VOLUME 86 NO. ST10
OCTOBER 1960

JOURNAL of the

Structural Division

PROCEEDINGS OF THE

AMERICAN SOCIETY
OF CIVIL ENGINEERS

BASIC REQUIREMENTS FOR MANUSCRIPTS

Original papers and discussions of current papers should be submitted to the Manager of Technical Publications, ASCE. Authors should indicate the technical division to which the paper should be referred. The final date on which a discussion should reach the Society is given as a footnote with each paper. Those who are planning to submit material will expedite the review and publication procedures by complying with the following basic requirements:

1. Titles must have a length not exceeding 50 characters and spaces.

2. A 50-word summary must accompany the paper.

3. The manuscript (a ribbon copy and two copies) should be double-spaced on one side of 8½-in. by 11-in. paper.

4. The author's full name, Society membership grade, and footnote reference stating present employment must appear on the first page of the paper.

5. Mathematics are recomposed from the copy that is submitted. Because of this, it is necessary that letters be drawn carefully, and that special symbols be properly identified.

6. Tables should be typed (ribbon copies) on one side of 8½-in. by 11-in. paper. Specific reference and explanation must be made in the text for each table.

7. Illustrations must be drawn in black ink on one side of 8½-in. by 11-in. paper. Because illustrations will be reproduced with a width of between 3-in. and 4½-in., the lettering must be large enough to be legible at this width. Photographs should be submitted as glossy prints. Explanations and descriptions must be made within the text for each illustration.

8. Papers should average about 12,000 words in length and must be no longer than 18,000 words. As an approximation, each full page of typed text, table, or illustration is the equivalent of 300 words.

9. Papers must be written in the third person.

Reprints from this Journal may be made on condition that the full title of the paper, name of author, page reference, and date of publication by the Society are given. The Society is not responsible for any statement made or opinion expressed in its publications.

This Journal is published monthly by the American Society of Civil Engineers. Publication office is at 2500 South State Street, Ann Arbor, Michigan. Editorial and General Offices are at 33 West 39 Street, New York 18, New York. $4.00 of a member's dues are applied as a subscription to this Journal. Second-class postage paid at Ann Arbor, Michigan.

The index for 1959 was published as ASCE Publication 1960-10 (list price $2.00); indexes for previous years are also available.

Journal of the

STRUCTURAL DIVISION

Proceedings of the American Society of Civil Engineers

STRUCTURAL DIVISION
EXECUTIVE COMMITTEE
Robert D. Dewell, Chairman; Emerson J. Ruble, Vice Chairman;
George S. Vincent; Nathan D. Whitman, Jr.; Charles T. G. Looney, Secretary

COMMITTEE ON PUBLICATIONS
Henry G. Schlitt, Chairman; Mace H. Bell; Gerald F. Borrmann;
Edwin S. Elcock; Kurt H. Gerstle; John E. Goldberg, Wayne C. Lewis;
Alfred L. Parme; Philip A. Upp; Halsted N. Wilcox

CONTENTS

October, 1960

Papers

Page

Matrix Formulation of the Folded Plate Equations
by A. C. Scordelis 1

Test of a Riveted Plate Girder with a Thin Web
by Desi D. Vasarhelyi, Jim C. Taylor, Naresh C.
Vasishth, and Chia-Yao Yuan 23

Buckling of One-Story Frames and Buildings
by John E. Goldberg 53

Long Span Prestressed Concrete Folded Plate Roofs
by John C. Brough, Jr. and B. H. Stephens, Jr. 87

Freezing and Thawing Effects on Prestressed Concrete
by M. J. Gutzwiller and F. E. Musleh 109

Flow Graphs in Structural Analysis
by Kurt H. Gerstle 125

(over)

Copyright 1960 by the American Society of Civil Engineers.

DISCUSSION

Page

Elasti-Plastic Analysis of Continuous Frames and Beams, by Lawrence P. Johnson, Jr., and Herbert A. Sawyer, Jr. (December, 1958. Prior discussion: June, 1959. Discussion closed.)
by Lawrence P. Johnson, Jr., and Herbert A. Sawyer, Jr. (closure) 141

Italian Arch Dam Design and Model Confirmation, by Guido Oberti. (March, 1960. Prior discussion: September, 1960. Discussion closed.)
by K. G. Harding and N. S. Trahair 145

The Impact of Computers on Engineering Education, by Gordon P. Fisher. (April, 1960. Prior discussion: September, 1960. Discussion closed.)
by Francis E. Swain 147

Dynamic Effects of Earthquake, by Ray W. Clough. (April, 1960. Prior discussion: August, 1960. Discussion closed.)
by A. A. Eremin. 151

Influence of Partial Base Fixity on Frame Stability, by Theodore V. Galambos. (May, 1960. Prior discussion: None. Discussion closed.)
by Eugene Guillard. 153

Various Instability Modes of the Fixed Base Column, by D. A. Sawyer. (July, 1960. Prior discussion: None. Discussion closes December 1, 1960.)
by Marvin A. Larson. 155

Basic Column Strength, by Lynn S. Beedle and Lambert Tall. (July, 1960. Prior discussion: None. Discussion closes December 1, 1960.)
by Donovan H. Lee 161

Errata 163

Journal of the
STRUCTURAL DIVISION
Proceedings of the American Society of Civil Engineers

A MATRIX FORMULATION OF THE FOLDED PLATE EQUATIONS

By A. C. Scordelis,[1] M. ASCE

SYNOPSIS

An analytical procedure, utilizing matrix algebra, is developed for determining longitudinal stresses, transverse moments, and vertical deflections in folded plate structures. The procedure provides an efficient and systematic method for analyzing structures of this type. The sequence of matrix operations can be readily programmed for a digital computer having available matrix subroutines. A sequence which has been programmed for the IBM 704 digital computer is described.

INTRODUCTION

Folded plate structures have gained increasing use and popularity in the United States during the past decade. They have proved to be especially economical in the construction of long span roof systems. These roofs have generally been made of reinforced concrete, but in some cases timber combined with plywood sheathing has been used. Folded plates have also been used for bins, silos, staircases, and floor systems. A description of a number of applications of folded plates in this country together with information on the economics of this type of construction has been given by Whitney, Anderson, and Birnbaum.[2]

Methods for analyzing folded plate structures were first developed in Germany in 1930 by Ehlers[3] and Craemer.[4] Since that time there have been

Note.—Discussion open until March 1, 1961. To extend the closing date one month, a written request must be filed with the Executive Secretary, ASCE. This paper is part of the copyrighted Journal of the Structural Division, Proceedings of the American Society of Civil Engineers, Vol. 86, No. ST 10, October, 1960.

[1] Assoc. Prof. of Civ. Engrg., Univ. of California, Berkeley, Calif.

[2] "Reinforced Concrete Folded Plate Construction," by C. S. Whitney, B. G. Anderson, and H. Birnbaum, Proceedings, ASCE, Vol. 85, No. ST 8, October, 1959, p. 15.

[3] "Ein neues Konstruktionsprinzip," by G. Ehlers, Bauingenieur, Vol. 9, 1930, p. 125.

[4] "Theorie der Faltwerke," by H. Craemer, Beton und Eisen, Vol. 29, 1930, p. 276.

numerous papers written on the subject, but no attempt will be made to review them here. This has been done to some extent by Gaafar[5] and Traum.[6] Perhaps the most extensive treatment of the subject to date is contained in a recently published book by Yitzhaki.[7] The general approach followed in this paper will be similar to his.

In contrast to the numerous papers on the analysis of folded plates structures very little information has been published on the experimental verification of the theories being used. However, Gaafar[5] has reported results on an experimental study of an aluminum folded plate that indicated fair correlation with theory.

The determination of longitudinal stresses, transverse moments, and vertical deflections is of primary interest in the analysis of a folded plate structure. These quantities may be obtained through the development and solution of a series of linear algebraic equations which are conveniently expressed in matrix form. Since the amount of computational effort is relatively large for even a simple case, the analysis can be most effectively carried out with the aid of a digital computer for which the matrix formulation is especially suited.

Notation.—The letter symbols adopted for use in this paper are defined where they first appear, in the illustrations or in the text, and are arranged alphabetically, for convenience or reference, in Appendix II.

METHOD OF ANALYSIS

A prismatic folded plate structure (Fig. 1) consists of a series of mutually supporting plates that frame into supporting diaphragms. A load applied to the structure is first carried by transverse slab action to the longitudinal joints. The reactions at the joints then resolve into forces parallel to the plates and are carried by longitudinal plate action to the diaphragms, each plate acting as a longitudinal beam spanning between supports.

The analysis is based on the following simplifying assumptions:

1. The material is elastic, isotropic, and homogeneous.
2. The structure is completely monolithic.
3. Slab action is defined by the behavior of transverse one way slabs spanning between longitudinal joints.
4. Longitudinal stresses developed in each plate due to longitudinal plate action may be calculated by the elementary beam theory; therefore, the longitudinal stresses vary linearly over the depth of each plate.
5. Supporting diaphragms are infinitely stiff parallel to their own plane, but perfectly flexible normal to their own plane.

For purposes of discussion the folded plate structure may be thought to consist of two systems intimately connected, Fig. 2. The slab system consists of a series of one way slab strips spanning between longitudinal joints. These strips are capable of transmitting shears and moments in a transverse direction only. The slab system is supported elastically by the plate system, which

---

5 "Hipped Plate Analysis Considering Joint Displacement," by I. Gaafar, Transactions, ASCE, Vol. 119, 1954.

6 "The Design of Folded Plates," by E. Traum, Proceedings, ASCE, Vol. 85, No. ST 8, October, 1959, p. 103.

7 "Prismatic and Cylindrical Shell Roofs," by D. Yitzhaki, Haifa Science Publishers, Haifa, Israel, 1958.

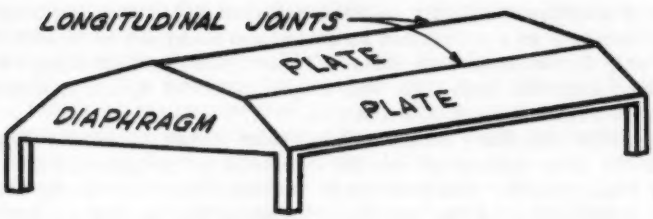

FIG. 1.—FOLDED PLATE STRUCTURE

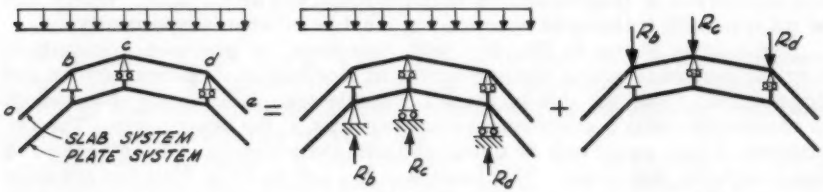

FIG. 2.—CONCEPT OF FOLDED PLATE STRUCTURE

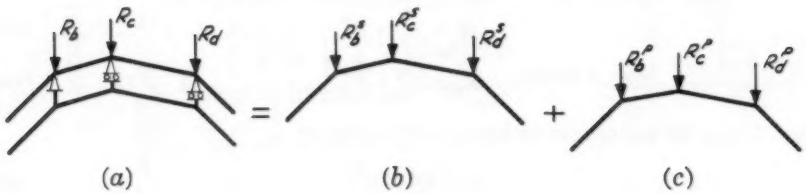

FIG. 3

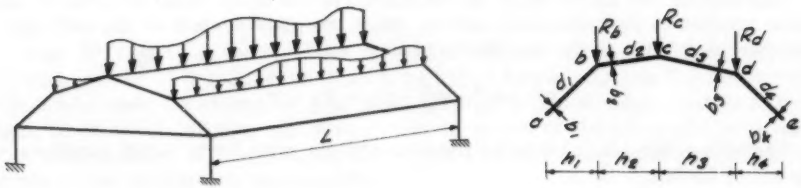

FIG. 4

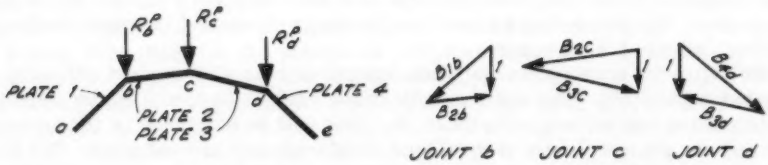

FIG. 5

consists of a series of plates spanning longitudinally between diaphragms. The plate system acts as a membrane structure and each plate is capable of transmitting only forces in its own plane. The analysis of a folded plate structure for a given external load, Fig. 2(a), may be obtained by the superposition of the loadings shown in Figs. 2(b) and 2(c).

In Fig. 2(b) imaginary supports have been placed under the longitudinal joints of the plate system so that the external load is carried entirely by the one-way slab system. The transverse moments may be readily obtained by moment distribution and the resulting reactions, R_b, R_c, and R_d, may then be found by equations of statics. This procedure may be followed in cases where the distributed external loads in each transverse span, shown in Fig. 2(b), have similar curves of longitudinal variation between end diaphragms. Where this is not true each transverse span loading must be treated independently.

The loading shown in Fig. 2(c) will, therefore, be assumed to consist of vertical line loads having similar curves of longitudinal variation between end diaphragms. Note that this includes a possible zero value at any of the joints in combination with a given longitudinal variation at the other joints. The remainder of this paper will be concerned with the response of the structure to these vertical line loads. The loads R_b, R_c, and R_d (Fig. 3(a)) are partially taken by the one-way slab strips (Fig. 3(b)) and partially by the longitudinal plate system (Fig. 3(c)), such that

$$R_b = R_b^s + R_b^p \quad \ldots\ldots\ldots\ldots\ldots\ldots (1a)$$

$$R_c = R_c^s + R_c^p \quad \ldots\ldots\ldots\ldots\ldots\ldots (1b)$$

$$R_d = R_d^s + R_d^p \quad \ldots\ldots\ldots\ldots\ldots\ldots (1c)$$

Eqs. 1 may be written, in an abbreviated form as

$$\underline{R} = \underline{R^s} + \underline{R^p} \quad \ldots\ldots\ldots\ldots\ldots\ldots (2)$$

in which the underlining indicates that the symbol represents a matrix.

The sum of the loads taken by the plate system must equal the sum of the loads applied to the combined system, since the plate system is the only system carrying loads to the end diaphragms.

$$R_b^p + R_c^p + R_d^p = R_b + R_c + R_d \quad \ldots\ldots\ldots\ldots (3)$$

Therefore, the loads taken by the slab system must form a self equilibrating set of forces.

$$R_b^s + R_c^s + R_d^s = 0 \quad \ldots\ldots\ldots\ldots\ldots (4)$$

The division of the total load between slab and plate system must be such as to produce the same displacement in the slab system and the plate system at each of the joints b, c, and d.

Initially, the solution for the plate system and the slab system will each be treated separately. The basic equations for each system will be developed in matrix form and subsequently these matrices will be combined in such a manner that the above criteria of equal joint displacements are satisfied. The final result will yield matrices defining longitudinal stresses, vertical deflections,

and transverse moments due to any combination of vertical line loads applied to the combined system.

As a typical case the structure shown in Fig. 4, which has a simple span L, will be considered. The structure has four plates, each of different thicknesses b, depths d, and horizontal transverse spans h. Edges a and e are free and the interior joints b, c, and d are subjected to vertical loads having different intensities R_b, R_c, and R_d at a given distance from one of the end diaphragms. All three loads have similar curves of longitudinal variation. The vertical joint loads R and the vertical joint deflections δ will be considered positive when they are in a downward direction.

PLATE SYSTEM

If the plates shown in Fig. 4 are assumed to have zero flexural stiffness normal to their own planes, the entire load will be carried by membrane action. The load intensities, R^p, at a given distance from the support, which are carried in this manner are shown in Fig. 5(a).

Longitudinal Stresses.—In this section a matrix will be developed defining the longitudinal stress σ at each plate edge produced by a given set of R^p loads. This matrix will be designated as the stress matrix $\underline{S}_p$ for the plate system.

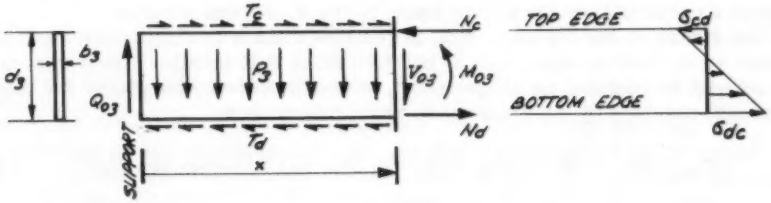

FIG. 6.—FREE BODY DIAGRAM OF A TYPICAL PLATE

The R^p loads can be resolved into plate loads P, which are loads parallel to each plate. This may be done with the aid of force triangles for unit vertical loads such as shown in Fig. 5(b). A force transformation matrix $\underline{B}$ may then be written defining the plate loads in terms of the vertical joint loads. Detailed makeup of this matrix, as well as others developed subsequently, is given in the example in the appendix.

$$\underline{p} = \underline{B}\,\underline{R}^p \quad \ldots\ldots\ldots\ldots\ldots\ldots \quad (5)$$

Plate loads in the direction a - b - c - d - e are considered positive, and the sign of each element in the $\underline{B}$ matrix should be taken accordingly.

A free body diagram of a portion of a typical plate (plate 3 in this case) is shown in Fig. 6 with all quantities indicated acting in a positive direction. Top and bottom edges of each plate are established by going successively in the direction a - b - c - d - e.

T_c and T_d are longitudinal shears per unit length on the top and bottom edges. N_c and N_d are forces normal to the cut section that are defined by

$$N_c = \int_o^x T_c \, dx \quad \ldots\ldots\ldots\ldots\ldots\ldots (6a)$$

$$N_d = \int_o^x T_d \, dx \quad \ldots\ldots\ldots\ldots\ldots\ldots (6b)$$

Q_{o3}, V_{o3}, and M_{o3} are the end reaction, shear, and bending moment assuming the plate spanning between diaphragms is subjected to the plate load P_3 alone. The term P_3 has the same longitudinal variation as R^p and the bending moment may be expressed as

$$M_{o3} = C_S \, P_3$$

in which C_S is a constant that is a function of span and load distribution. For M_{o3} at midspan of a simple span this constant has the following values: $C_S = L^2/8$ for a uniform load; $C_S = L^2/\pi^2$ for a first harmonic sine loading in which P_3 is the maximum load intensity; and $C_S = L/4$ if P_3 is a concentrated load at midspan.

For the given case of similar longitudinal variation of P in all plates the N versus x curve will be similar in shape to the M_o versus x curve and the T versus x curve will be similar in shape to the V_o versus x curve.

The stress at the top edge, σ_{cd}, is positive when it is compressive and the stress at the bottom edge, σ_{dc}, is positive when it is tensile. The σ versus x curve will be similar in shape to M_o versus x curve. Formulas for these stresses, obtained by the elementary beam theory, are

$$\sigma_{cd} = C_S \left[(6/bd^2)_3 \, (P_3) + (4/bd)_3 \, (N_c/C_S) + (2/bd)_3 \, (N_d/C_S) \right] \quad \ldots (8a)$$

$$\sigma_{dc} = C_S \left[(6/bd^2)_3 \, (P_3) + (2/bd)_3 \, (N_c/C_S) + (4/bd)_3 \, (N_d/C_S) \right] \quad \ldots (8b)$$

A similar set of equations may be written for each plate so that

$$\sigma = C_S \left[\underline{\sigma_o} + \underline{\sigma_N} \right] \quad \ldots\ldots\ldots\ldots\ldots\ldots (9a)$$

$$\sigma = C_S \left[\underline{S_o} \, \underline{P} + \underline{S_N} \, \underline{(N/C_S)} \right] \quad \ldots\ldots\ldots\ldots\ldots\ldots (9b)$$

in which $\underline{S_o}$ and $\underline{S_N}$ are matrices that are functions of the width b and depth d of each plate. Using the relationship established in Eq. 5 between the plate loads and the vertical joint loads, Eq. 9 may be written as

$$\sigma = C_S \left[\underline{S_o} \, \underline{B} \, \underline{(R^p)} + \underline{S_N} \, \underline{(N/C_S)} \right] \quad \ldots\ldots\ldots\ldots\ldots\ldots (10)$$

The only unknown quantities on the right hand side of this expression are the $\underline{(N/C_S)}$ values at each interior joint of the plate system. These may be found by noting that the algebraic sum of the stresses at each interior joint must equal zero to satisfy the condition of compatibility of longitudinal strains

$$\underline{\Sigma \sigma} = \underline{D_o} \, \underline{R^p} + \underline{D_N} \, \underline{(N/C_S)} = 0 \quad \ldots\ldots\ldots\ldots\ldots\ldots (11)$$

in which $\underline{D_o}$ and $\underline{D_N}$ are obtained by adding the proper rows of the $\underline{S_N}$ and $\underline{S_o\ B}$ matrices in Eq. 10 or by pre-multiplying the latter matrices by a matrix designated as an ADRO matrix. For example for the case shown in Fig. 5(a) there are four plates and three interior joints so that

$$\underline{ADRO} = \begin{bmatrix} 0 & 1 & 1 & 0 & 0 & 0 & 0 & 0 \\ 0 & 0 & 0 & 1 & 1 & 0 & 0 & 0 \\ 0 & 0 & 0 & 0 & 0 & 1 & 1 & 0 \end{bmatrix} \quad \ldots\ldots (12)$$

Eq. 11 may be solved for $\underline{N/C_S}$ and the result substituted back into Eq. 10 to obtain a final relationship between longitudinal stresses at the plate edges and external vertical joint loads.

$$\underline{N/C_S} = -\underline{D_N^{-1}}\ \underline{D_o}\ \underline{R^p} \quad \ldots\ldots\ldots\ldots\ldots (13a)$$

$$\underline{\sigma} = C_S\left[\underline{S_o}\ \underline{B} - \underline{S_N}\ \underline{D_N^{-1}}\ \underline{D_o}\right]\underline{R^p} \quad \ldots\ldots\ldots\ldots (13b)$$

or letting

$$\underline{S_p} = \left[\underline{S_o}\ \underline{B} - \underline{S_N}\ \underline{D_N^{-1}}\ \underline{D_o}\right] \quad \ldots\ldots\ldots\ldots\ldots (14)$$

$$\boxed{\underline{\sigma} = C_S\ \underline{S_p}\ \underline{R^p}} \quad \ldots\ldots\ldots\ldots\ldots\ldots (15)$$

$\underline{S_p}$ is the stress matrix for the plate system and is a function of only the dimensions and geometry of the folded plate structure cross-section.

Vertical Joint Deflections.—In this section a matrix will be developed defining the vertical deflection δ at each interior joint produced by a given set of R^p loads. This matrix will be designated as the flexibility matrix, $\underline{F_p}$, for the plate system. The inverse of this matrix will be designated as the stiffness matrix $\underline{K_p}$ for the plate system. $\underline{K_p}$ defines the vertical load R^p at each interior joint produced by a given set of vertical joint deflections δ.

The vertical deflection δ at any interior joint can be expressed in terms of the plate displacements v of the two plates adjoining the joint. The latter displacements are parallel to the plates and will be considered positive when in the direction a - b - c - d - e. Using a Williot diagram, Fig. 7(a) depicts the real displacement, cc', at a typical joint that results from plate displacements v_2 and v_3. Fig. 7(b) indicates a free body diagram of joint c subjected to a virtual force system in which B_{2c} and B_{3c} are forces parallel to plates 2 and 3 respectively and are equal to similarly designated quantities in the force transformation matrix $\underline{B}$ of Eq. 5. All quantities shown in Fig. 7(a) and 7(b) are acting in a positive direction.

Applying the real displacements in Fig. 7(a) to the virtual forces on joint c in Fig. 7(b) the total virtual work must equal zero.

$$1 \times \delta_c - B_{2c}\ v_2 - B_{3c}\ v_3 = 0 \quad \ldots\ldots\ldots\ldots (16a)$$

$$\delta_c = B_{2c}\ v_2 + B_{3c}\ v_3 \quad \ldots\ldots\ldots\ldots\ldots (16b)$$

A similar expression may be written for each interior joint so that

$$\underline{\delta} = \underline{G}\ \underline{v} = \underline{B}^T\ \underline{v} \quad \ldots\ldots\ldots\ldots\ldots\ldots (17)$$

in which the displacement transformation matrix $\underline{G}$ is equal to the transpose of the force transformation matrix $\underline{B}$ of Eq. 5. Neglecting shear deformations a typical plate displacement v_3 (Fig. 8) at a given distance x from the support can be expressed as

$$v_3 = C_V \frac{M_p}{E\, I_p} \quad \ldots\ldots\ldots\ldots\ldots\ldots (18)$$

in which C_V is a constant that depends on the span and the distribution of angle

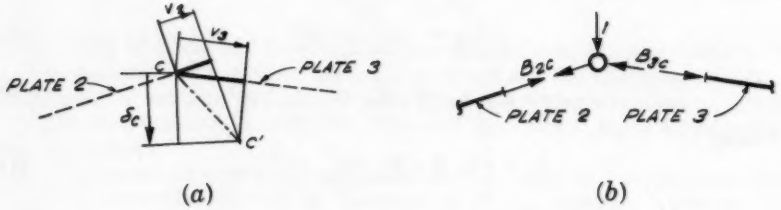

FIG. 7

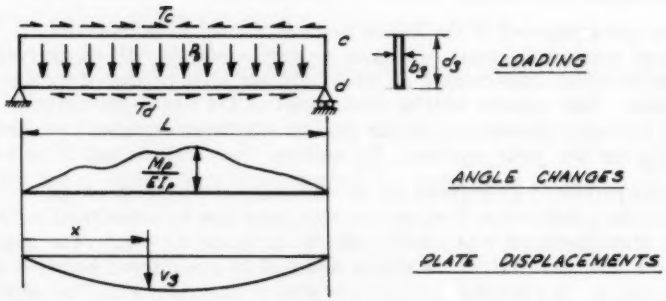

FIG. 8.—PLATE DISPLACEMENTS

changes and $M_p/E\, I_p$ is a specified angle change ordinate, usually the maximum ordinate.

From Fig. 6

$$M_p = M_{o3} + N_c \frac{d_3}{2} + N_d \frac{d_3}{2} \quad \ldots\ldots\ldots\ldots (19a)$$

$$M_p = C_S\, P_3 + N_c \frac{d_3}{2} + N_d \frac{d_3}{2} \quad \ldots\ldots\ldots\ldots (19b)$$

and

$$I_p = \frac{b_3\, d_3^3}{12} \quad \ldots\ldots\ldots\ldots\ldots\ldots\ldots (19c)$$

Substituting these values into Eq. 18

$$v_3 = C_D\left[(12/b\,d^3\,E)_3\,(P_3) + (6/b\,d^2\,E)_3\,(N_c/C_S) + (6/b\,d^2\,E)_3\,(N_c/C_S)\right] \quad . . (20)$$

in which $C_D = C_V \cdot C_S$ is a deflection constant. For v_3 at midspan of a simple span: $C_D = 5\,L^4/384$ for a uniform load; $C_D = L^4/\pi^4$ for a first harmonic sine loading with P_3 being a midspan value; $C_D = L^3/48$ if P_3 is a concentrated load at midspan. An equation similar to Eq. 20 may be written for each plate so that

$$\underline{v} = C_D\left[\underline{v_o} + \underline{v_N}\right] \quad . . . . . (20a)$$

$$\underline{v} = C_D\left[\underline{F_o}\;\underline{P} + \underline{F_N}\;\underline{N/C_S}\right] \quad . . . . . (20b)$$

in which $\underline{F_o}$ and $\underline{F_N}$ are matrices that are functions of the width b, depth d, and modulus of elasticity E of each plate. Since $\underline{P}$ and $\underline{N/C_S}$ have already been expressed in terms of $\underline{R^p}$ by Eqs. 5 and 13 respectively, these substitutions may be made in Eq. 20 to yield

$$\underline{v} = C_D\left[\underline{F_o}\;\underline{B} - \underline{F_N}\;\underline{D_N^{-1}}\;\underline{D_o}\right]\underline{R^p} \quad . . . . . (21)$$

A final relationship between vertical joint deflections and loads taken by the plate system may now be written;

$$\underline{\delta} = \underline{G}\;\underline{v} = \underline{B^T}\;\underline{v} \text{ from (3.1)} \quad . . . . . (22a)$$

$$= C_D\;\underline{B^T}\left[\underline{F_o}\;\underline{B} - \underline{F_N}\;\underline{D_N^{-1}}\;\underline{D_o}\right]\underline{R^p} \quad . . . . . (22b)$$

or, letting

$$\underline{F_p} = \underline{B^T}\left[\underline{F_o}\;\underline{B} - \underline{F_N}\;\underline{D_N^{-1}}\;\underline{D_o}\right] \quad . . . . . (23)$$

$$\boxed{\underline{\delta} = C_D\;\underline{F_p}\;\underline{R^p}} \quad . . . . . (24a)$$

$$\boxed{\underline{R^p} = \underline{C_D^{-1}}\;\underline{K_p}\;\underline{\delta}} \quad . . . . . (24b)$$

in which $\underline{K_p} = \underline{F_p^{-1}}$. $\underline{F_p}$ and $\underline{K_p}$ are, respectively, the flexibility and stiffness matrices for the plate system and both are functions only of the dimensions and geometry of the folded plate structure cross section and the modulus of elasticity.

By substituting the value of $\underline{R^p}$ from Eq. 24 into Eq. 15 the longitudinal stresses at the plate edges σ may be expressed directly in terms of the vertical joint deflections δ.

$$\sigma = C_S\;C_D^{-1}\left[\underline{S_p}\;\underline{K_p}\right]\underline{\delta} \quad . . . . . (25)$$

SLAB SYSTEM

Fig. 9(a) shows a typical slab strip of unit width that has been taken from the slab system at a given distance from an end diaphragm. The slab strip is

subjected to vertical joint loads, R^s, that form a self equilibrating system of forces. A given set of R^s loads and transverse moments m are associated with a given set of vertical joint deflections δ.

Transverse Moments.—In this section a matrix will be developed defining the transverse moment, m, at each plate edge produced by a given set of vertical joint deflections δ. This matrix will be designated as the moment matrix $\underline{S_s}$ for the slab system.

Fig. 9(b) shows a free body diagram of a typical span of the slab strip (span 3 in this case) with all quantities shown acting in a positive direction. The

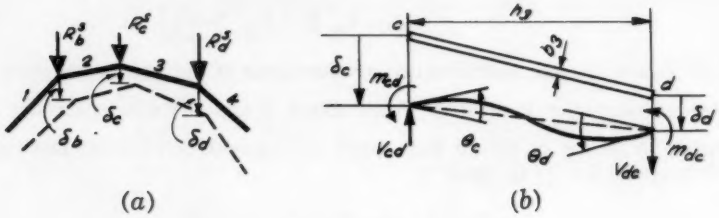

(a) (b)

FIG. 9

moment at each end of span 3 can be expressed by the slope-deflection equations as

$$m_{cd} = 2\,E\,I_s/d\left[2\,\theta_c + \theta_d - 3\,\psi_{cd}\right]$$

$$= \left(b^3\,E/3\,d\right)_3\,\theta_c + \left(b^3\,E/6\,d\right)_3\,\theta_d$$

$$- \left(b^3\,E/2\,d\,h\right)_3\,\delta_c + \left(b^3\,E/2\,d\,h\right)_3\,\delta_d \quad \ldots\ldots (26a)$$

$$m_{dc} = 2\,E\,I_s/d\left[\theta_c + 2\,\theta_d - 3\,\psi_{cd}\right]$$

$$= \left(b^3\,E/6\,d\right)_3\,\theta_c + \left(b^3\,E/3\,d\right)_3\,\theta_d$$

$$- \left(b^3\,E/2\,d\,h\right)_3\,\delta_c + \left(b^3\,E/2\,d\,h\right)_3\,\delta_d \quad \ldots\ldots (26b)$$

in which $I_s = (1)\,b_3^3/12$, is the moment of inertia of a unit width of slab and $\psi_{cd} = (\delta_c - \delta_d)/h_3$, is the chord rotation. A pair of equations similar to Eqs. 26 may be written for each span so that

$$\underline{m} = \underline{m_\theta} + \underline{m_\delta} \quad \ldots\ldots (27a)$$

$$m = \underline{K_\theta}\,\underline{\theta} + \underline{K_\delta}\,\underline{\delta} \quad \ldots\ldots (27b)$$

The joint rotations θ may be found in terms of vertical joint deflections δ by noting that the algebraic sum of the moments at each interior joint must equal zero to satisfy equilibrium.

$$\underline{\Sigma m} = \underline{D_\theta}\,\underline{\theta} + \underline{D_\delta}\,\underline{\delta} = 0 \quad \ldots\ldots (28)$$

in which D_θ and D_δ are obtained by adding the proper rows of the K_θ and K_δ matrices in Eq. 27, or by multiplying the latter matrices by the ADRO matrix of Eq. 12. Eq. 28 may be solved for θ and the result substituted back into Eq. 27 to obtain a final relationship between transverse moments at the plate edges and vertical joint deflections.

$$\underline{\theta} = -\underline{D_\theta^{-1}}\ \underline{D_\delta}\ \underline{\delta} \quad \ldots\ldots\ldots\ldots\ldots\ldots (29a)$$

$$\underline{m} = \left[\underline{K_\delta} - \underline{K_\theta}\ \underline{D_\theta^{-1}}\ \underline{D_\delta}\right]\ \underline{\delta} \quad \ldots\ldots\ldots\ldots (29b)$$

or, letting

$$S_s = \left[\underline{K_\delta} - \underline{K_\theta}\ \underline{D_\theta^{-1}}\ \underline{D_\delta}\right] \quad \ldots\ldots\ldots\ldots\ldots (30)$$

$$\boxed{\underline{m} = \underline{S_s}\ \underline{\delta}} \quad \ldots\ldots\ldots\ldots\ldots\ldots (31)$$

$\underline{S_s}$ is the moment matrix for the slab system and it is a function only of the geometry and dimensions of the folded plate structure cross section and the modulus of elasticity.

Vertical Joint Loads Taken by Slab System.—The vertical joint load R^s at each joint can be computed in terms of transverse slab moments, m, at each plate edge using equations of statics. For example, in Fig. 9(a)

$$R_c^s = \left(\frac{m_{bc} + m_{cb}}{h_2}\right) - \left(\frac{m_{cd} + m_{dc}}{h_3}\right) \quad \ldots\ldots\ldots\ldots (32)$$

One equation, similar to Eq. 32 may be written for each interior joint so that

$$\underline{R^s} = \underline{H}\ \underline{m} \quad \ldots\ldots\ldots\ldots\ldots\ldots (33)$$

The $\underline{H}$ matrix is a function of the horizontal spans h of the transverse slab system. Substituting the value of $\underline{m}$ in Eq. 31 into Eq. 33 a final relationship between vertical joint deflections and loads taken by the slab system may be obtained.

$$\underline{R^s} = \underline{H}\ \underline{S_s}\ \underline{\delta} \quad \ldots\ldots\ldots\ldots\ldots\ldots (34)$$

or letting

$$\underline{K_s} = \underline{H}\ \underline{S_s} \quad \ldots\ldots\ldots\ldots\ldots\ldots (35)$$

$$\boxed{\underline{R^s} = \underline{K_s}\ \underline{\delta}} \quad \ldots\ldots\ldots\ldots\ldots\ldots (36)$$

$\underline{K_s}$ is the stiffness matrix for the slab system. While a single vertical joint deflection will produce a set of R^s loads in equilibrium, a set of vertical joint deflections cannot exist for a single R^s joint load since the slab strip would not be in equilibrium. Thus the $\underline{K_s}$ matrix cannot be inverted.

COMBINED PLATE AND SLAB SYSTEM; HARMONIC LOADING

One approach to the analysis of the combined plate and slab system, represented in Fig. 4, is to replace the given longitudinal distribution of the vertical joint loads, R, by the superposition of harmonic loadings obtained from a

Fourier series representation of the actual loading. A harmonic loading has the property that it produces R versus x, R^p versus x, v versus x, σ versus x, R^s versus x, m versus x, and δ versus x curves of the same shape. For example, the first harmonic is a single sine wave. Each harmonic is analyzed in a similar manner, and, therefore, only the first harmonic will be considered in the following discussion.

Recalling Eq. 2 and the requirement that the plate system and the slab system must have the same vertical joint deflections, the following relationship may be written for the combined system. From Eq. 2

$$\underline{R} = \left[\underline{K_s} + C_D^{-1}\ \underline{K_p}\right] \underline{\delta} \quad \ldots\ldots\ldots\ldots\ldots\ldots (37)$$

in which values for R^s and R^p are obtained from Eqs. 36 and 24b, respectively.

Letting

$$\underline{K} = \left[\underline{K_s} + C_D^{-1}\ \underline{K_p}\right] \quad \ldots\ldots\ldots\ldots\ldots\ldots (38)$$

$$\boxed{\underline{R} = \underline{K}\ \underline{\delta}} \quad \ldots\ldots\ldots\ldots\ldots\ldots (39)$$

$$\boxed{\underline{\delta} = \underline{F}\ \underline{R}} \quad \ldots\ldots\ldots\ldots\ldots\ldots (40)$$

in which $\underline{F} = \underline{K}^{-1}$. $\underline{K}$ and $\underline{F}$ are, respectively, the stiffness and flexibility matrices for the combined system under a harmonic loading. For a first harmonic $C_D^{-1} = \pi^4/L^4$ and R and δ are the maximum ordinates of sine curves.

Thus, to analyze the folded plate structure in Fig. 4 for any set of harmonic vertical joint loads $\underline{R}$, Eq. 40 is used to compute the vertical joint deflections $\underline{\delta}$ and then Eqs. 25 and 31 are used to compute longitudinal plate stresses, $\underline{\sigma}$, and transverse slab moments, $\underline{m}$. The quantities found are maximum ordinates of the particular harmonic curve.

Sequence of Matrix Operations for Harmonic Loading.—The entire sequence of matrix operations can be readily programmed for a digital computer. In a general case a folded plate structure will have n plates, j interior joints, and will be subjected to q different combinations of vertical joint loads. To recapitulate, the steps required for a first harmonic loading on a simple span are listed below with appropriate remarks. Detailed makeup of the input matrices is illustrated in the example given in Appendix I.

Step	Matrix Description	Matrix Size	Remarks
1	[B]	nxj	Input
2	$[S_N]$	2nxj	Input
3	$[S_o]$	2nxn	Input
4	[ADRO]	jx2n	Input
5	$[F_N]$	nxj	Input
6	$[F_o]$	nxn	Input
7	$[K_\theta]$	2nxj	Input

8	$[K_\delta]$	2nxj	Input
9	$[H]$	jx2n	Input
10	C_{SH}	Constant	Input = L^2/π^2 for first harmonic
11	C_{DH}	Constant	Input = L^4/π^4 for first harmonic
12	$[R]$	jxq	End of input = joint loading
13	$[S_oB] = [S_o][B]$	2nxj	
14	$[D_N] = [ADRO][S_N]$	jxj	
15	$[D_o] = [ADRO][S_oB]$	jxj	
16	$[D_N^{-1}] = [D_N]^{-1}$	jxj	
17	$[D_N^{-1}D_o] = [D_N^{-1}][D_o]$	jxj	
18	$[S_ND_N^{-1}D_o] = [S_N][D_N^{-1}D_o]$	2nxj	
19	$[S_p] = [S_oB] - [S_ND_N^{-1}D_o]$	2nxj	Output - stress matrix, plate system
20	$[F_oB] = [F_o][B]$	nxj	
21	$[F_ND_N^{-1}D_o] = [F_N][D_N^{-1}D_o]$	nxj	
22	$[F_oB - F_ND_N^{-1}D_o] = [F_oB] - [F_ND_N^{-1}D_o]$	nxj	
23	$[G] = [B]^T$	jxn	G = transpose of B
24	$[F_p] = [G][F_oB - F_ND_N^{-1}D_o]$	jxj	Output - flexibility matrix, plate system
25	$[K_p] = [F_p]^{-1}$	jxj	Output - stiffness matrix, plate system
26	$[D_\theta] = [ADRO][K_\theta]$	jxj	
27	$[D_\delta] = [ADRO][K_\delta]$	jxj	
28	$[D_\theta^{-1}] = [D_\theta]^{-1}$	jxj	
29	$[D_\theta^{-1}D_\delta] = [D_\theta^{-1}][D_\delta]$	jxj	
30	$[K_\theta D_\theta^{-1}D_\delta] = [K_\theta\ [D_\theta^{-1}D_\delta]$	2nxj	
31	$[S_s] = [K_\delta] - [K_\theta D_\theta^{-1}D_\delta]$	2nxj	Output - moment matrix, slab system

32	$[K_s] = [H][S_s]$	jxj	Output - stiffness matrix, slab system
33	$[C_{DH}^{-1} K_p] = C_{DH}^{-1}[K_p]$	jxj	
34	$[K] = [C_{DH}^{-1} K_p] + [K_s]$	jxj	Output - stiffness matrix, combined system
35	$[F] = [K]^{-1}$	jxj	Output - flexibility matrix, combined system
36	$[\delta] = [F][R]$	jxq	Output - midspan joint deflections
37	$[m] = [S_s][\delta]$	2nxq	Output - midspan transverse moments
38	$[C_{SH}S_p] = C_{SH}[S_p]$	2nxj	
39	$[C_{SH}S_p C_{DH}^{-1} K_p] = [C_{SH}S_p][C_{DH}^{-1} K_p]$	2nxj	
40	$[\sigma] = [C_{SH}S_p C_{DH}^{-1} K_p][\delta]$	2nxq	Output - midspan longitudinal stresses

To obtain results for second, third, and so on numbers of harmonic loadings only steps 33 to 40 have to be repeated using new values of C_S, C_D, and $\underline{R}$ corresponding to the particular harmonic. Input matrices in steps 1 to 9 and matrices computed in steps 13 to 32 are functions of only the dimensions and geometry of the folded plate cross section and the modulus of elasticity.

COMBINED PLATE AND SLAB SYSTEM; NON-HARMONIC LOADING

While the method described in the preceding section is generally applicable to any loading, the number of harmonics necessary to represent a given loading may be excessive in certain cases. An alternate procedure suggested by Yitzhaki,[7] offers definite advantages in these cases.

For simplicity of discussion let the beam of Fig. 10(a) represent, symbolically, an entire folded plate structure consisting of the combined plate and slab system.

1. The loading shown in Fig. 10(a), in this case a set of concentrated vertical joint loads R at midspan, is obtained by the superposition of those shown in Figs. 10(b), 10(c), and 10(d).

2. In Fig. 10(b) the entire load R is assumed to be taken by the plate system alone acting as a membrane structure. Longitudinal stresses σ_1 and vertical joint deflections σ_1 are computed.

3. The deflection curve in Fig. 10(b) can be closely approximated by a first harmonic sine wave. Thus, in Fig. 10(c), the harmonic load R_1 and the transverse slab moments m_1, both resulting from this deflection curve being applied to the slab system alone, are computed.

4. In Fig. 10(d), the harmonic load R_1 is applied to the combined plate and slab system and σ_2, m_2, and δ_2 are computed by the method developed in the preceding section on harmonic loadings.

5. Thus, final values for the loading in Fig. 10(a) are obtained by superposition.

$$\underline{R} = \underline{R} + \underline{R_1} - \underline{R_1} \quad \ldots\ldots\ldots\ldots\ldots\ldots (41)$$

$$\underline{\sigma} = \underline{\sigma_1} - \underline{\sigma_2} \quad \ldots\ldots\ldots\ldots\ldots\ldots\ldots (42)$$

$$\underline{m} = \underline{m_1} - \underline{m_2} \quad \ldots\ldots\ldots\ldots\ldots\ldots\ldots (43)$$

and

$$\underline{\delta} = \underline{\delta_1} - \underline{\delta_2} \quad \ldots\ldots\ldots\ldots\ldots\ldots\ldots (44)$$

The advantage of the above procedure is that only the deflection curve of the given loading rather than the loading itself need be represented by a harmonic series.

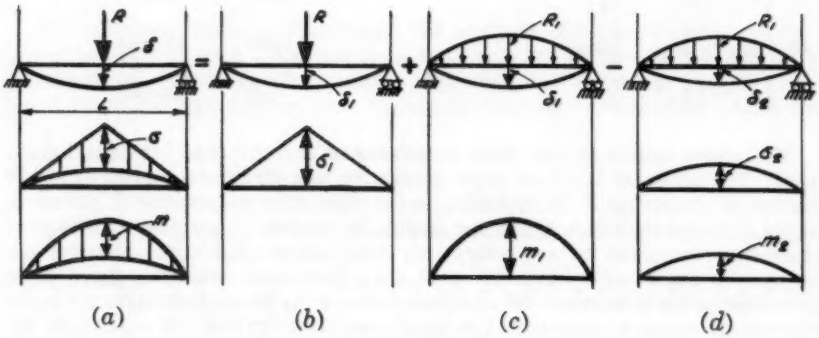

FIG. 10

Sequence of Matrix Operations for Non-Harmonic Loading.—Steps 1 to 35 are exactly the same for this sequence as for the harmonic loading with the exception that in steps 9 and 10 two constants are input rather than one.

9. $C_{SH} = L^2/\pi^2$; C_{SW} is the stress constant for given loading; such as $L/4$ for concentrated load at midspan; $L^2/8$ for a uniformly distributed load.

10. $C_{DH} = L^4/\pi^4$; C_{DW} is the deflection constant for given loading; e.g. $L^3/48$ for concentrated load at midspan; $5L^4/384$ for a uniformly distributed load.

Beyond step 35 the following sequence should be used.

Step	Matrix Description	Matrix Size	Remarks
36	$[C_{SW}S_p] = C_{SW}[S_p]$	2nxj	
37	$[\sigma_1] = [C_{SW}S_p][R]$	2nxq	Output
38	$[C_{DW}F_p] = C_{DW}[F_p]$	jxj	
39	$[\delta_1] = [C_{DW}F_p][R]$	jxq	Output

40	$[R_1] = [K_s]\,[\delta_1]$	jxq	
41	$[m_1] = [S_s]\,[\delta_1]$	2nxq	Output
42	$[\delta_2] = [F]\,[R_1]$	jxq	
43	$[m_2] = [S_s]\,[\delta_2]$	2nxq	
44	$[C_{SH}S_p] = C_{SH}\,[S_p]$	2nxq	
45	$[C_{SH}S_p\,C_{DH}^{-1}\,K_p] = [C_{SH}S_p]\,[C_{DH}^{-1}\,K_p]$	2nxj	
46	$[\sigma_2] = [C_{SH}\,S_p\,C_{DH}^{-1}\,K_p]\,[\delta_2]$	2nxq	
47	$[\sigma] = [\sigma_1] - [\sigma_2]$	2nxq	Output
48	$[m] = [m_1] - [m_2]$	2nxq	Output
49	$[\delta] = [\delta_1] - [\delta_2]$	jxq	Output

The above sequence has been programmed for the IBM 704 digital computer. The program has been made applicable to a structure composed of any number of plates up to 24 by adding to the input data the number of plates, n, number of interior joints, j, and the number of loading conditions, q. The program then computes the necessary addresses and storage space required for the matrix sizes involved in the analysis. Numerous examples have been solved using the computer. As an illustration of the above procedure a simple example is given in Appendix I in which numerical values are given only for the input matrices and the final answers for $\underline{\sigma_1}$, $\underline{m_1}$, $\underline{\delta_1}$, $\underline{\sigma}$, $\underline{m}$, and $\underline{\delta}$.

CONCLUSIONS

A matrix procedure has been developed for the determination of longitudinal stresses, transverse moments, and vertical deflections in the typical case of a simple span folded plate structure with free longitudinal edges. However, the method can be applied, with proper modifications, to cases involving other boundary conditions. Certain modifications are also necessary when the structure contains interior vertical plates. Advantage may also be taken of symmetry or antisymmetry, in cases where they exist, to decrease the amount of computation. Some of the advantages of the matrix procedure developed are as follows:

1. It can be readily programmed for a digital computer.
2. The basic matrices are functions only of the geometry and dimensions of the folded plate structure cross section and the modulus of elasticity. Thus they need not be recomputed for each different loading condition.
3. The analysis of the plate system and the slab system are separated so that the effect of changes in slab thickness or in span length for a particular cross section can be studied.

The folded plate equations, which were developed in matrix form in this paper, are based on the simplifying assumptions regarding slab and longitudinal

plate behavior generally used in this type of analysis. A more precise analysis based on the theory of elasticity can also be developed in matrix form.

ACKNOWLEDGMENTS

The author wishes to express his sincere appreciation to his colleagues Frank Baron and Ray Clough for their critical review of the paper.

APPENDIX I

The following example illustrates the analysis of a folded plate roof subjected to vertical joint loads that have a uniform distribution in the longitudinal direction. The procedure used is that described in the section on "Combined Plate and Slab System; Non-Harmonic Loading." Numerical values are

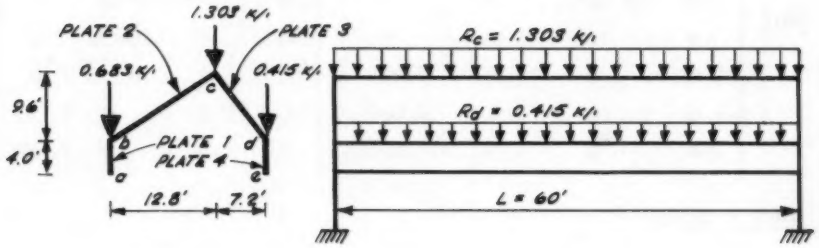

FIG. 11.—DIMENSIONS AND LOADING OF FOLDED PLATE ROOF

only given for input and final answer matrices and kip and feet units are used throughout. In this example there are four plates (n = 4), three interior joints (j = 3), and one loading condition (q = 1).

Dimensions and Loading.—simple span L = 60 ft, plate thickness b = 4 in. = 1/3 ft for all plates, modulus of elasticity E = 432 x 10^3 ksf.

Input Matrices:—

Step 1: $\underline{B}$ in Eq. 5 $\underline{P} = \underline{B}\,\underline{R}^p$

$$[B] = \begin{bmatrix} B_{1b} & 0 & 0 \\ B_{2b} & B_{2c} & 0 \\ 0 & B_{3c} & B_{3d} \\ 0 & 0 & B_{4d} \end{bmatrix} = \begin{bmatrix} -1.00 & 0 & 0 \\ 0 & -0.60 & 0 \\ 0 & +0.80 & 0 \\ 0 & 0 & +1.00 \end{bmatrix}$$

Steps 2 and 3: $\underline{S_N}$ and $\underline{S_O}$ in Eq. 9 $\underline{\sigma} = C_s \left[\underline{S_O}\ \underline{P} + \underline{S_N}\ \left(\underline{N/C_S}\right) \right]$

$$\left[S_N\right] = \begin{bmatrix} (2/bd)_1 & 0 & 0 \\ (4/bd)_1 & 0 & 0 \\ (4/bd)_2 & (2/bd)_2 & 0 \\ (2/bd)_2 & (4/bd)_2 & 0 \\ 0 & (4/bd)_3 & (2/bd)_3 \\ 0 & (2/bd)_3 & (4/bd)_3 \\ 0 & 0 & (4/bd)_4 \\ 0 & 0 & (2/bd)_4 \end{bmatrix} = \begin{bmatrix} 1.500 & 0 & 0 \\ 3.000 & 0 & 0 \\ 0.750 & 0.375 & 0 \\ 0.375 & 0.750 & 0 \\ 0 & 1.000 & 0.500 \\ 0 & 0.500 & 1.000 \\ 0 & 0 & 3.000 \\ 0 & 0 & 1.500 \end{bmatrix}$$

$$\left[S_o\right] = \begin{bmatrix} (6/bd^2)_1 & 0 & 0 & 0 \\ 6/bd^2)_1 & 0 & 0 & 0 \\ 0 & (6/bd^2)_2 & 0 & 0 \\ 0 & (6/bd^2)_2 & 0 & 0 \\ 0 & 0 & (6/bd^2)_3 & 0 \\ 0 & 0 & (6/bd^2)_3 & 0 \\ 0 & 0 & 0 & (6/bd^2)_4 \\ 0 & 0 & 0 & (6/bd^2)_4 \end{bmatrix} = \begin{bmatrix} 1.125 & 0 & 0 & 0 \\ 1.125 & 0 & 0 & 0 \\ 0 & 0.070312 & 0 & 0 \\ 0 & 0.070312 & 0 & 0 \\ 0 & 0 & 0.125 & 0 \\ 0 & 0 & 0.125 & 0 \\ 0 & 0 & 0 & 1.125 \\ 0 & 0 & 0 & 1.125 \end{bmatrix}$$

Step 4: ADRO

$$\left[\text{ADRO}\right] = \begin{bmatrix} 0 & 1 & 1 & 0 & 0 & 0 & 0 & 0 \\ 0 & 0 & 0 & 1 & 1 & 0 & 0 & 0 \\ 0 & 0 & 0 & 0 & 0 & 1 & 1 & 0 \end{bmatrix}$$

Steps 5 and 6: $\underline{F_N}$ and $\underline{F_O}$ in Eq. 20 $\underline{v} = C_D \left[\underline{F_O}\ \underline{P}\ +\ \underline{F_N}\ \left(\underline{N/C_S}\right) \right]$

$$\left[F_N\right] = \begin{bmatrix} (6/bd^2E)_1 & 0 & 0 \\ (6/bd^2E)_2 & (6/bd^2E)_2 & 0 \\ 0 & (6/bd^2E)_3 & (6/bd^2E)_3 \\ 0 & 0 & (6/bd^2E)_4 \end{bmatrix} = \begin{bmatrix} 2.604166 & 0 & 0 \\ 0.162759 & 0.162759 & 0 \\ 0 & 0.289352 & 0.289352 \\ 0 & 0 & 2.604166 \end{bmatrix} \times 10^{-6}$$

$$[F_o] = \begin{bmatrix} (12/bd^3E)_1 & 0 & 0 & 0 \\ 0 & (12/bd^3E)_2 & 0 & 0 \\ 0 & 0 & (12/bd^3E)_3 & 0 \\ 0 & 0 & 0 & (12/bd^3E)_4 \end{bmatrix}$$

$$= \begin{bmatrix} 1.302083 & 0 & 0 & 0 \\ 0 & 0.020345 & 0 & 0 \\ 0 & 0 & 0.048225 & 0 \\ 0 & 0 & 0 & 1.302083 \end{bmatrix} \times 10^{-6}$$

Steps 7 and 8: $\underline{K_\theta}$ and $\underline{K_\delta}$ in Eq. 27 $\underline{m} = \underline{K_\theta}\ \underline{\theta} + \underline{K_\delta}\ \underline{\delta}$

$$[K_\theta] = \begin{bmatrix} (b^3E/6d)_1^* & 0 & 0 \\ (b^3E/3d)_1^* & 0 & 0 \\ (b^3E/3d)_2 & (b^3E/6d)_2 & 0 \\ (b^3E/6d)_2 & (b^3E/3d)_2 & 0 \\ 0 & (b^3E/3d)_3 & (b^3E/6d)_3 \\ 0 & (b^3E/6d)_3 & (b^3E/3d)_3 \\ 0 & 0 & (b^3E/3d)_4^* \\ 0 & 0 & (b^3E/6d)_4^* \end{bmatrix} = \begin{bmatrix} 0 & 0 & 0 \\ 0 & 0 & 0 \\ 333.333 & 166.666 & 0 \\ 166.666 & 333.333 & 0 \\ 0 & 444.444 & 222.222 \\ 0 & 222.222 & 444.444 \\ 0 & 0 & 0 \\ 0 & 0 & 0 \end{bmatrix}$$

$$[K_\delta] = \begin{bmatrix} (b^3E/2dh)_1^* & 0 & 0 \\ (b^3E/2dh)_1^* & 0 & 0 \\ -(b^3E/2dh)_2 & (b^3E/2dh)_2 & 0 \\ -(b^3E/2dh)_2 & (b^3E/2dh)_2 & 0 \\ 0 & -(b^3E/2dh)_3 & (b^3E/2dh)_3 \\ 0 & -(b^3E/2dh)_3 & (b^3E/2dh)_3 \\ 0 & 0 & -(b^3E/2dh)_4^* \\ 0 & 0 & -(b^3E/2dh)_4^* \end{bmatrix} = \begin{bmatrix} 0 & 0 & 0 \\ 0 & 0 & 0 \\ -39.0625 & 39.0625 & 0 \\ -39.0625 & 39.0625 & 0 \\ 0 & -\ 9.25926 & 9.25926 \\ 0 & -\ 9.25926 & 9.25926 \\ 0 & 0 & 0 \\ 0 & 0 & 0 \end{bmatrix}$$

The values marked with an asterik are zero for a cantilever span.

Step 9: $\underline{H}$ in Eq. 33 $\underline{R^S} = \underline{H}\,\underline{m}$

$$[H] = \begin{bmatrix} 1/h_1^* & 1/h_1^* & -1/h_2 & -1/h_2 & 0 & 0 & 0 & 0 \\ 0 & 0 & 1/h_2 & 1/h_2 & -1/h_3 & -1/h_3 & 0 & 0 \\ 0 & 0 & 0 & 0 & 1/h_3 & 1/h_3 & -1/h_4^* & -1/h_4^* \end{bmatrix}$$

$$= \begin{bmatrix} 0 & 0 & -0.078125 & -0.078125 & 0 & 0 & 0 & 0 \\ 0 & 0 & 0.078125 & 0.078125 & -0.138889 & -0.138889 & 0 & 0 \\ 0 & 0 & 0 & 0 & 0.138889 & 0.138889 & 0 & 0 \end{bmatrix}$$

Step 10: $C_{SH} = L^2/\pi^2 = 364.756$

$C_{SW} = L^2/8 = 450.000$

Step 11: $C_{DH} = L^4/\pi^4 = 133047$

$C_{DW} = 5L^4/384 = 168750$

Step 12: $\underline{R}$ = load matrix

$$\begin{bmatrix} R_b \\ R_c \\ R_d \end{bmatrix} = \begin{bmatrix} 0.683 \\ 1.303 \\ 0.415 \end{bmatrix}$$

C. Final answers.

Steps 37 and 47: Longitudinal Stresses

$$\begin{bmatrix} \sigma_{1ab} \\ \sigma_{1ba} \\ \sigma_{1bc} \\ \sigma_{1cb} \\ \sigma_{1cd} \\ \sigma_{1dc} \\ \sigma_{1de} \\ \sigma_{1ed} \end{bmatrix} = \begin{bmatrix} -194.17 \\ -\ 42.57 \\ 42.57 \\ -\ 3.81 \\ 3.81 \\ -\ 17.04 \\ 17.04 \\ 113.57 \end{bmatrix} \qquad \begin{bmatrix} \sigma_{ab} \\ \sigma_{ba} \\ \sigma_{bc} \\ \sigma_{cb} \\ \sigma_{cd} \\ \sigma_{dc} \\ \sigma_{de} \\ \sigma_{ed} \end{bmatrix} = \begin{bmatrix} -175.66 \\ -\ 33.43 \\ 33.43 \\ -\ 12.16 \\ 12.16 \\ -\ 1.04 \\ 1.04 \\ 80.79 \end{bmatrix}$$

Steps 41 and 48: Transverse moments

$$\begin{bmatrix} m_{1ab} \\ m_{1ba} \\ m_{1bc} \\ m_{1cb} \\ m_{1cd} \\ m_{1dc} \\ m_{1de} \\ m_{1ed} \end{bmatrix} = \begin{bmatrix} 0 \\ 0 \\ 0 \\ -1.199 \\ 1.199 \\ 0 \\ 0 \\ 0 \end{bmatrix} \quad \begin{bmatrix} m_{ab} \\ m_{ba} \\ m_{bc} \\ m_{cb} \\ m_{cd} \\ m_{dc} \\ m_{de} \\ m_{ed} \end{bmatrix} = \begin{bmatrix} 0 \\ 0 \\ 0 \\ -0.869 \\ 0.869 \\ 0 \\ 0 \\ 0 \end{bmatrix}$$

Steps 39 and 49: Vertical joint deflections

$$\begin{bmatrix} \delta_{1b} \\ \delta_{1c} \\ \delta_{1d} \end{bmatrix} = \begin{bmatrix} 0.05138 \\ -0.00303 \\ 0.02834 \end{bmatrix} \quad \begin{bmatrix} \delta_{b} \\ \delta_{c} \\ \delta_{d} \end{bmatrix} = \begin{bmatrix} 0.04554 \\ -0.00010 \\ 0.01805 \end{bmatrix}$$

APPENDIX II.—NOTATION

An underlined symbol represents a matrix.

b = plate thickness;

d = plate depth between longitudinal edges;

h = horizontal projection of plate depth d;

m = transverse slab moment at a plate edge;

n = number of plates;

j = number of interior joints;

q = number of loading conditions;

v = plate displacement (parallel to a plate);

x = distance from a support along length of plate;

C_D = deflection constant;

C_S = stress constant;

E = modulus of elasticity;

I_p = moment of inertia of a plate = $bd^3/12$;

I_s = moment of inertia of a unit width of slab = $b^3/12$;

L = longitudinal span;

M_p = total plate moment;

M_o = plate moment due to P alone;

N = summation of plate longitudinal edge shear T;

P = plate load (parallel to a plate);

Q_o = plate end reaction due to P alone;

R = vertical joint load taken by combined plate and slab system;

R^p = vertical joint load taken by plate system;

R^s = vertical joint load taken by slab system;

T = longitudinal shear per unit length along plate edge;

V_o = plate shear force due to P alone;

δ = vertical joint deflection;

σ = longitudinal stress at the plate edge; and

θ = joint rotation in transverse slab system.

Journal of the
STRUCTURAL DIVISION
Proceedings of the American Society of Civil Engineers

TEST OF A RIVETED PLATE GIRDER WITH A THIN WEB

By Desi D. Vasarhelyi,[1] M. ASCE, Jim C. Taylor,[2]
Naresh C. Vasishth,[3] and Chia-Yao Yuan[4]

SYNOPSIS

A detailed record of the experimental results obtained from tests on a full-size riveted plate girder with a web plate thinner than that required under the present design specifications is reported herein.

Both the web-buckling phenomenon and the diagonal-tension phenomenon of the web plate under load were carefully observed. Comparison was then made between the computed buckling loads and the values determined from experimental data. Particular emphasis was laid on the behavior of the web after being loaded beyond the conventionally termed "buckling load", with a view to evaluating the importance of the buckling of the web with respect to practical design. Study was also made on the change in the shear-carrying behavior of the web after buckling occurred and on the ability of the web to withstand loads in excess of the buckling value.

Note.—Discussion open until March 1, 1961. Separate discussions should be submitted for the individual papers in this symposium. To extend the closing date one month, a written request must be filed with the Executive Secretary, ASCE. This paper is part of the copyrighted Journal of the Structural Division, Proceedings of the American Society of Civil Engineers, Vol. 86, No. ST 10, October, 1960.

[1] Assoc. Prof. of Civ. Engrg., Univ. of Washington, Seattle, Wash.
[2] Engr., Dominion Bridge Co., Vancouver, B. C., Canada.
[3] Engr., Moffett, Nichol and Taylor, Portland, Ore.
[4] Engr., Star Iron and Steel Co., Tacoma, Wash.

The behavior of the flanges of this girder was also carefully observed and the results are reported herein. Particular emphasis has been given to the stress distribution in the region of the cover plate cutoffs.

INTRODUCTION

Object and Scope.—This test was conducted primarily to investigate the effect of a thin web on the load-carrying capaicty of a plate girder. A reasonable amount of information was also obtained concerning the behavior of the built-up flanges.

The test specimen, with the exception of the thin web, was typical of many of the riveted plate girders in common use. Much of the testing procedure was governed by the behavior of the web. At the conclusion of the test, selected sections of the flange were cut from the girder and examined. Saw cuts were made through the rivets at various sections of the flange. Inspection of these exposed rivets helped to interpret some of the information gathered during the testing procedure.

Buckling of the Web Plate.—As shown in some earlier research, (10), (11),[5] and in observations made in this experiment, the web plate of a plate girder does not behave exactly in the same manner as a theoretical, flat rectangular plate of the same material and dimensions, when being loaded to the critical buckling stress.

The theoretical buckling stress of a flat plate is defined as the stress at which an exchange of stable equilibrium configurations occurs between the straight and the slight bent form. It marks the region in which continued application of load results in an accelerated growth of deflections perpendicular to the plane of the plate. Its importance lies in the fact that buckling initiates the physical processes that lead to the eventual failure of the plate (3).

In comparison with the theoretical, flat rectangular plate previously mentioned, the web plate of a plate girder behaves quite differently when the girder is under load. Because it is impossible, under ordinary fabrication conditions, to keep the web plate absolutely flat, the presence of small initial curvature will cause the web to deflect laterally as soon as the load is applied. The rate of deflection increases as the load increases until a point is reached at which the rate of deflection begins to decrease. Physically, this point marks the transition from a shear resistant web to a diagonal tension web.

If we assume, for the purpose of approximation, that the web plate is free from initial imperfection, then the web plate must be approaching a state of instability when this occurs; otherwise, the change in the shear resisting behavior in the web would not have resulted. We can, therefore, say that the load at this point is synonymous to the buckling load of the web.

Accordingly, in describing the significance of the buckling load of the web plate of a plate girder, we can say that it represents the point of transition in the shear-carrying action of the web from a state of pure shear resistance to a state of incomplete diagonal tension.

Method of Estimation of the Buckling Load by Using the Theoretical Formulas.—Due to the indeterminate nature of the edge restraint on the web plate

[5] Numbers in parentheses refer to references listed in the Bibliography. See Appendix.)

that is developed in the riveted connection between the flange angles and the web plate, and between the vertical stiffeners and the web, and because of the complexities of the bending and shearing stress distribution along the four edges of the web plate, there does not seem to be an exact analytical method for computing the buckling load of the web plate of a plate girder.

According to Timoshenko, (1), (9), the web-plate buckling can be analyzed by considering the following three cases of loading:

a. Near the supports, the shearing force is the most important factor; the part of the web between the two stiffeners can be considered as a rectangular plate subjected to the action of uniform shear;

b. At the middle of the span of the plate girder, the shearing stresses can be neglected in comparison with the normal stress; then the part of the web between two stiffeners is in a condition of pure bending;

c. In the intermediate cross sections, there is a combination of normal and shearing forces.

As to the supporting conditions at the boundary, we can tell by intuition that it must be an intermediate case between simply-supported edges and clamped edges. Timoshenko suggested that for design purposes all four edges of the web plate could be considered as freely supported, because this boundary condition would yield a more conservative result and hence insure that the design was safe.

The assumption that the bending stress is constant between two stiffeners at the edges of the plate is a further simplification, since these stresses vary along the girder with the bending moment. However, to permit a solution of the buckling problem without undue complication of the analysis, the simplification of the loading condition is the first step necessary in dealing with the stability of the web plates in a plate girder.

General Formulae for the Buckling Stress.—This discussion will be confined to the critical stresses for elastic buckling. The general expression for theoretical buckling stresses of a flat rectangular plate under various types of loadings and different boundary conditions can be given as

$$\sigma_{cr} \left(\text{cr}\, \tau_{cr} \right) = K \frac{\pi^2 E}{12\left(1-\mu^2\right)} \left(\frac{t}{b}\right)^2 \quad \ldots\ldots\ldots\ldots (1)$$

in which σ_{cr} is the critical bending stress, τ_{cr} refers to the critical shearing stress, t denotes the thickness of the plate, b is the width of the plate, and K denotes the elastic buckling coefficient. The value of the elastic buckling coefficient, (K), is dependent upon the aspect ratio, the type of loading, and the condition of restraint along the edges. Numerical values of the elastic buckling coefficients, (K), for various loading and boundary conditions were computed, and tables giving values of K corresponding to certain ranges of the aspect ratios of the plate are available. However, due to the large variety of cases of loading and boundary conditions, the information is by no means complete. Values of K, covering various cases of loading and boundary conditions, are given by Bleich (2). For plates subjected to uniform shearing stress on four edges only, Paul Kuhn, (4), gives an empirical formula.

The Post-Buckling Phenomenon.—The post-buckling behavior of the web plate of a plate girder was explained by Paul Kuhn and others in the theory of

incomplete diagonal tension in a series of papers published by the National Advisory Council on Aeronautics (NACA), (4),(5),(6),(7),(8),(39).

As the applied load increases and buckling occurs, the principal tensile stresses increase rapidly and undertake to carry most of the additional shear in truss action, while the principal compressive stresses increase at a much slower rate. This state of stress in the web plate is called incomplete diagonal tension, because a part of the additional shearing force is still carried by the shear action due to the continued increase in the principal compressive force; however, most of the additional shear is carried by the truss action.

The main physical characteristic of the diagonal tension action that can be observed in the web plate is the formation of diagonal buckles. The process of buckle formation is accompanied by the appearance and development of axial stresses in the stiffeners. This is due to the fact that the truss action in the web plate produces vertical and horizontal components of compressive stresses in the direction of the stiffeners as well as the flanges. The vertical compression is assumed to be resisted by the stiffener together with a certain effective width of the web. This accounts for the appearance of axial compressive stresses in the stiffeners at the buckling of the web plate. In the same manner, the diagonal tension may produce some secondary compressive stresses in the flanges.

Determination of Flange Stresses.—The analysis of flange stresses in a riveted plate girder is complicated by the fact that the girder is not a solid beam, but is composed of components that are connected by an elastic medium, namely, the rivet. Both the elastic properties of the rivet, and the rivet hole itself, affect the distribution of stresses in the beam in a somewhat uncertain manner. The solution of the problem in the past has been to treat the girder as a solid beam, and to adopt one of the standard procedures for determining the flange stresses. The rate at which stress builds up in the ends of the cover plates does not seem to be fully understood, as a result of which there are several opinions as to how far cover plates should extend past their theoretical cutoff points.

DESCRIPTION OF SPECIMEN AND TEST

Design of Specimen.—The design, workmanship, and material of this girder was in compliance with current American Assn. of State Highway Officials (AASHO) specifications, with several exceptions. For one half of the girder a 1/4-in. web was used, while on the other half, the web thickness was 5/16-in. The spacing of the vertical stiffeners has been so determined that buckling will occur sequentially during the test, rather than maintaining a spacing to comply with the specifications. Based on the expected buckling loads for the web, the flanges were designed for a total two-point load of 350 kips at basic design stresses. In computing the resisting moment of the section, the net section was used with rivet holes in both flanges deducted. Since the top flange was to be fully supported, the compression stress in the top flange did not govern the design. At the end of the girder, with 1/4-in. thick web, the cover plates were extended 12 in. past their theoretical cutoff points. At the other end, with 5/16-in. thick web, they were extended far enough to accommodate a sufficient number of rivets to develop the computed initial force that the plate had to support at the theoretical cutoff point. The general dimensions and properties of the girder cross section are shown in Table 1.

Description of Test.—The girder was tested in the 2,400,000-lb Baldwin testing machine at the University of Washington, Seattle, Wash. The general arrangement of the test is illustrated in Fig. 2. The top flange of the girder was supported by bracing frames at seven points along its length, while the bottom flange was supported at the ends and at the center line.

The location of all strain gages is shown in Fig. 1. Seventy type A-11 SR4 gages were used. Strain gages on the stiffeners were placed at mid-height on the edge of the outstanding leg of the stiffener angles. These gages were placed at symmetrical positions so that by averaging the readings in the two gages, any possible bending effect present in the stiffeners could be eliminated, thus leaving only the axial strains.

TABLE 1.—GENERAL PROPERTIES OF THE GIRDER

Specification	AASHO
Material	ASTM A-7 Steel (Rivets—ASTM A-141)
Length	56 ft - 0 in. c. to c. end brgs. (56 ft - 7 in. overall)
Depth	6 ft - 2 1/2 in. b. to b. of angles
Flange	2-L^S 6 in. x 6 in. x 3/4 in., 3 cover plates : 14 in. x 1/2 in.
Length of cover plates	1. 38 ft - 8 1/4 in. 2. 31 ft - 5 in. 3. 23 ft - 10 1/4 in.
Web	1/4 in. x 74 in. and 5/16 in. x 74 in.
Intermediate stiffeners	2-L^S — 3 1/2 in. x 5 in. x 3/8 in.
Yield stress	Web 41.4 ksi Angles 36.9 ksi Cover Plates 39.4 ksi } [a]
Dead weight	Approx. 20^k
Working load	350^k total for two-point loading @ 14 ft - 0 c. to c. load
Moment of inertia (in^4)	Gross: 111,677; 90,930; 70,717; 51,029 Net: 95,700; 77,547; 59,860; 42,634
Rivets	3/4 in ϕ: holes subpunched 11/16 in. ϕ, Reamed 13/16 in ϕ

[a] From coupon tests as shown in Table 2.

Vertical deflection gages were placed along the bottom of the girder, at mid-span, at stiffener points and at each end of the girder. The gages used were 1/1000-in. dial gages; the general arrangement is shown in Fig. 1. The two deflection gages at each end of the girder served to indicate any settlement of the supports.

For the measurement of lateral deflections of the web, a special fixture was used to hold the dial gages against the web. Both 1/10,000-in. and 1/1000-in. dial gages were used.

At three selected points, 0.0001-in. dial gages were mounted directly to the flange to measure the "slip" or relative motion at the ends of a cover plate.

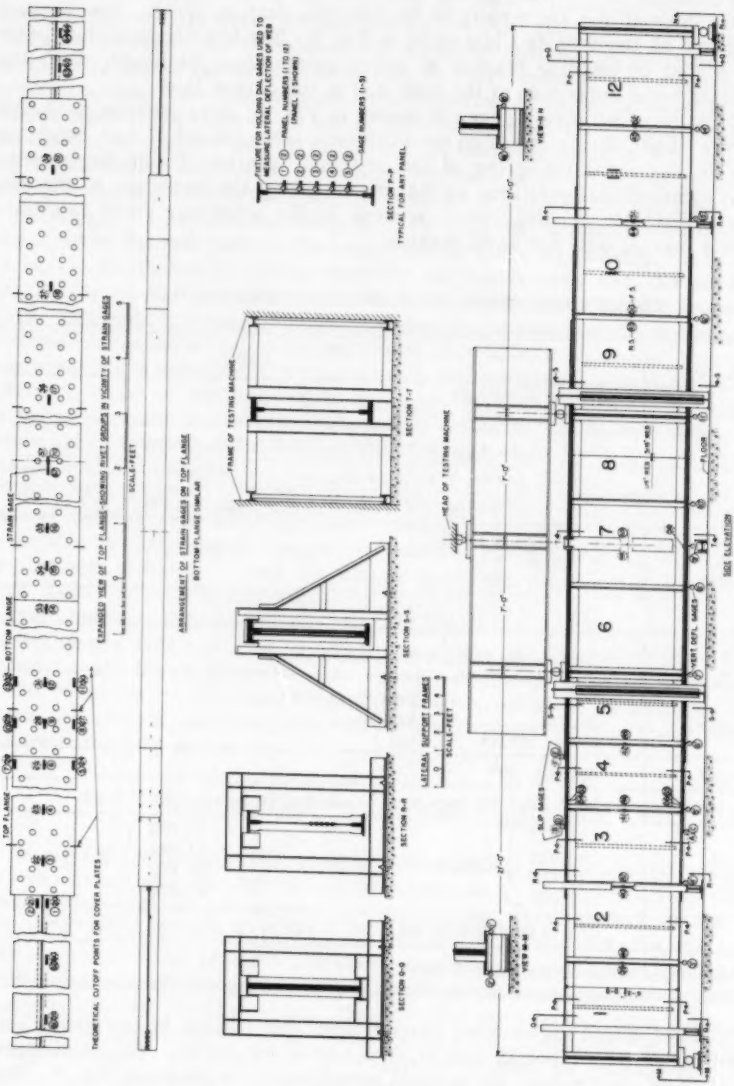

FIG. 1.—GENERAL SETUP OF THE TESTS

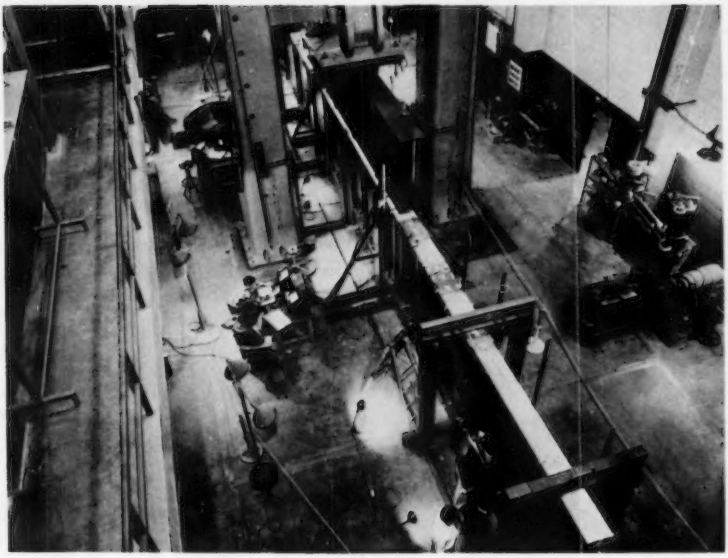

FIG. 2.—GENERAL SETUP OF THE TEST

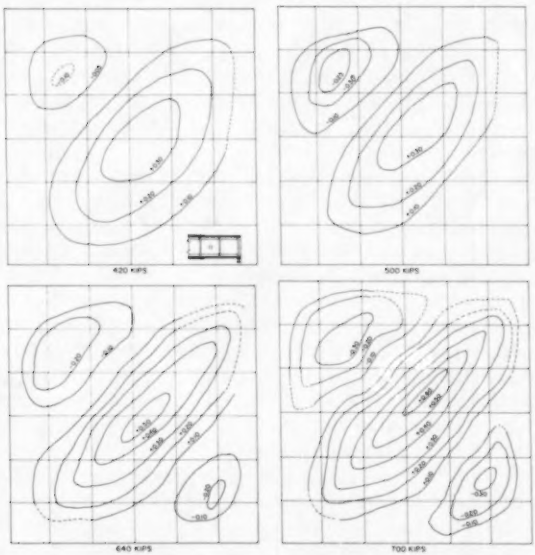

FIG. 3.—CONTOUR PLOTS SHOWING DEFLECTED SHAPES OF THE WEB IN PANEL 11 UNDER VARIOUS APPLIED LOADS

These gages were mounted in pairs, one gage on each side of the cover plate. The top flange and one side of the girder was sprayed with a coat of "white-wash", so that yielding at any point could readily be detected.

To obtain the contour plot of the deflected shape of the web, a photographic method was used (42). Samples of contour plots thus obtained are shown in Fig. 3.

Test Procedure.—In general, load was applied to the beam in 20-kip increments, and all gages were read immediately after each increment was added. The maximum load applied was increased by 60 kips each day a test was run, except when certain panels of the web buckled to the extent that yielding was indicated and had to be stiffened before more load could be added. Loading was continued in this manner until a maximum load of 740 kips was applied. At this load, it became apparent that the capacity of the web was reached, and since yielding was also observed at many places along the flange, no further load was added. The girder was, however, tested in the working range (0-350 kips) after being subjected to the maximum load.

Observation of web deflection was concentrated first on the end panels and the rest of the 1/4-in. web panels. In order to measure very small deflections at small loads, the 1/10,000-in. dial gages were used first; when the deflection became larger, 1/1000-in. dial gages were substituted. Occasionally the loading was removed in order to check for any residual deflection in the plate.

In order to make sure that the point of maximum deflection of the web panel had been detected, the measuring fixture with five dial gages was used first. The five dial gages measured the deflections at five equidistant points (including the one at the center) along the vertical line at the middle of the panel. When plotting the deflections along the vertical center line of the panel to scale, it would be apparent where the point of maximum deflection was located. It was found that this point was usually very close to the center of the panel. When the diagonal tension action appears in the web plate, the point of maximum deflection shifts slightly from the center position. In order to catch the maximum point, two or three dial gages were placed around the center of the panel at an estimated distance of 2 in. to 3 in. apart. This method usually took care of the shifting of the maximum point.

Due to the different thicknesses of the web plates, failure of the thinner web would most probably cause the failure of the beam as a whole, and thus, there would be no opportunity to observe the yielding of the thicker web plates. In order to avoid such an early failure of the girder, failure of the weaker panels was prevented by the addition of bolted stiffeners in the panels concerned. The angles used for the stiffeners were of the same cross sections as the intermediate stiffeners (5 in. x $3\frac{1}{2}$ in. x 3/8 in.) and were 62 in. long, so that they fit in between the top edge of the bottom flange angle and the bottom edge of the top flange angle, with a clearance of 1/4-in. on each end. One pair of stiffener angles was attached to each side of the web plate with 3/4-in. high tension bolts which had the same spacing as the rivets on the intermediate stiffeners. The bolts were tightened by the one-half turn method.

At the completion of the test, selected portions of the flange were cut from the girder and saw cuts were made through the rivets. The clearance between the rivets and the holes was measured and some rivets were removed for inspection. The clamping force exerted by the rivets was also measured by placing a strain gage on the rivet before removing it from the flange.

Correlation of Stress and Strain.—The measurement of strain in a structure is very easily and exactly accomplished through the use of the SR-4 strain

gage; however, relating this strain to stress often is not so straightforward. In the case of a riveted structure, biaxial and triaxial stress conditions are known to exist in the region of the rivet holes, although at points away from the rivets a uniaxial stress field is approached. However, even if the gages were located far enough from the rivets to be in a field of uniaxial stress, there would be some doubt as to what gages located on the net section, through a row of rivets, measured in terms of the average stress or strain on that section. There would also be some doubt as to how far from a rivet the stress disturbances extended.

To establish a correlation between the measured strain and the average stress on a section, a specimen having the same dimensions and hole pattern as a typical section from the girder cover plates was tested under axial tension. By locating gages on this test specimen at the same relative position as on the girder cover plates, a relation between the average stress in the plate and the measured strain was obtained.

All graphs and curves presented herein are plotted on the basis of strain. In general, however, the equivalent stress, in kips per square inch across the gross section, can be obtained approximately by taking 3% of the strain in micro inches per inch. Where theoretical lines or curves have been shown for comparison with the experimental results, a modulus of 30,000 ksi has been assumed.

The dead load of the girder has been taken into account by converting it to an equivalent applied load and adding it to the load applied through the testing machine. Where the term "total load" is given herein the previous conversion has been included.

TEST RESULTS

Behavior of Web Plates Under Loadings Below their Buckling Loads.—It was noticed from the beginning of the tests that the web plates of the plate girder started to deflect as soon as the load was applied. This might be due to the presence of initial curvature in the web plates, which could hardly be avoided during the manufacturing procedure. Table 2 shows the values of these initial deflections as measured prior to the application of any load to the girder. However, the direction of the lateral deflection of the web plate did not necessarily follow the direction of the initial curvature.

Behavior of Web at Buckling Load.—As explained earlier, the so-called buckling load of the web plate of the plate girder can be regarded as the transition load under which there appears a change in the manner in which the shear in the panel is carried, that is the change from a shear resisting web to a diagonal tension web. For this reason, a characteristic change in the deflected surface of web began to take place at the buckling load. The web deflected in a dish. like surface at smaller loads. When the load was increased, and approached the buckling load of the panel, diagonal buckles were formed. The inclination of the buckle, which depended on the proportion of the panel, generally made a 45° to 50° angle with the longitudinal axis of the girder.

The magnitude of the lateral deflection of the web at the buckling load depended on the aspect ratio and the position of the panel. The measured deflections ranged from 45% to 85% of the thickness of the plate. A list of the buckling loads and the corresponding web deflections is shown in Table 3. (See also Figs. 4(a) and 4(b)). Residual deflections in web plates after unloading (Table

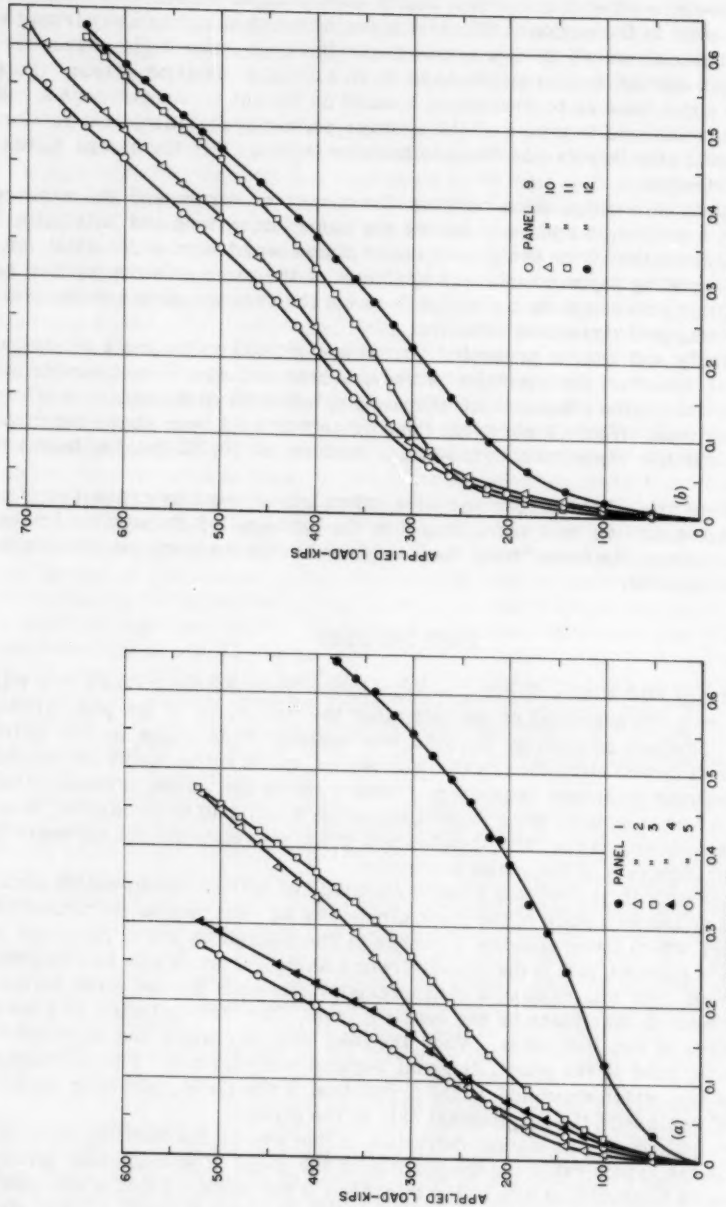

FIG. 4.—TOTAL APPLIED LOAD ON GIRDER VERSUS LATERAL DEFLECTION OF WEB

2) were generally under one hundredth of an inch and were therefore less than the initial deflections.

Web Behavior at Allowable Load of the Girder.—The allowable load of the girder was computed as 350 kips, based on the allowable stress of 18 ksi (AASHO specification), since the compression flange of the girder was completely supported against lateral deflection.

It can be seen from the list of buckling loads in Table 3 that the allowable load of 350 kips is about 25% higher than the buckling loads of panels 1 to 5 (the 1/4-in. thick webs) and is above or close to the buckling loads of panels 9 to 12 (the 5/16-in. webs). The behavior of the web plates is described separately.

TABLE 2.—INITIAL DEFLECTIONS IN THE WEBS AND RESIDUAL DEFLECTIONS AT DIFFERENT STAGES OF LOADING

Panel No.	Initial Deflection in.	Residual Deflection after Removal of Load				
		Buckling Load (k)	δ (in.)	Residual Deflection at allowable load of 350k (in.)	Max. Test Load (k)	δ (in.)
(1)	(2)	(3)	(4)	(5)	(6)	(7)
1	−0.095	130	+0.006	+0.008	450	+0.044
2	−0.045	260	0	−0.002	480	+0.022
3	+0.040	260	+0.002	+0.006	500	+0.028
4	+0.066	280	+0.002	+0.004	490	+0.004
5	+0.062	280	0	0	520	+0.030
9	+0.073	360	0	0	640	−0.007
10	+0.048	350	0	0	640	−0.012
11	−0.069	320	0	0	620	−0.033
12	−0.072	260	0	0	620	−0.085

Notes: + sign indicates deflection towards the west side of the girder.
− sign indicates deflection towards the east side of the girder (the whitewashed side).

Panels 1 to 5.—Observation of the buckling pattern of the web plates indicated that the diagonal tension effect had fully developed in the webs. The lateral deflections in the web plates ranges from 64% to 121% of the thickness of the web plate. Panel 1 had the maximum deflection of 0.303 inches. However, the residual deflections after removal of the load was still within 0.01 inch. This indicated that no yielding of the web plate had taken place. An inspection of the web of flange and web to stiffener connections did not reveal any damage in this area.

Panels 9 to 12.—Lateral deflection in webs ranged from 43% to 91% of the thickness of the plate (5/16-in.). The largest deflection, which amounted to 0.285 in., was in the end panel (panel 12). Web plates were still found to be elastic upon removal of the load.

As a whole, it can be concluded that, the girder performed satisfactorily under the allowable load. Although the deflections at the end panels were close to or above 100% of the web thickness, the magnitude of the actual deflections seemed to be still tolerable. A list of the web deflections at the allowable load is given in Table 4.

Post-Buckling Behavior of the Webs.—As the applied load was increased beyond the buckling load of a panel, it was observed that the effect of diagonal tension became more and more pronounced. There are two points that are worth noticing.

Contrary to the general concept of buckling, the rate of increase of the lateral deflection of the web became slower, instead of faster, when passing the buckling load. This can be seen in the load-lateral deflection plot (Fig. 4 and

TABLE 3.—COMPARISON OF WEB DEFLECTIONS UNDER BUCKLING LOADS AND YIELDING LOADS

Panel No.	Aspect Ratio	Buckling Load			Maximum Test Load		
		Load (k)	Deflection (in.)	Percentage of web Thickness	Load (k)	Deflection (in.)	Percentage of web Thickness
(1)	(2)	(3)	(4)	(6)	(6)	(7)	(8)
1	0.935	130	0.213	85.2	450	0.712	284
2	0.744	260	0.150	60.0	480	0.423	169
3	0.744	260	0.200	80.0	500	0.454	182
4	0.632	280	0.138	55.2	490	0.283	113
5	0.640	280	0.112	44.8	520	0.270	108
9	0.944	360	0.150	48.1	640	0.492	157
10	0.935	350	0.160	51.3	640	0.531	171
11	0.935	320	0.165	52.9	620	0.587	188
12	0.935	260	0.152	48.7	620	0.595	191

Notes: 1. Loads shown are total applied loads on girder.
2. The buckling loads are determined from the load-deflection curves of the webs.
3. Aspect ratio = $\frac{\text{clear width of the web}}{\text{clear depth of the web}}$.

5) in that the slope of the part of the deflection curve above the buckling load became steeper than that immediately under the buckling load.

Another point is the gradual reorientation of the direction of the inclined buckle due to diagonal tension. As mentioned previously, the plate deflected in a dished surface when the load was relatively small. As the effect of diagonal tension gradually set in, the contour of the deflected surface was seen to elongate towards the direction of the corners, and a main buckle thus formed. This buckle first made an angle of approximately 45° with the longitudinal axis of the girder. As the load was increased the inclination of the buckle was seen to alter, and the angle that the buckle made with the longitudinal axis kept increasing, until finally, at maximum test load, there appeared one large dominate wave running diagonally from corner to corner of the panel.

Illustrations of the elongation of the web deflection contours in the direction of the diagonal can be seen in Fig. 3, for panel 11. It is very apparent that, at the final stage of loading, the main buckles always extend from one corner to the opposite corner of the plate.

The Web Plates at Maximum Test Load.—

The 1/4-in. web.—Due to the thin web and large aspect ratio, panel 1 was the first to show signs of yielding. During the process of loading, there had been no sign of any gradual damage or excessive increment of lateral deflection in the web up to 440 kips. However, when the load was increased from 440 to 460 kips, cracks, which represented Lueders' lines in the plate, showed that localized yielding was beginning at the corner. The Lueders' lines appeared at a distance of approximately $\frac{1}{2}$ it from the upper outside corner of the panel extending from the upper edge of the plate toward the diagonal buckle. They ran perpendicular to the edge of the plate and vanished close to the middle of the buckle. Thus, they formed approximately 45° angles with the diagonal. Since the Lueders' lines appeared in between the loading from 440 to 460 kips, the

TABLE 4.—LATERAL DEFLECTION OF WEB PLATES AT ALLOWABLE LOAD OF GIRDER—350^k

Panel No. (1)	Plate thickness t (in.) (2)	Lateral Deflection (in.) (3)	Percentage t (4)
1	1/4	0.303	121
2	1/4	0.292	117
3	1/4	0.317	127
4	1/4	0.194	77.6
5	1/4	0.159	63.7
9	5/16	0.134	42.9
10	5/16	0.156	50.0
11	5/16	0.222	71.2
12	5/16	0.285	91.3

maximum test load was estimated at 450 kips. The maximum lateral deflection of the web was measured to be 0.712 in. An inspection was made of the rest of the panels, and no other sign of yielding was detected. Stiffener angles were then bolted in the first panel to restrain the buckling.

Tests on panels 2, 3, 4, and 5 were carried out in the same manner. The loading was continued until localized yielding was observed in a panel. Stiffeners were then bolted in the panel and the same loading process was carried on again. Lueders' lines were noticed in the web plates of panels 2 and 3 during the same test run; therefore, these two panels were stiffened at the same time. Panels 4 and 5 showed localized yielding during separate tests and were reinforced with stiffeners. A list of the maximum test loads and the maximum deflections in the plates is given in Table 3.

During the loading, it is interesting to note the following: (a) Localized yielding in the web plates started at the same corresponding positions in each

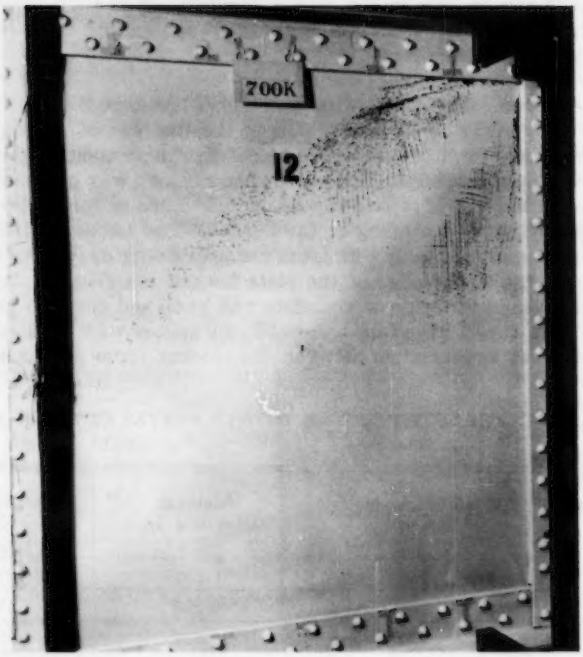

FIG. 5.—THE DIAGONAL BUCKLE AND THE LUEDERS' LINES DEVELOPED IN PANEL 12, AS VIEWED FROM THE EAST SIDE OF THE GIRDER

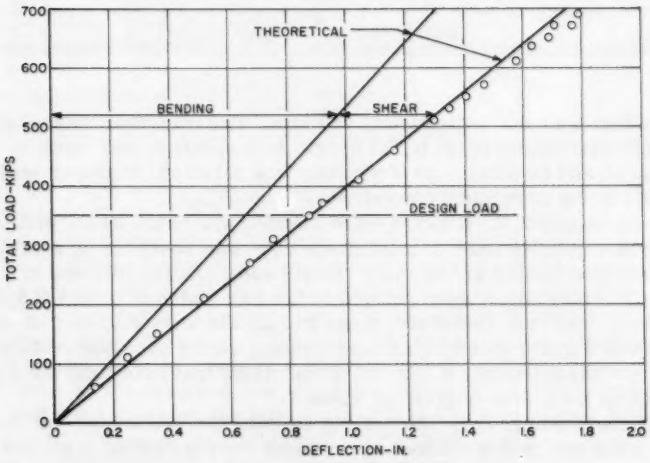

FIG. 6.—VERTICLE DEFLECTION AT MID-LENGTH

panel (that is the upper outer corner) and the Lueders' lines appeared in similar pattern as in panel 1. (b) As shown in Table 3, panels 4 and 5 showed localized yielding under applied loads of 490 kips and 520 kips, after all the panels preceding them were stiffened. Before the stiffeners were in the preceding panels, panels 4 and 5 had been subjected to loadings as high as the above and showed no sign of yielding.

The 5/16-in. web.—The web plates of panels 9, 10, 11, and 12 were of the same thickness (5/16-in.) and approximately the same dimensions. Therefore, it could be expected that these four panels would show signs of yielding at the same load. At a load of 620 kips, yielding in the upper, outer corner of the web, plates appeared in panels 11 and 12. Panel 12 showed distinct Lueders' lines similar to those that occurred before, and only a few spots of paint cracks appeared in panel 11. As the load was increased to 640 kips, the same kind of paint cracks were found at identical corners of panels 9 and 10. As the load was further increased, more distinct Lueders' lines developed at the corners of panels 9, 10, 11. The maximum deflections and residual deflections after the removal of the load are also shown in Table 3.

In order to observe the crippling of the web panel, the girder was further loaded in 20-kip increments from 640 kips to 700 kips and finally to 740 kips. At loadings from 640 to 680 kips, there was only gradual multiplication of Lueders' lines at the corners of the web plates. When loading was increased from 680 to 700 kips, noticeably large deformations took place in panel 12. A deep buckle suddenly developed along the diagonal of the panel, and the two minor buckles on each side of the principal diagonal buckle deepened more appreciably. The shape of the main diagonal buckle is shown in Fig. 5. It can be seen that yield lines ran both in the vertical and horizontal directions along the two sides of the ridge formed by the buckle. On the reverse side of the plate horizontal and vertical Lueders' lines were distributed along the low points of the diagonal buckle.

Finally the load was increased to 740 kips. Observations were made as follows: (a) In panel 12, besides the spread of the yielding zone along the diagonal line, Lueders' lines were also noticed on the plate starting from the position of the outer third rivet connecting the upper flange to the web plate. The Lueders' lines ran also in a direction approximately perpendicular to the upper edge of the plate and spread along the depth of the upper minor buckle mentioned above. (b) In panels 9, 10, and 11 similar paint cracks were found in the plate near the outer third rivets in addition to the Lueders' lines previously formed. (c) On the other end of the girder, in spite of the fact that these panels were already reinforced with vertical stiffeners, further deformation occurred in the web plate of the subdivided panels, and Lueders' lines spread extensively over the web plate in panels 1 and 2.

General Observations.—No yielding in the flanges of the girder was detected, either visually in the "white-wash," or by the strain-gage readings, up to a total applied load of 660 kips. At 680 kips load, gage 57 (see Fig. 1) indicated yielding at this point. Gage 58, however, did not indicate yielding, although it was located on the same cross section of the tension flange.

Loads above 680 kips began to produce some cracking of the white-wash along with Lueders' lines, at various points along the compression flange. Gage 1 was the only other strain gage that indicated yielding at 740 kips load.

Inspection of the rivets cut from the girder revealed that the rivets did not completely fill the holes. The actual clearance varied considerably along the

length of the rivet but was generally less near the shop-formed head. The average clearance on each side of the rivet was approximately 0.010 in.; however, it was found to be two or three times this value in several instances.

Vertical Deflection.—The vertical deflection of the girder at center line is shown in Fig. 6. The theoretical bending deflection was computed using the gross section and assuming the cover plates were effective from their theoretical cutoff points. The shear deflection was computed assuming all shear was carried by the web, and no account was made for the buckling of the web.

The measured deflection is remarkably close to the total theoretical deflection. At loads over about 400 kips, considerable buckling of the web took place, and this may account for the somewhat higher measured deflections at these loads. The fact that the theoretical and measured deflections are in such close agreement may be somewhat of a coincidence, since the use of the theoretical cover-plate lengths in computing the deflections was arbitrary.

Flange Stresses.—The difference in strain between the top and bottom flanges is almost insignificant except at the highest loads. While yielding at the center of the outside cover plate was indicated at 680 kips total load, no yielding was indicated at the gage on the inside of the flange angle, up to the maximum total load of 740 kips. The measured strains agree very closely with the theoretical values based on the gross cross section. The load at which yielding in the center of the outside cover plate occurred was 1.93 times the AASHO design load. Yielding, however, was not detected in the center section of the compression flange or on the inside face of the tension flange at 2.13 times the AASHO design load.

The flange strain at the center of panels 9, 10, and 12 is shown in Fig. 7. Both flanges follow the theoretical line up to the load at which the web buckled. For loads higher than this, the stress in the top flange increases at a much faster rate than the theoretical, while the stress in the tension flange increases much slower. In panel 12, over loads of 650 kips, no increase in the tension flange strain was observed, but the strain in the compression flange increased at a much greater rate than previously. Buckling of the web became very severe over 650 kips load, and it is likely that high secondary stresses were induced in the flanges. Below the load at which yielding was noticed on the buckles of the web (620 kips) the behavior of the flanges appeared to be completely elastic.

The flange strain near the center of panel 10 is also shown in Fig. 7. These gages were located at the theoretical cutoff point of the middle cover plate. As mentioned previously, the cover plates on this end of the girder were extended far enough past their theoretical cutoff points so as to accommodate sufficient rivets to develop the initial forces coming into them. Up to the load at which the web buckled, the strain in both flanges agreed with the theoretical. Over this load, the strains followed the same pattern as was observed in panel 12. The theoretical line shown on Fig. 7 is based on the assumption that the outer cover plate is acting integrally with the rest of the flange at this point.

The flange strain in panel 9, at the theoretical cutoff point of the outer cover plate in both flanges, agrees with the theoretical based on the assumption that the outer cover plate is acting integrally with the rest of the flange. The web of this panel buckled at about 370-kips load, but no marked change in the flange strain could be noted. Only at much higher loads could some reduction in the tension flange strain be observed. It was noted, however, that the load at which the web of this panel buckled was not so clearly defined as in the other panels, and the lateral deflection was less than for panels 10, 11, and 12.

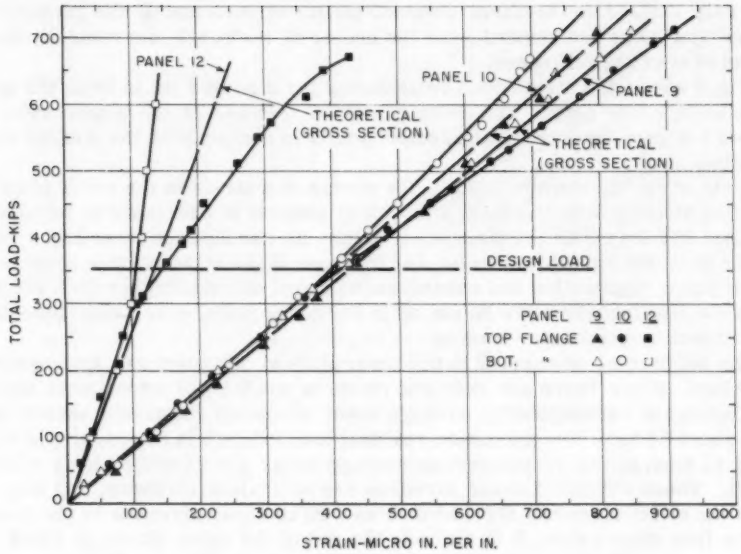

FIG. 7.—FLANGE STRAIN AT CENTER OF PANELS 9, 10, 12

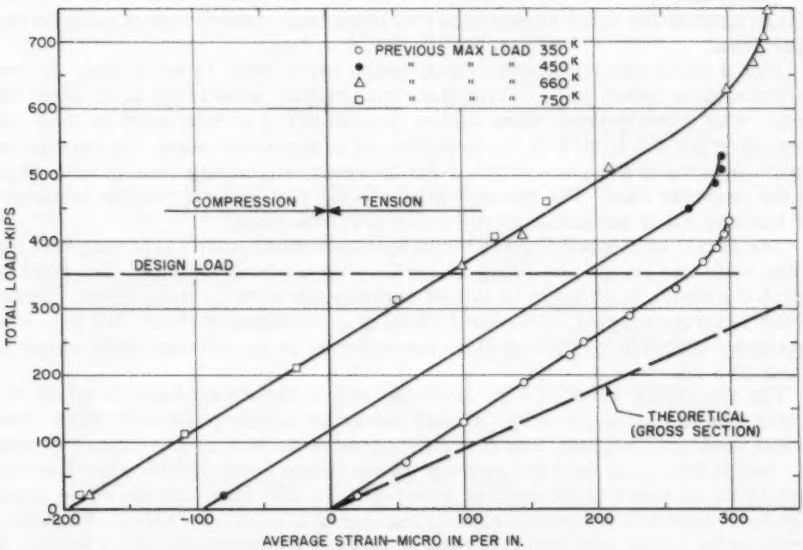
PREVIOUS MAX LOAD 350 K
" " " 450 K
" " " 660 K
" " " 750 K
COMPRESSION
TENSION
DESIGN LOAD
THEORETICAL (GROSS SECTION)
TOTAL LOAD-KIPS
AVERAGE STRAIN-MICRO IN. PER IN.
-200 -100 0 100 200 300
0 100 200 300 400 500 600 700

FIG. 8.—STRAIN IN MIDDLE COVER PLATE 8 INCHES FROM THE END—BOTTOM FLANGE

In general, this change in the flange strain at the buckling load of the web was only noticed in the three exterior panels at each end of the girder. The effect was more pronounced near the center of the panel and could hardly be detected over the stiffeners.

Fig. 8 shows the strain-load relationship for a point 8 in. in from the end of the middle cover plate. The cover plates on this end of the girder were extended 1 ft past their theoretical cutoff points to comply with the AASHO specification.

Up to about the working load of the girder, the strain in the cover plate increased directly with the load, although in general it was found to be between 20% and 30% less than the theoretical value. As can be seen from Fig. 8, loads higher than 400 kips did not cause any increase in the strain at this point on the cover plate. Application and subsequent removal of loads higher than 400 kips caused a residual stress to be set up in the cover plate, which was opposite in sign to that induced under loading.

The maximum load carried by the cover plate at this point was approximately 60 kips. Since there are only six rivets in the 8 in. of cover plate beyond this point, the corresponding average shear stress in the rivets should have been about 22 ksi. The maximum residual load induced in the cover plate was about 40 kips, and corresponds to an average shear stress in the rivets of about 13 ksi. These computed shear stresses are equivalent stresses, and may include the effect of frictional resistance as well as shear stresses in the rivets.

The five other points, 8 in. in from the end of the cover plates, at which the strain was measured, behaved similarly to the point just described, except that the apparent maximum shear stress in the rivets varied considerably. The lowest value observed was about 19 ksi, while the highest was about 31 ksi. The observations made at all points seemed to have only random variance, and no particular trend could be noticed either by comparing the results of one flange against the other or by comparing the areas of the flange at each particular point.

Fig. 9 shows the strain-load relationship for a point 16 in. in from the end of the middle cover plate. (The theoretical cutoff point is 12 in. in from the end). The same general phenomenon was observed at this point as was just described for the point 8 in. in from the end of the cover plate. The maximum strain induced in the plate at this point, however, was not so clearly defined as in the previous case. The residual strain in the plate did not reach a maximum or limiting value as was observed in the previous case.

The strain at this point agreed with the theoretical value (assuming that the outer plate and flange are acting integrally) up to about 450 kips. The point at which the strain first began to fall off corresponds to an average shear stress, in the 12 rivets connecting the first 16 in. of cover plate, of about 17.7 ksi. The maximum strain in the cover plate corresponds to an average rivet shear of about 22.6 ksi.

The five other points, 16 in. from the end of the cover plate, at which the strain was measured, behaved almost the same as the point described. The strain readings indicated that the outer cover plate was acting integrally with the rest of the flange until the average shear stress in the rivets connecting the last 16 in. of cover plate reached about 17 ksi. The strain in the cover plate then increased in a somewhat erratic manner to a maximum value. The maximum-value varied and corresponded to an average maximum shear stress of between 20 ksi and 31 ksi. As before, the variation seemed to be only random.

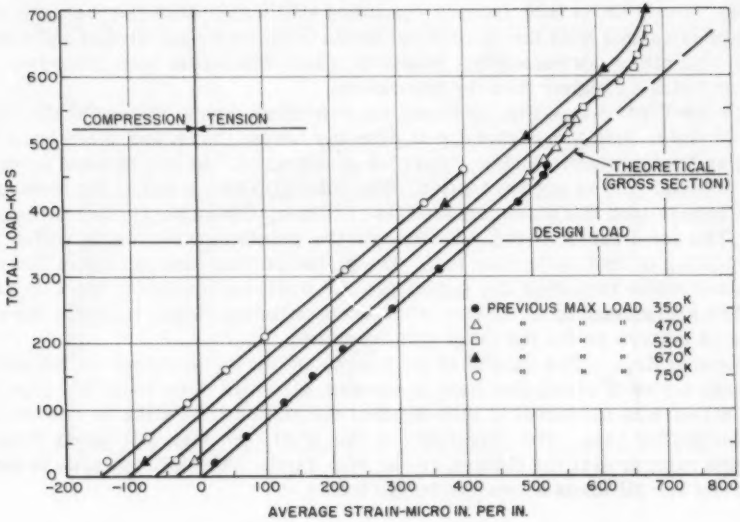

FIG. 9.—STRAIN IN MIDDLE COVER PLATE, 16 INCHES FROM THE END—BOTTOM FLANGE

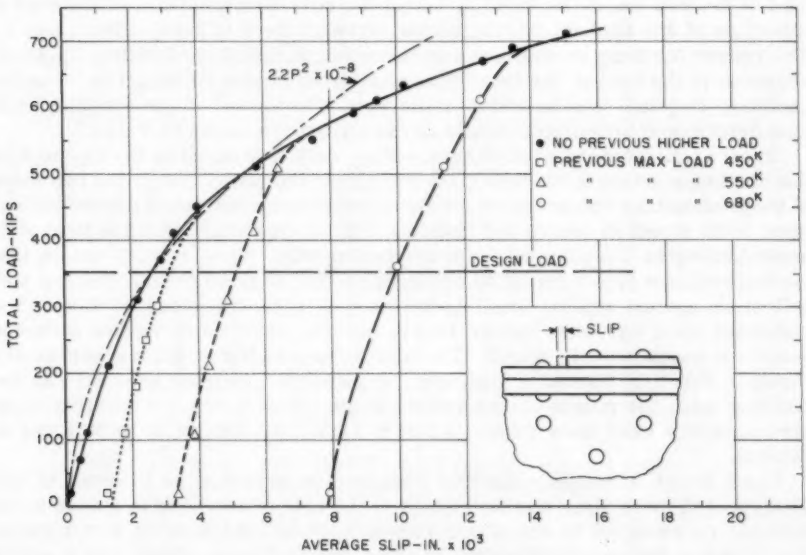

FIG. 10.—SLIP AT THE END OF THE MIDDLE COVER PLATE—BOTTOM FLANGE

In the second cover plate, at the point where the third cover plate terminates, the strain in both flanges was about 16% higher than the theoretical and happens to agree with the theoretical strain based on the net area of the flanges. The four other corresponding points at which the strain was measured also showed strains higher than the theoretical.

Cover Plate Slip.—Fig. 10 shows the slip measured at the end of the middle cover plate. Slip was measured at even the lowest loads, and there is no particular load at which a sudden "jump" was observed. As can be seen from Fig. 10, the load-slip is not reversible. The total slip at the end of the cover plate will depend upon the maximum load that has been previously applied to the girder. The solid curve in Fig. 10 connects the points corresponding to the first application of that particular load. The dashed curves connect points that were obtained while reloading the girder after a previous maximum load, as noted.

The slip measured at the two other points on the top flange followed the same general pattern as for the point just described.

Neutral Axis.—The strain at mid-depth of the girder on a cross section through a row of rivets has been measured. At loads over about 200 kips, tensile strain was measured at mid-depth of the girder, indicating an upward shift of the neutral axis. The magnitude of this shift has been calculated from the strains measured at the flanges and at mid-depth. The shift upwards is nearly constant for all loads above the design load.

ANALYSIS OF TEST RESULTS

The Determination of Buckling Load.—

From load vs. lateral deflection curves.—In this experiment, the buckling load of the web was determined by taking the corresponding load at the point of inflection of the load-lateral deflection curve of the web panel (Fig. 4 and 5). The reason for doing so was based on the assumption that the buckling load corresponds to the load at the transition point from a pure shear action to an incomplete diagonal tension action in the web. The values of the buckling loads thus determined for various panels of the girder are shown in Table 3.

From axial stresses in stiffeners.—This method is based on the assumption that the truss action in the web plate will cause the stiffeners on the two sides of the panel to take compressive stresses, while these stiffeners should be free from axial stresses before the buckling load is reached. Since the total stiffener load up to the point where truss action takes place is very small, this method could not give a result as accurate as that obtained from a graph of web deflection against applied load. In the present case, the cross section of the stiffeners used has been rather heavy, and the axial compressive stresses therefore comparatively small. The load versus stiffener-stress curves are shown in Fig. 11. Instead of indicating any specific point on the curve as the buckling load, the ranges of the applied loads within which the buckling must have occurred have been given. A list of such load ranges is to be found in Table 5.

From flange stresses.—Another phenomenon observed as a result of the buckling of the web plate was the change of the rate of increase in stress in the flanges. As revealed by the strain versus applied load plots on strain gages placed on the flanges at mid-point between two stiffeners, there was a sharp change of slope in the curve at a load corresponding to the buckling load of the panel. Since the strain versus load curves are straight lines, the breaking point

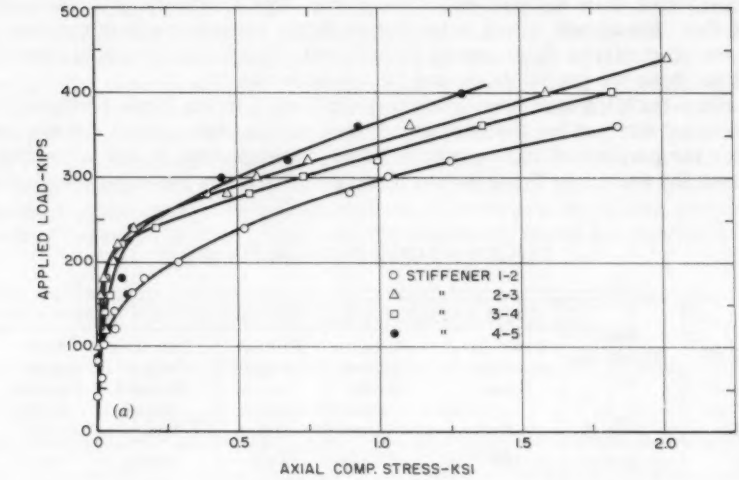

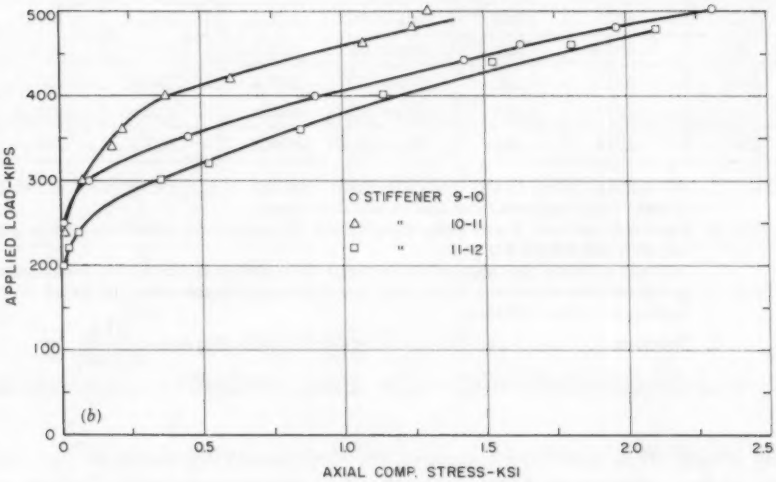

FIG. 11.—TOTAL APPLIED LOAD ON GIRDER VERSUS AXIAL COMPRESSIVE STRESSES IN STIFFENERS

is very apparent, and the buckling load can easily be located. The buckling load, indicated by the strain-gage plots, appeared to be about 5% higher than that determined from the load-deflection curve. One shortcoming of this method was that this abrupt break in the flange strain curves was only apparent in the cases of the three outer panels at each end. The flange strain against applied load plots for panels 9, 10, and 12 are shown in Fig. 7.

By plate-buckling formulae.—As pointed out earlier, the plate-buckling formula was not derived for the buckling of the web of a plate girder, but has been used for the purpose of approximation only. Nevertheless, it is interesting to note from the values in Table 5, that in certain instances the approximation is

TABLE 5.—TABLE OF BUCKLING LOADS

Panel No.	Web Thickness (in.)	FROM EXPERIMENT		THEORETICALLY COMPUTED		
		From deflection (kips)	From stiffener stress (kips)	Freely supported edges (kips)	Two long edges clamped (kips)	Four edges clamped (kips)
(1)	(2)	(3)	(4)	(5)	(6)	(7)
1	1/4	130	100 - 140	119.6	169.2	249.4
2	1/4	260	200 - 250	171.4	265.2	300.0
3	1/4	260	200 - 240	174.4	268.2	282.2
4	1/4	280	200 - 250	228.0	362.2	335.2
5	1/4	280	200 - 250	228.6	354.4	335.2
9	5/16	360	250 - 320	257.0	353.0	420.0
10	5/16	350	350 - 320	258.4	355.8	440.0
11	5/16	320	250 - 320	254.6	352.0	430.0
12	5/16	260	200 - 250	250.8	348.2	480.0

Notes:
1. All values shown in the table are total applied loads on girder at which elastic buckling occurred in the various panels.
2. Values in column 3 are determined from the points of inflection of the load vs. web deflection curves.
3. Column 4 shows the approximate range of machine loads within which diagonal tension appeared in the web by observing the presence of axial compression in the stiffners.
4. Columns 5, 6 and 7 are computed by the formula $T_{cr} = k \frac{\pi^2 E}{12(1-\mu^2)} \left(\frac{t}{b}\right)^2$.

fairly close. This table was computed for the cases: (a) assuming all four edges of the web plate as freely supported and consider shearing stresses on edges only, (b) assuming the edges along the flanges as clamped, and the other two edges freely supported and consider shearing stresses only, and (c) assuming all four edges as clamped, and considering both bending and shearing stresses.

The k value used in case (b) was taken from Iguchi (2a) and the computation for case (c) has been made by using the interaction curve and computing the critical shear and bending stress under the boundary conditions of case (c).

In comparing the experimental result with the computed values, it may be observed that computation based on case (a) gave a closer approximation for the two end panels, case (b) was in good agreement with the results of panels 2, 3, 9, 10, and 11, and case (c) yielded closer values for panels 4 and 5.

Comparison of the Buckling Load and the Maximum Test Load.—It is of interest now to compare the buckling loads with the loads that caused failure. The load which caused signs of yielding in the web plate has been considered as the maximum test load of the panel. The relations, if any, that exist between the buckling load and the maximum test load of a panel are of interest. In order to show better the interrelation between the buckling loads, the maximum test loads, and the respective web deflections, the two sets of figures are tabulated under Tables 6 and 3, together with the necessary ratios for comparison.

TABLE 6.—COMPARISON BETWEEN BUCKLING LOADS AND MAXIMUM TEST LOADS OF WEB PANELS

Panel No.	Aspect Ratio	Buckling Loads (P_{cr}) kips	Maximum Test Loads (P_{yp}) kips	$\frac{P_{cr}}{P_{yp}}$, in percentage	Reserve strength after buckling, in percentage
(1)	(2)	(3)	(4)	(5)	(6)
1	0.935	130	450	28.9	71.1
2	0.744	260	480	54.2	45.8
3	0.744	260	500	52.0	48.0
4	0.632	280	490	57.2	42.8
5	0.640	280	520	53.8	46.2
9	0.944	360	640	56.2	43.8
10	0.935	350	640	54.7	45.2
11	0.935	320	620	51.7	48.3
12	0.935	260	620	42.0	58.0

Notes: 1. Loads shown are total applied load on girder.
2. The buckling loads are determined from the load-deflection curves of the webs.
3. Aspect ratio = $\frac{\text{clear width of the web}}{\text{clear depth of the web}}$.

1. The buckling loads vary as the $\frac{d}{t}$ ratio (clear depth to thickness) the aspect ratio and the location of the panel in the girder (that is end or inner panels). Dividing the panels into two groups according to the plate, it may be observed that the difference between the largest value for the buckling load (280 k) and the smallest value (130 k) in the first group (1/4-in. web) is 53.5%, and the difference in the second group (5/16-in. web) is 27.8%.

2. The maximum test loads vary mainly with the plate thickness and to a certain extent with the aspect ratio. Comparing the highest and the lowest maximum test loads in the same manner as in 1, a difference of 13.5% for the first

group, and 3.1% for the second group is revealed. The difference in the maximum test load apparently is very small when the plate thicknesses and aspect ratios of the panels are the same.

3. Due to the redistribution of stresses in the web plate as a result of adding the stiffeners in the adjacent panel, the maximum test loads of the panels in the first group might not represent the true picture. Therefore, no comparisons between the buckling loads and the maximum test loads were made on the basis of the results in the first group. Taking the second group for comparison, it was found that while the plate thicknesses and aspect ratios were the same for the four panels, the maximum test loads were almost the same but the buckling loads differed by as much as 27.8%.

4. Comparing the buckling loads with the maximum test loads revealed that for panel 1, the ratio of the buckling load to the maximum test load was 28.9%; that is, the plate still had a reserved strength of 72.1% after it buckled, and for panel 12, the ratio was 42%, or the reserve strength was 58%, and for all other panels the reserve strengths after buckling were approximately 50%. This shows that buckling of a web panel does not mean immediate failure. If the design were to be based on the requirement that buckling of the web plate should not take place under the working load, and a certain factor of safety were added, at least 50% of the reserve strength of the plate would be wasted.

5. As shown in the preceding analysis, the buckling load only serves to indicate that the load-carrying behavior of the web is changing from one pattern to another. It is doubtful whether the buckling load may be used as a measure of the load-carrying capacity of a panel. It has been shown that extensive yielding of the web does not take place either at the buckling load or immediately afterwards.

Flange Stresses.—The flange strains measured during the testing of this girder showed good agreement with the theoretical values based on the gross moment of inertia, except in the vicinity of the ends of the cover plates. It should not be concluded, however, that the gross moment of inertia should be used to compute the design stresses for a riveted plate girder, since the average stress across the net section of the flange will be higher than that measured by the strain gages. Yielding across the net section of the tension flange begins before the design load is ever reached, and spreads across the flange as the load increases. Noting, from Table 1, that the yield stress of the cover plates was 39.4 ksi, the AASHO design procedure implies that yielding across the net section of the tension flange should have occurred at $\frac{39.4}{18} = 2.19$ times the design load, whereas yielding was detected at the center of the outside cover plate at 1.93 times the design load. However, yielding did not occur across the net section of the outstanding leg of the flange angles at 2.13 times the design load (maximum test load).

No particular change in the location of the neutral axis or in the behavior of the compression flange was apparent after yielding across the outside cover plate of the tension flange was observed. Yielding, as indicated by cracking of the "white-wash," was observed near the rivets in the center section of the compression flange at about the same load as yielding was measured across the tension flange.

The examination of the rivets in this girder revealed that the clearance between the rivet and the hole varied considerably, but only in rare cases could

it be said that there was no clearance between the rivet and the hole. In view of these observations, it is evident that before a rivet could be loaded in direct shear and bearing (as is generally assumed) some slipping of the adjoining parts must take place. Before the adjoining surfaces slip far enough to take up the clearance in the holes, the frictional resistance between the surfaces must be overcome and the rivet must undergo considerable bending distortion. (Bending of the rivet must take place since the rivet is apparently tight in the hole, just under the head).

The transfer of stress by the rivets in a plate girder is similar to the transfer of stress in a very long riveted joint, inasmuch as slipping between the connected parts results only through a difference in strain between the adjoining surfaces. If there is no difference in strain between adjoining surfaces then the stresses in a built-up girder should be no different from those in a solid beam. Furthermore, if there is no relative sliding between the connected parts of a plate girder, and load transferred by the rivets must be by means of friction alone. The strains measured during the testing of this girder agreed very well with those computed by the flexure formula, and it will be shown that the relative slip measured at the ends of the cover plates can be attributed to the difference in strain in the first few feet at the end of the cover plate. Because the deflections also agreed with those computed for a solid beam, it can be concluded that the action of this riveted plate girder is not different from a solid beam, except locally at the ends of the cover plates. It also follows that the load transferred by the rivets is mainly through friction between the connected surfaces only, except at the ends of the cover plates.

At the ends of the cover plates the stresses are not so simply distributed as in the remainder of this girder. Before any cover plate may act integrally with the rest of the flange, the strain in it must reach the value of the strain in the rest of the flange. The strain in the outer cover plate builds from zero to some steady state value, while the strain in the balance of the flange decreases to some new steady state value. This difference in strain between the connected surfaces results in a relative slipping of the surfaces, which accumulates at the end of the cover plate. It is this co-called slip that was measured during the testing of the girder and is shown in Fig. 10. When this slip is small, the stress transferred to the outer cover plate will be a result of friction between the sliding surfaces, but when the slip is large enough to absorb the clearance between the rivets and the rivet holes, the load will be transferred by the rivets acting in shear and bearing. The load on the rivets will depend on the clearance in the holes, but those rivets closest to the end of the cover plates will suffer the greatest distortions. Extending the cover plates any reasonable distance beyond their theoretical cutoff points will not avoid overstressing of these end rivets. The load on the end rivets will be reduced most effectively by decreasing the spacing of the rivets at the ends of the cover plates.

Cover Plate Slip.—The distribution of strain in a highly idealized manner may be assumed in the outer cover plate to build up linearly at a rate proportional to the shear resistance that can be developed between the cover plate and the adjoining flange. If the transfer of load to the outer cover plate was only through the medium of friction, the strain distribution would be very similar to that ideal one. Assuming such a distribution exists, and using the equivalent average rivet shear stress at first determined by the strain gage readings, an expression for the slip may be evaluated at the point that corresponds

with Fig. 10. The expression for this girder reduces to

$$\Delta = P^2 \times 2.2 \times 10^{-8} \text{in.}$$

in which Δ is the slip at the end of cover plate, and P denotes the load on girder in kips. This result has been plotted on Fig. 10. The theoretical slip is of the same magnitude as that measured, and follows the same general shape of curve.

The slip measured can therefore be attributed to the strain distribution at the ends of the cover plate, and it can be concluded that, in this immediate vicinity only, relative sliding between the component parts of the girder takes place.

Effect of the Thin Web on Flange Stresses.—The results of this test clearly indicate that the flange stresses in the buckled web framework cannot accurately be computed by the flexure formula. Fig. 7 seems to suggest that the load-strain relationship is still linear after buckling. This same observation was made in four other panels of the girder. The apparent additional increase in total flange load after buckling is also shown, and seems to be about 40% of the shear increment. It has been assumed that the surface strains measured on the top of the flange are representative of the average strain in the flange, but of course this assumption could be in error if the buckled web induces secondary bending stresses in the flange.

This redistribution of flange stress at the buckling load of the web follows the same pattern as was predicted and observed in connection with the investigation of the bending of thin-walled box beams (28).

CONCLUSIONS

Any conclusions drawn from this experiment must, of course, be made with certain reservations since it is not possible to assess all the variables involved on the basis of a single experiment.

1. The buckling behavior of the web of a plate girder is different from the theoretical behavior of a flat plate in the following ways: (a). Due to unavoidable initial curvature in the plate, the web starts to deflect laterally as soon as it is loaded; (b). The laterial deflection of the web does not become disproportionately large when it is loaded beyond its theoretical buckling load; (c). In the range of slenderness tested the web remains elastic and acquires no residual deflection under loads higher than the theoretical buckling load, unless the maximum test load is approached.

2. When using the theoretical buckling formula for an initially straight plate, in order to approximate the load at which diagonal tension action develops in the web, reasonably close results can be obtained if appropriate assumptions are made for the supporting and loading conditions.

3. The web of a plate girder is capable of carrying loads far in excess of its theoretical buckling load. In this experiment, the maximum test loads that caused local yielding in the web panels were from 1.75 to 3.45 times their respective buckling loads.

4. Local yielding in both the 1/4-in. web and the 5/16-in. web of this plate girder started as the maximum test load was approached, and occurred in advance of the localized yielding of the flanges.

5. After considering the theoretical buckling loads and the maximum test loads of the various panels of the plate girder, it is evident that the slenderness of the web is not a good criterion for the design of the web thickness.

6. The vertical deflection of a riveted plate girder could be accurately computed using the gross moment of inertia.

7. The neutral axis of a riveted plate girder remained very close to the center of gravity of the gross cross section for all loads.

8. Except locally, at the ends of the cover plates and across sections containing rivets, the flange stresses in a riveted plate girder can be accurately computed by the flexure formula by using the gross moment of inertia.

9. The transfer of horizontal shear stresses in this riveted plate girder was mainly accomplished through frictional resistance between the adjoining surfaces.

10. Extending the cover plates far enough past their theoretical cutoff point to develop the initial forces coming into them will insure that for all static loads the outer cover plate acts integrally with the rest of the flange at the theoretical cutoff point.

APPENDIX.—BIBLIOGRAPHY ON RIVETED PLATE GIRDERS

---

1. Timoshenko, S., "Theory of Elastic Stability," McGraw Hill Book Co., Inc., New York, 1936.

2. Bleich, F., "Buckling Strength of Metal Structures," McGraw Hill Book Co., New York, Inc., 1952. (a) p. 396.

3. Gerard, G. and H. Becker, "Handbook of Structural Stability," CNAC TN 3781-3784, July, 1957.

4. Kuhn, P., J. P. Peterson and L. R. Levin, "A Summary of Diagonal Tension," Part I, Methods of Analysis, CNAC TN 2661, May, 1952.

5. Kuhn, P., J. P. Peterson and L. R. Levin, "A Summary of Diagonal Tension," Part II, Experimental Evidence, CNAC TN 2662, May, 1952.

6. Kuhn, P. and J. P. Peterson, "Strength Analysis of Stiffened Beam Webs," NACA TN 1364, 1947.

7. Kuhn, P., "Investigations on the Incompletely Developed Plane Diagonal Tension Field," NACA Rep. 697, 1940.

8. Kuhn, P. and P. T. Chiarito, "The Strength of Plane Web Systems in Incomplete Diagonal Tension," NACA ARR, August, 1942.

9. Timoshenko, S., "Stability of the Webs of Plate Girders," Engineering, vol. 138, p. 207, 1935.

10. Mackey, S. and D. M. Brotton, "Investigation of the Behavior of Riveted Plate Girder," Structural Engineer, Vol. 30, No. 4, pp. 73-81, April, 1952.

11. Mackey, S. and D. M. Brotton, "Discussion on Investigation of Behavior of Riveted Plate Girder," Structural Engineer, Vol. 30, No. 11, pp. 273-8, November, 1952.

12. Mackey, S. and D. M. Brotton, "An Investigation of the Stress Distribution in a Welded Plate Girder for the Margam Plant," Structural Engr., Vol. 28, No. 2, February, 1950.

13. Mackey, S. and D. M. Brotton, Discussion on "An Investigation of the Stress Distribution in a Welded Plate Girder for the Margam Plant," Structural Engr., Vol. 29, No. 2, February, 1951.

14. Rockey, K. C., "Stability Problems Associated with the Design of Plate Girder Webs," Civil Engineering and Public Works Review, Vol. 47, Nos. 556-8 and Vol. 48, No. 559, London, 1953.

15. Rockey, K. C., "Plate Girder Design: Flange Stiffness and Web Plate Behavior," Engineering, Vol. 184, pp. 788-792, 1957.

16. Rockey, K. C. and F. Jenkins, "The Behavior of Web Plates of Plate Girders Subjected to Pure Bending," Structural Engineer, Vol. 35, No. 5, May, 1957.

17. Moore, H., "The Strength of I-Beams in Flexure," Bul. 68 Engr. Experiment Station, Univ. of Illinois, 1913.

18. Moore, H. and W. M. Wilson, "The Strength of I-Beams and Girders," Bul. 86, Engr., Experiment Station, Univ. of Illinois, 1916.

19. Kerensky, O. A., A. R. Flint and W. C. Brown, "The Basis for Design of Beams and Plate Girders," Revised British Standard 153, Structural Paper No. 48, Proc., I.C.E., 1956.

20. Longbottom, E. and J. Heyman, "Experimental Verification of the Strength of Plate Girders Designed in Accordance with the Revised British Standard 153: Tests on Full Size and on Model Plate Girders," Structural Paper Proc., I.C.E., 1956.

21. Southwell, R. V., "On the Analysis of Experimental Observations in Problems of Elastic Stability," Proc. Royal Society of London, Series A- 135, 1932.

22. Cox, H. L., "Notes on the Southwell Method for Estimating Critical Load," Aeronautical Research Council, R. and M., No. 2696, February, 1947.

23. Budiansky and Connor, "Buckling Stresses of Clamped Rectangular Flat Plates in Shear," NACA TN 1559, May, 1948.

24. Inge, Lyse and H. J. Godfrey, "Investigation of Web Buckling in Steel Beams," Transactions, ASCE, Vol. 100, p. 675, 1935.

25. Massonnet, Ch., "Buckling Experiments on Girder with Stiffened Web," International Association for Bridge and Structural Engineering, Vol. 14, 1954.

26. American Association of State Highway Officials, "Standard Specification for Highway Bridges," Sixth Edition, 1953.

27. American Railway Engineering Association, "Specifications for Steel Railway Bridges for Spens not Exceeding 400 Feet in Length," 1956.

28. Vasarhelyi, D. D. and R. O. Knudson, "Thin Walled Box Beams Under Pure Bending," International Association for Bridge and Structural Engineering, Vol. 15, 1955.

29. Timbey, E. K., "Neutral Axis and Centre of Gravity Do Not Coincide," Civil Engineering, Vol. 8, p. 270, April, 1938.

30. Lilly, S. B. and S. T. Carpenter, "Effective Moment of Inertia of a Riveted Plate Girder," Proceedings, ASCE, Vol. 65, pp. 1407-21, October, 1939.

31. Garrelts, J. M. and I. E. Madsen, "An Investigation of Plate Girder Web Splices," Transactions, ASCE, Vol. 107, p. 1303, 1942.

32. Chesson, E. and W. H. Munse, "Behavior of Riveted Connections in Truss-Type Members," University of Illinois Structural Research Series No. 115, January, 1956.

33. Moore, L. E., "Design of Plate Girders," McGraw-Hill Book Co., Inc., New York, 1913.

34. Gaylord, E. H. and C. N. Gaylord, "Design of Steel Structures," McGraw-Hill Book Co., Inc., New York, 1957.

35. Fleming, R., "Frictional Resistance of Riveted Joints," Engineering News Record, Vol. 84, pp. 1104-1107, June 3, 1920.

36. Hrennikoff, A., "Work of Rivets in Riveted Joints," Transactions, ASCE, Vol. 99, pp. 437-389, 1934.

37. Richard deJonge, A. E., "Riveted Joints," Research Publication, ASME, 1945.

38. Moore, R. L., "Observations on the Behavior of Aluminum Alloy Test Girders," Paper No. 2315, ASCE Transactions, Vol. 112, p. 901, 1947.

39. Moore, R. L., "An Investigation of Stiffeners on Shear-Resistant Plate-Girder Webs," NACA Tech. Note 862, September, 1942.

40. Bergman, G. A. and G. Westlund, "Buckling of Webs in Deep Steel I Girders," Inst. Struct. Eng. and Bridge Bldg., R. Inst. of Technology, Stockholm, January, 1947.

41. Bergman, G. A., "Behavior of Buckled Rectangular Plates under the Action of Shearing Forces," Royal Inst. of Technology, Stockholm, January, 1948.

42. Yuan, Ch. Y., and D. D. Vasarhelyi, "A Photographic Method for Determining the Deflected Shapes of Buckled Plates," The Trend, Vol. 12, pp. 13-15, January, 1960.

Journal of the
STRUCTURAL DIVISION
Proceedings of the American Society of Civil Engineers

BUCKLING OF ONE-STORY FRAMES AND BUILDINGS

By John E. Goldberg,[1] F. ASCE

SYNOPSIS

Buckling of plane frames and of complete one-story building structures is considered herein. The theory of buckling of plane, one-story frames is described and applied to the collapse of rectilinear frames using a generalization of the slope-deflection method. Both the symmetrical and anti-symmetrical or lurching modes of collapse of plane frames are considered. The relation of the buckling of plane frames to the buckling of the complete structure is pointed out and a theory for the buckling of such space structures is presented. It is shown that the buckling analysis of the complete structure can be reduced to a sequence of computationally simple problems. Illustrative examples are included.

INTRODUCTION

The theory of buckling of plane frames is now well established, and no serious difficulties are met in the determination of the critical loads of, at least, elementary plane frames. The proper application of valid methods based upon this theory leads to a generally satisfactory, if not overly conservative, design for such frames, from the standpoint of possible collapse, by reason of instability or buckling.

Plane frames, however, generally do not exist singly. A building structure normally consists of a set of such frames. These are inter-connected by floors

Note.—Discussion open until March 1, 1961. To extend the closing date one month, a written request must be filed with the Executive Secretary, ASCE. This paper is part of the copyrighted Journal of the Structural Division, Proceedings of the American Society of Civil Engineers, Vol. 86, No. ST 10, October, 1960.

[1] Assoc. Prof., Dept. of Civ. Engrg., Purdue Univ., LaFayette, Ind.

or roofs or by structural systems designed specifically to resist or to aid in the distribution of lateral loads. Under certain circumstances, these floors, roofs, or lateral systems may perform an additional function, that of providing a bracing system against a lurching or sidesway mode of buckling.

Plane frames may buckle in either a lurching or sidesway mode, involving lateral displacement of the joints, or in a mode that does not involve lateral

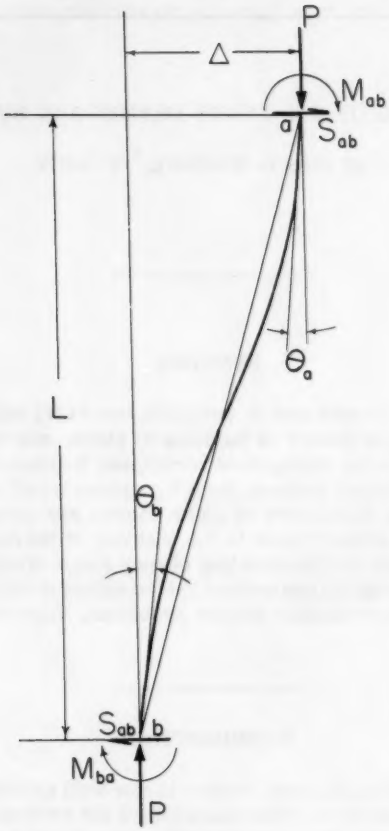

FIG. 1.—APPLIED FORCES AND DISTORTION OF A COLUMN

displacement of the joints. These modes are frequently called the "anti-symmetrical" and "symmetrical" modes, respectively, although these designations are applicable strictly to the corresponding modes of symmetrical, symmetrically loaded frames.

It is generally assumed that a plane frame will buckle in a lurching mode at a lesser loading than would be required to cause buckling in the symmetrical

mode. This assumption, however, is not necessarily valid if lateral support is provided in the form of floors, roofs, or explicit lateral bracing systems. A relatively small amount of lateral support in any of these forms may be sufficient to increase the critical loading for the sidesway mode to a level at which it exceeds the critical loading for the so-called symmetrical mode. Under these circumstances, and with the added condition that the frame and loading are symmetrical, the symmetrical mode of buckling takes on the greater significance.

This situation leaves the designer or analyst with two alternatives. He may accept, as a basis of design, the overly conservative critical loading for the lurching mode of buckling of the unbraced frame, or determine the critical loadings for both the lurching and symmetrical modes, if the latter is possible for the braced frame, and use the lower of these as a design basis.

The determination of the critical loading for the symmetrical mode of buckling of each of a set of plane frames is easily accomplished. The determination of the critical loading for unbraced frames or for independently braced frames in the lurching mode of buckling is also simple. The critical loadings of a set of mutually braced frames in the lurching modes presents a slightly more complicated but still straight-forward problem. This problem is analyzed in the present paper.

A procedure is presented for determining whether or not a complete one-store structure will buckle in a sidesway or lurching mode under a specified set of loads. The procedure is relatively simple, and has the advantage that is based upon concepts of rigid frame theory that are familiar to civil and structural engineers.

BASIC FORMULAS

If a member ab is subjected to a constant axial load as shown in Fig. 1, the bending moments at the end a and the end b may be expressed in terms of the angular and transverse displacements of its ends

$$M_{ab} = K_{ab}\left[A_{ab}\theta_a + B_{ab}\theta_b - (A_{ab} + B_{ab})\ \frac{\Delta_{ab}}{L_{ab}}\right] \quad \ldots\ldots\ldots (1a)$$

$$M_{ba} = K_{ab}\left[A_{ab}\theta_b + B_{ab}\theta_a - (A_{ab} + B_{ab})\ \frac{\Delta_{ab}}{L_{ab}}\right] \quad \ldots\ldots\ldots (1b)$$

in which $K_{ab} = E\,I/L$, E is the appropriate modulus of elasticity, I denotes the moment of inertia of cross section, L is the length of member, A, and B are constants, θ is the angular displacement at end designated by subscript, and Δ refers to relative transverse displacement of ends.

The values of the constants A and B depend upon the sign and magnitude of the axial load and may be expressed completely[2] as functions of the ratio of the axial load to the Euler load of the member, due consideration being given to the use of the appropriate modulus in the Euler formula for compressive axial load,

---

[2] "Stiffness Charts for Gusseted Members Under Axial Load," by John E. Goldberg, Transactions, ASCE, Vol. 119, 1954, p. 43.

$$A = \frac{\sin p L - p L \cos p L}{\frac{2}{p L}(1 - \cos p L) - \sin p L} \quad \ldots\ldots\ldots\ldots (2a)$$

$$B = \frac{p L - \sin p L}{\frac{2}{p L}(1 - \cos p L) - \sin p L} \quad \ldots\ldots\ldots\ldots (2b)$$

TABLE 1.—SLOPE DEFLECTION COEFFICIENTS A AND B FOR VARIOUS VALUES OF LOAD RATIO ρ

ρ	A	B		A	B
3.9	-78.34	78.58	0.3	3.589	2.109
3.8	-39.05	39.54	0.2	3.730	2.070
3.7	-24.69	25.39			
3.6	-17.87	18.79	0.1	3.865	2.033
3.5	-13.73	14.86	0	4.000	2.000
3.4	-10.91	12.24	0	4.000	2.000
3.3	- 8.86	10.40	-0.1	4.131	1.968
3.2	- 7.30	9.02	-0.2	4.255	1.938
3.1	- 6.05	7.96	-0.3	4.384	1.910
3.0	- 5.03	7.12	-0.4	4.502	1.883
2.8	- 3.449	5.884	-0.5	4.619	1.857
2.6	- 2.252	5.019	-0.6	4.736	1.834
2.5	- 1.749	4.678	-0.7	4.849	1.811
2.4	- 1.300	4.383	-0.8	4.959	1.789
2.2	- 0.519	3.901	-0.9	5.069	1.769
2.0	0.143	3.521	-1.0	5.175	1.749
1.8	0.717	3.224	-1.2	5.383	1.713
1.6	1.224	2.980	-1.4	5.583	1.681
1.5	1.457	2.873	-1.6	5.777	1.651
1.4	1.673	2.778	-1.8	5.964	1.623
1.2	2.090	2.610	-2.0	6.147	1.598
1.0	2.468	2.468	-2.5	6.580	1.544
0.9	2.645	2.404	-3.0	6.99	1.499
0.8	2.816	2.346	-4.0	7.75	1.43
0.7	2.981	2.291	-5.0	8.42	1.38
0.6	3.140	2.241	-7.0	9.62	1.30
0.5	3.295	2.194	-9.0	10.69	1.26
0.4	3.444	2.150			

and for tensile axial load,

$$A = \frac{p L \cosh p L - \sinh p L}{\frac{2}{p L}(1-\cosh p L) + \sinh p L} \quad \ldots\ldots\ldots\ldots (3a)$$

$$B = \frac{\sinh p L - p L}{\frac{2}{p L}(1-\cosh p L) + \sinh p L} \quad \ldots\ldots\ldots\ldots (3b)$$

in which

$$p L = \pi \sqrt{|\rho|} \quad \ldots\ldots\ldots\ldots (4a)$$

and

$$\rho = \frac{P}{P_e} = \frac{P}{\pi^2 E I/L^2} \quad \ldots\ldots\ldots\ldots\ldots\ldots (4b)$$

and P is the axial load, denoted as positive when compression. The values of the slope-deflection coefficients A and B may be taken from Table 1 or Figs. 2 and 3. A more extensive set of charts which gives the values of these coefficients for gusseted members has been presented[2] previously. It may be noted that, when the axial load is zero, the coefficients A and B take on the values 4 and 2, respectively.

Referring to Fig. 1 and taking moments about either end leads to the following formula for the transverse shear:

$$S_{ab} = \frac{-1}{L_{ab}} \left(M_{ab} + M_{ba} + P_{ab}\, \Delta_{ab}\right) \quad \ldots\ldots\ldots (5)$$

Substitution of Eq. 1 into Eq. 5 yields

$$S_{ab} = \frac{-K_{ab}}{L_{ab}} \left(A_{ab} + B_{ab}\right)\left(\theta_a + \theta_b - 2\,\frac{\Delta_{ab}}{L_{ab}}\right) - P_{ab}\ \frac{\Delta_{ab}}{L_{ab}} \quad \ldots\ldots (6)$$

It is of interest to investigate the effect of various end conditions at the base of the column upon Eqs. 1 and 6. If the lower end, a, is elastically restrained by a rotational spring having a spring rate Q_a, the moment at the lower end has the magnitude

$$M_{ab} = Q_a\, \theta_a \quad \ldots\ldots\ldots\ldots\ldots\ldots (7)$$

By Eq. (1), therefore,

$$K_{ab}\left[A_{ab}\, \theta_a + B_{ab}\, \theta_b - \left(A_{ab} + B_{ab}\right) \frac{\Delta_{ab}}{L_{ab}}\right] = - Q_a\, \theta_a \quad \ldots (8)$$

which leads to

$$\theta_a = \frac{1}{A_{ab} + \dfrac{Q_a}{K_{ab}}} \left[- B_{ab}\, \theta_b + \left(A_{ab} + B_{ab}\right) \frac{\Delta_{ab}}{L_{ab}}\right] \quad \ldots\ldots (9)$$

Substitution of Eq. 9 into Eqs. 1 and 6 yields

$$M_{ba} = K_{ab}\left[\left(A_{ab} - \frac{B_{ab}^2}{A_{ab} + \dfrac{Q_a}{K_{ab}}}\right)\theta_b \right.$$

$$\left. - \left(A_{ab} + B_{ab}\right)\left(1 - \frac{B_{ab}}{A_{ab} + \dfrac{Q_a}{K_{ab}}}\right) \frac{\Delta_{ab}}{L_{ab}}\right] \quad \ldots\ldots (10)$$

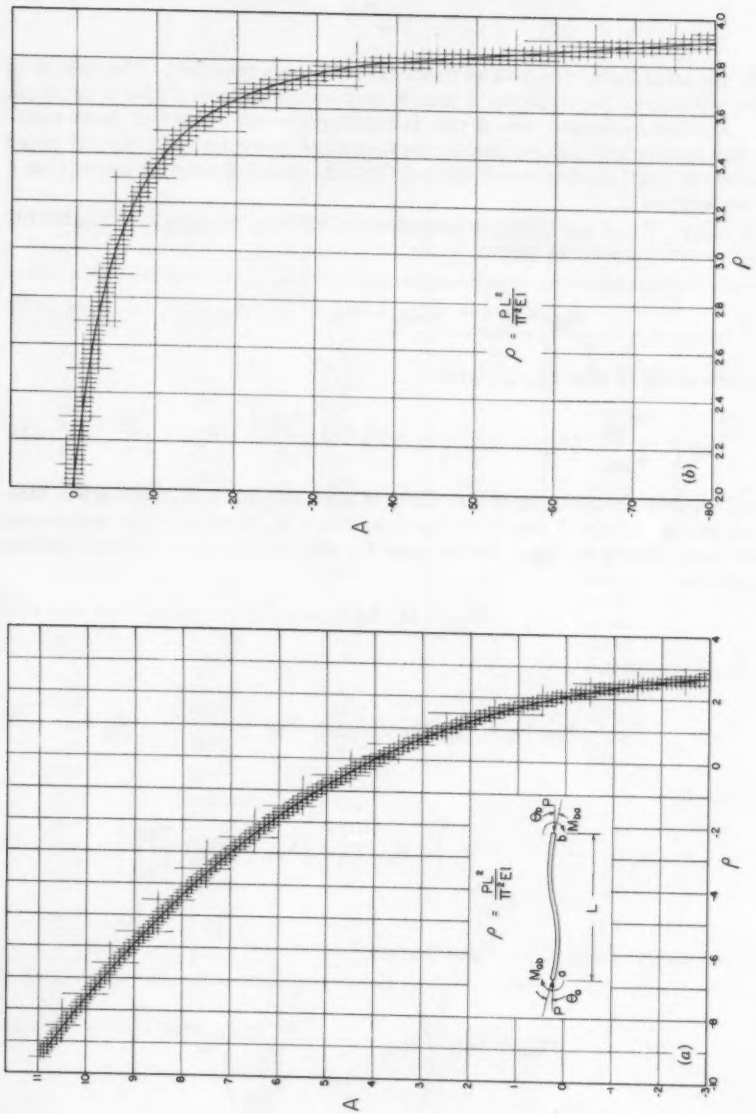

FIG. 2.—VALUES OF A

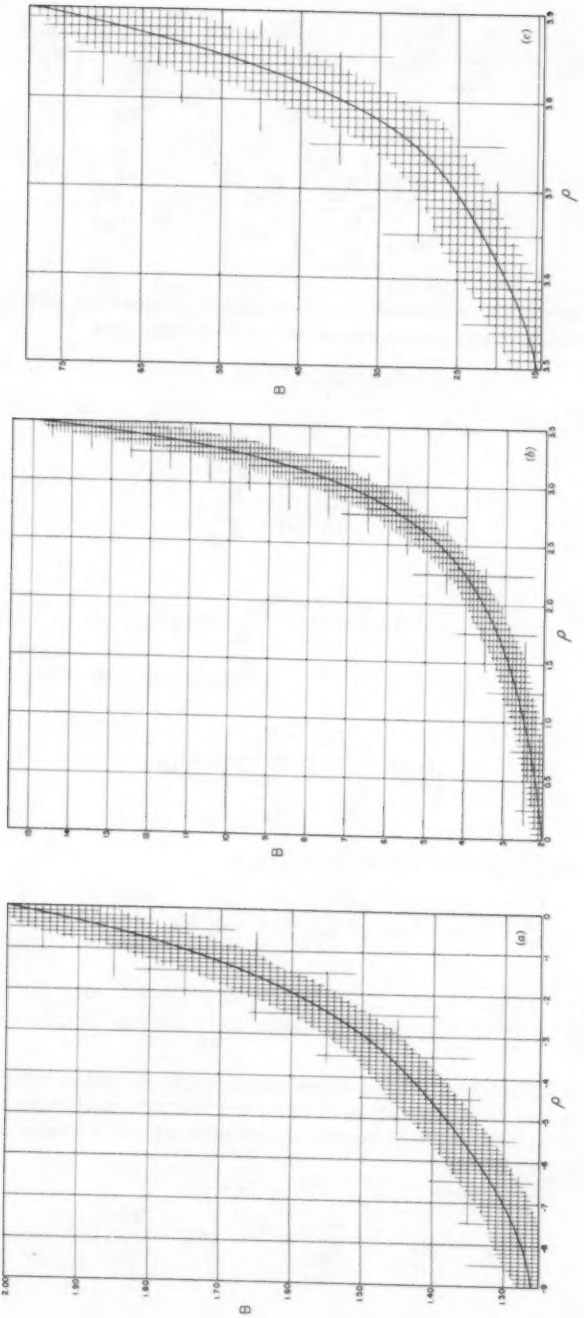

FIG. 3.—VALUES OF B

and

$$S_{ab} = -\frac{K_{ab}}{L_{ab}}\left(A_{ab} + B_{ab}\right)\left[\left(1 - \frac{B_{ab}}{A_{ab} + \frac{Q_a}{K_{ab}}}\right)\theta_b - \left(2 - \frac{A_{ab} + B_{ab}}{A_{ab} + \frac{Q_a}{K_{ab}}}\right)\frac{\Delta_{ab}}{L_{ab}}\right] - P_{ab}\frac{\Delta_{ab}}{L_{ab}} \quad \ldots\ldots (11)$$

These may be written somewhat more compactly, if desired, with the introduction of several new and easily evaluated coefficients. Let

$$A_{ab} + B_{ab} = C_{ab} \quad \ldots\ldots\ldots\ldots\ldots (12a)$$

$$A_{ab} - \frac{B^2_{ab}}{A_{ab} + \frac{Q_a}{K_{ab}}} = A'_{ab} \quad \ldots\ldots (12b)$$

$$1 - \frac{B_{ab}}{A_{ab} + \frac{Q_a}{K_{ab}}} = c_{ab} \quad \ldots\ldots\ldots (12c)$$

and

$$2 - \frac{A_{ab} + B_{ab}}{A_{ab} + \frac{Q_a}{K_{ab}}} = c'_{ab} \quad \ldots\ldots\ldots\ldots (12d)$$

Then Eqs. 10 and 11 may be written in the form

$$M_{ba} = K_{ab}\left(A'_{ab}\,\theta_b - C_{ab}\,c_{ab}\,\frac{\Delta_{ab}}{L_{ab}}\right) \quad \ldots\ldots\ldots (13)$$

$$S_{ab} = -\frac{K_{ab}}{L_{ab}}\,C_{ab}\left(c_{ab}\,\theta_b - c'_{ab}\,\frac{\Delta_{ab}}{L_{ab}}\right) - P_{ab}\frac{\Delta_{ab}}{L_{ab}} \quad \ldots\ldots (14)$$

It may be noted that Eqs. 10 and 11 reduce directly, to rather simple forms, when Q takes on the limiting values of zero and infinity, corresponding to the pinned condition and the built-in condition, respectively, at the base of the column. Thus, for pinned base

$$M_{ba} = K_{ab}\,\frac{\left(A^2_{ab} - B^2_{ab}\right)}{A_{ab}}\left(\theta_b - \frac{\Delta_{ab}}{L_{ab}}\right) \quad \ldots\ldots\ldots (15a)$$

or

$$M_{ba} = K_{ab} \frac{C_{ab}}{A_{ab}} (A_{ab} - B_{ab}) \left(\theta_b - \frac{\Delta_{ab}}{L_{ab}}\right) \quad \ldots\ldots\ldots\ldots (15b)$$

and

$$S_{ab} = - \frac{K_{ab}}{L_{ab}} \frac{(A^2 - B^2)}{A_{ab}} \left(\theta_b - \frac{\Delta_{ab}}{L_{ab}}\right) - P_{ab} \frac{\Delta_{ab}}{L_{ab}} \quad \ldots\ldots\ldots (16a)$$

or

$$S_{ab} = - \frac{K_{ab}}{L_{ab}} \frac{C_{ab}}{A_{ab}} (A_{ab} - B_{ab}) \left(\theta_b - \frac{\Delta_{ab}}{L_{ab}}\right) - P_{ab} \frac{\Delta_{ab}}{L_{ab}} \quad \ldots\ldots\ldots (16b)$$

also

$$A'_{ab} = A_{ab} - \frac{B^2_{ab}}{A_{ab}} = \frac{A^2_{ab} - B^2_{ab}}{A_{ab}} = \frac{C_{ab}}{A_{ab}} (A_{ab} - B_{ab}) \quad \ldots (17a)$$

$$c_{ab} = 1 - \frac{B_{ab}}{A_{ab}} = \frac{A_{ab} - B_{ab}}{A_{ab}} \quad \ldots\ldots\ldots (17b)$$

and

$$c'_{ab} = 2 - \frac{A_{ab} + B_{ab}}{A_{ab}} = c_{ab} \quad \ldots\ldots\ldots\ldots (17c)$$

whereas for the built-in base

$$M_{ba} = K_{ab} \left[A_{ab}\, \theta_b - (A_{ab} + B_{ab}) \frac{\Delta_{ab}}{L_{ab}} \right] \quad \ldots\ldots (18a)$$

or

$$M_{ba} = K_{ab} \left(A_{ab}\, \theta_b - C_{ab} \frac{\Delta_{ab}}{L_{ab}} \right) \quad \ldots\ldots\ldots (18b)$$

and

$$S_{ab} = - \frac{K_{ab}}{L_{ab}} (A_{ab} + B_{ab}) \left(\theta_b - 2 \frac{\Delta_{ab}}{L_{ab}}\right) - P_{ab} \frac{\Delta_{ab}}{L_{ab}} \quad \ldots (19a)$$

or

$$S_{ab} = - \frac{K_{ab}}{L_{ab}} C_{ab} \left(\theta_b - 2 \frac{\Delta_{ab}}{L_{ab}}\right) - P_{ab} \frac{\Delta_{ab}}{L_{ab}} \quad \ldots (19b)$$

In addition

$$A'_{ab} = A_{ab} \quad \ldots\ldots\ldots\ldots\ldots\ldots \quad (20a)$$

$$c_{ab} = 1 \quad \ldots\ldots\ldots\ldots\ldots\ldots \quad (20b)$$

and

$$c'_{ab} = 2 \quad \ldots\ldots\ldots\ldots\ldots\ldots \quad (20c)$$

The formulas presented in this section will be applied to buckling problems of certain rectangular frames, in particular one-story frames, in the following sections.

SYMMETRICAL BUCKLING

One-Story Single-Bay Frame.—Under certain conditions, a frame may buckle in a mode which does not involve lateral displacement of the joints. If one considers a one-story, single-bay rectangular frame under symmetrical conditions, as shown in Fig. 4 and setting $\Delta_{ab} = 0$, and $\theta_c = -\theta_b$. Eq. 13 for the column and girder become

$$M_{ba} = K_{ab} A'_{ab} \theta_b \quad \ldots\ldots\ldots\ldots \quad (21a)$$

and

$$M_{bc} = K_{bc} \left(4 \theta_b + 2 \theta_c\right) = K_{bc} \theta_b \quad \ldots\ldots\ldots \quad (21b)$$

The sum of the moments acting about joint b must vanish, and, therefore,

$$\left(K_{ab} A'_{ab} + 2 K_{bc}\right) \theta_b = 0 \quad \ldots\ldots\ldots\ldots \quad (22)$$

Eq. 22 determines the magnitude of A'_{ab} which will maintain equilibrium in the symmetrically buckled configuration. The stability criterion therefore is

$$A'_{ab} = -2 \frac{K_{bc}}{K_{ab}} \quad \ldots\ldots\ldots\ldots\ldots\ldots \quad (23)$$

To determine the critical load, one first computes the required value of A'_{ab} by using Eq. 23. If the base of each column is fixed, the corresponding value of ρ may be read directly from Fig. 2 (a) since $A'_{ab} = A_{ab}$. In other cases, the corresponding value of ρ is best obtained by trial-and-error. A value of ρ is assumed, and A'_{ab} is computed by means of Eqs. 12 or 17 using values of A and B from the charts of Figs. 2 and 3. The process is repeated until the value of ρ that corresponds to the required value of A'_{ab} is determined. Interpolation will be helpful in improving the successive trials. Normally, the proper value of ρ will be determined with satisfactory accuracy with only three or four trials. After establishing the correct value of ρ, the critical load is determined by use of Eq. 4b.

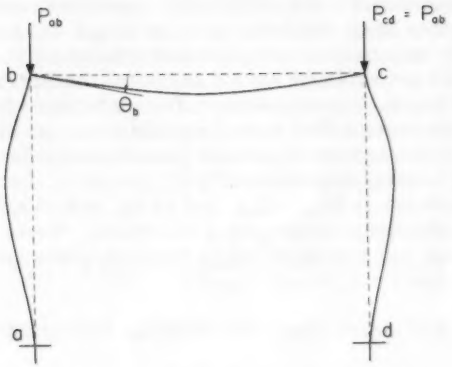

FIG. 4.—SYMMETRICAL BUCKLING OF A ONE-STORY SINGLE BAY RECTANGULAR FRAME

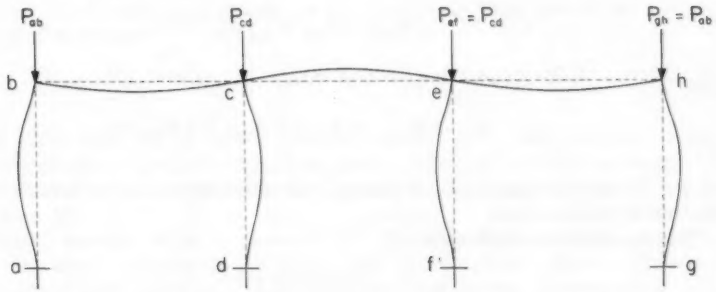

FIG. 5.—SYMMETRICAL BUCKLING OF A ONE-STORY THREE BAY FRAME

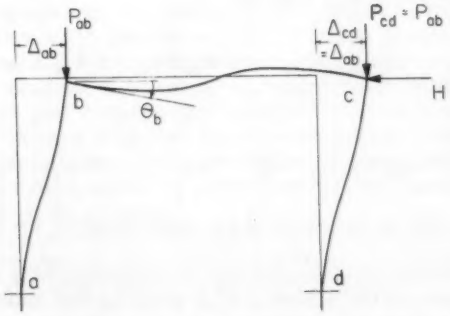

FIG. 6.—ANTI-SYMMETRICAL BUCKLING OF SINGLE BAY RIGID FRAME

One-Story, Three-Bay Frame.—The basic equations used in the case of multi-bay frames are those which are used for single-bay frames. Because of the greater number of joint rotations, however, the procedure for determining whether or not given column loads form a critical set must differ from that used for the single-bay frame. The single-bay frame may also be treated as a special case of the multi-bay frame. The three-bay frame, such as shown in Fig. 5, offers an opportunity to describe a general procedure for the analysis of symmetrical buckling in multi-bay frames.

The beam shears due to M_{bc}, M_{cb}, and so on, induce axial strains in columns and cause differential settlement of the beams. These effects, however, are generally small and are neglected in this and subsequent analyses. The relevant moments are

$$M_{ba} = K_{ab} A'_{ab} \theta_b \quad \ldots\ldots\ldots\ldots\ldots (24a)$$

$$M_{bc} = K_{bc} (4 \theta_b + 2 \theta_c) \quad \ldots\ldots\ldots\ldots (24b)$$

$$M_{cb} = K_{bc} (4 \theta_c + 2 \theta_b) \quad \ldots\ldots\ldots\ldots (24c)$$

$$M_{cd} = K_{cd} A'_{cd} \theta_c \quad \ldots\ldots\ldots\ldots\ldots (24d)$$

and

$$M_{ce} = K_{ce} (4 \theta_c + 2 \theta_e) = 2 K_{ce} \theta_c \quad \ldots\ldots\ldots (24e)$$

where, in the last equation, advantage has been taken of the symmetry of the angular displacements.

The equilibrium equations,

$$M_{ba} + M_{bc} = 0 \quad \ldots\ldots\ldots\ldots\ldots (25a)$$

and

$$M_{cb} + M_{cd} + M_{ce} = 0 \quad \ldots\ldots\ldots\ldots (25b)$$

become, upon substitution of Eqs. 24,

$$(K_{ab} A'_{ab} + 4 K_{bc}) \theta_b + 2 K_{bc} \theta_c = 0 \quad \ldots\ldots\ldots (26a)$$

and

$$2 K_{bc} \theta_b + (4 K_{bc} + K_{cd} A'_{cd} + 2 K_{ce}) \theta_c = 0 \quad \ldots\ldots (26b)$$

These equations will be satisfied, if the axial loads on the columns have their critical values.

There are several available procedures for determining whether a given set of column loads provide the values of A'_{ab} and A'_{cd} that make it possible to satisfy this pair of simultaneous equations. A trial-and-error procedure generally will be most practical.

One such procedure consists of the following steps: after selecting trial values for the column loads and computing the value of A'_{ab} and of A'_{cd}, either of the

equilibrium equations may be solved for one rotation in terms of the other. For example, the second of Eq. 26 may be solved for θ_c in terms of θ_b. This result now may be substituted into the remaining equation, and it can be determined whether or not this transformed equation can be satisfied. This, it will be seen, is tantamount to the vanishing of the coefficient of θ_b in the transformed equation. If both equations can be satisfied, then the assumed loads form a critical set. If not, new values are chosen, and the process is repeated.

Following this line of attack, the elimination of θ_c from the pair of equations yields

$$\left(K_{ab} A'_{ab} + 4 K_{bc} - \frac{4 K^2_{bc}}{4 K_{bc} + K_{cd} A'_{cd} + 2 K_{ce}} \right) \theta_b = 0 \quad \ldots (27)$$

which can be satisfied if the coefficient of θ_b vanishes. Thus, the stability criterion is

$$K_{ab} A'_{ab} + 4 K_{bc} - \frac{4 K^2_{bc}}{4 K_{bc} + K_{cd} A'_{cd} + 2 K_{ce}} = 0 \quad \ldots\ldots (28)$$

An alternate form may be obtained by placing the entire expression over a common denominator and setting the numerator equal to zero, in other words, multiplying through by the denominator of the fraction. This yields the stability criterion in the form,

$$(K_{ab} A'_{ab} + 4 K_{bc})(4 K_{bc} + K_{cd} A'_{cd} + 2 K_{ce}) - 4 K^2_{bc} = 0 \ldots (29)$$

It may be noted that Eq. 29 would also be obtained if θ_b had first been eliminated from the pair of equilibrium equations. One may observe also that Eq. 29 is the expansion of the determinant formed by the coefficients of the rotations in Eqs. 26.

There are several ways to describe or define a critical set of loads. For example, the ratio between P_{ab} and P_{cd} may be specified. Thus, trial values will conform to this ratio, as will subsequent trial values, if necessary, in the trial-and-error process. Alternatively, the set may be defined by specifying the actual magnitude of one of the column loads. In the associated trial-and-error process, the remaining load is adjusted until the proper value is found that permits the two equilibrium equations to be satisfied. If the critical set is to be defined in this manner, the first procedure might be found to be convenient. Suppose, for example, that the magnitude of P_{bc} is specified, and P_{ab} is subject to variation. Then the coefficients in Eq. 26 b are completely defined, and θ_c may be determined in terms of θ_b. Substitution of this result into the first equation of the pair reduces this equation to a homogeneous expression in θ_b. The proper value of A'_{ab} now may be computed in a simple manner, and the corresponding critical value of ρ for this column may be found. The analogous sequence of operations may be performed directly upon Eq. and will, of course, yield the same result.

A third procedure introduces the concept of "reserve stiffness" as a stability criterion. Imagine that an external moment M_o is applied to joint b; the equilibrium equations at joints c and b, respectively, become

$$2 K_{bc} \theta_b + (4 K_{bc} + K_{cd} A'_{cd} + 2 K_{ce}) \theta_c = 0 \quad \ldots\ldots\ldots (30a)$$

$$(K_{ab} A'_{ab} + 4 K_{bc}) \theta_b + 2 K_{bc} \theta_c = M_o \quad \ldots\ldots\ldots (30b)$$

in which the positive direction of M_o is the same as the positive direction for joint rotations. Assuming a value of unity for θ_b, the first equation is solved for θ_c. These values are now substituted into the second equation, and M_o is determined. The sign of M_o establishes whether the frame is stable or unstable under the loads corresponding to the values of A'_{ab} and A'_{cd} that have been used. If M_o is positive, that is, if M_o acts in the direction of θ_b, then the frame has "reserve stiffness," and is stable under the applied loads. Conversely, if M_o is negative, the critical loads have been exceeded, and the frame is unstable. If M_o has the value zero, the applied loads exactly constitute a critical set. Since the sign and magnitude of M_o serve as a criterion of stability, one may again use a trial-and-error procedure to determine the magnitudes of the column load that form a critical set. The sign of the computed value of M_o indicates whether the column loads should be increased or decreased for the next trial.

By an extension of these methods, the symmetrical modes of buckling of multi-story frames may be investigated, and the magnitudes of the critical loads may be established. A further generalization leads to a related procedure for treating the lurching or anti-symmetrical modes of buckling of multi-story frames. Whereas these methods already have been developed, they are beyond the scope of the present paper.

ANTI-SYMMETRICAL MODE

Unbraced Single-Bay Frame.—The critical values of the column loads for the anti-symmetrical or lurching mode of buckling may be determined through the use of Eq. 1 and its particularized variations.

In the case of a single-bay rigid frame, the deformed or buckled structure appears somewhat as shown in Fig. 6. If the frame is symmetrical and symmetrically loaded, then only two equilibrium equations need be written. These state that the sum of the moments at either upper joint, say b, vanishes, and that the force H, which is shown in Fig. 6, also vanishes. In which case, Eq. 25a and

$$- S_{ab} - S_{cd} = H = 0 \quad \ldots\ldots\ldots\ldots\ldots\ldots \quad (31a)$$

hold true. By virtue of the assumed symmetry, Eq. 31a may be written simply as

$$- S_{ab} = \frac{H}{2} = 0 \quad \ldots\ldots\ldots\ldots\ldots\ldots \quad (31b)$$

Noting that Δ_{bc} is zero, these equations become, through the use of Eqs. 1, 13, and 14

$$K_{ab}\left(A'_{ab}\,\theta_b - C_{ab}\,c_{ab}\,\frac{\Delta_{ab}}{L_{ab}}\right) + 2\,K_{bc}\,\theta_b = 0 \quad \ldots\ldots \quad (32a)$$

and

$$\frac{K_{ab}}{L_{ab}}\,C_{ab}\left(c_{ab}\,\theta_b - c'_{ab}\,\frac{\Delta_{ab}}{L_{ab}}\right) + P_{ab}\,\frac{\Delta_{ab}}{L_{ab}} = \frac{H}{2} = 0 \quad \ldots\ldots \quad (32b)$$

or, upon collecting terms,

$$\left(K_{ab}\,A'_{ab} + 2\,K_{bc}\right)\,\theta_b - K_{ab}\,C_{ab}\,c_{ab}\,\frac{\Delta_{ab}}{L_{ab}} = 0 \quad \ldots\ldots \quad (33a)$$

and

$$\frac{K_{ab}}{L_{ab}} C_{ab} c_{ab} \theta_b - \left(\frac{K_{ab}}{L_{ab}} C_{ab} c'_{ab} - P_{ab} \right) \frac{\Delta_{ab}}{L_{ab}} = \frac{H}{2} = 0 \quad \ldots \quad (33b)$$

One may again note that the constants have very simple forms when the base conditions are either fixed or hinged.

As in the previous cases, a trial-and-error procedure for the solution of Eqs. 33 and the determination of the critical load will be found to be convenient and relatively rapid. Noting that, for a frame such as shown in Fig. 6, the critical load must be less than the Euler load computed with an appropriate modulus, a trial value is selected for P_{ab} and the coefficients evaluated. Assuming Δ_{ab} to have unit magnitude, the value of θ_b is found from Eq. 33a. Substitution of this value of θ_b and the unit value of Δ_{ab} into the Eq. 33b yields the value of H that would be required to hold the frame in the deflected position with the prescribed column loads. The sign of the computed value of H determines whether

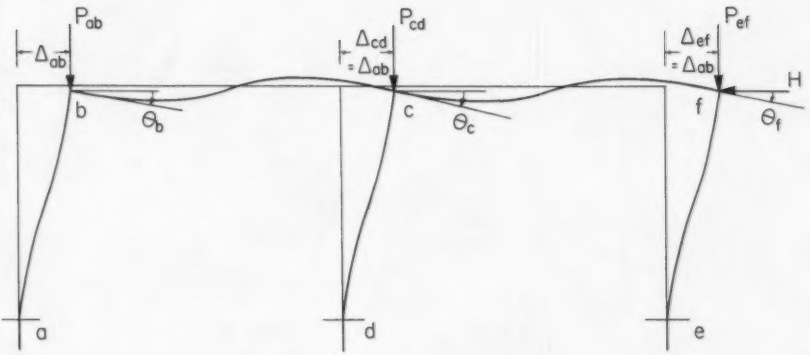

FIG. 7.—LURCHING MODE OF BUCKLING OF TWO BAY FRAME

the axial loads are greater or less than the critical loads. If H is positive, the assumed column loads exceed the critical loads, since the force H is now supporting the frame against further deflection. If H is negative, the assumed column loads are less then the critical loads, since the direction of H now implies that the frame has "reserve stiffness." If H vanishes, the assumed column loads are equal to the critical loads. In the trial-and-error procedure, if H is not zero, its sign clearly indicates whether the next trial value for the axial load should be larger or smaller.

SIDESWAY BUCKLING

Multi-Bay Frames.—A two-bay frame serves to illustrate the procedure for determining the critical loads of a multi-bay frame in the lurching mode of collapse (Fig. 7).

The equilibrium equations, Eq. 25a,

$$M_{cb} + M_{cd} + M_{cf} = 0 \quad \ldots\ldots\ldots\ldots \quad (34a)$$

$$M_{fc} + M_{fe} = 0 \quad \ldots\ldots\ldots\ldots\ldots \quad (34b)$$

$$S_{ab} + S_{cd} + S_{ef} = - H = 0 \quad \ldots\ldots\ldots\ldots \quad (34c)$$

become, upon substitution of the appropriate expressions,

$$\left(K_{ab} A'_{ab} + 4 K_{bc}\right) \theta_b + 2 K_{bc} \theta_c - K_{ab} C_{ab} c_{ab} \frac{\Delta_{ab}}{L_{ab}} = 0 \quad \ldots \quad (35a)$$

$$2 K_{bc} \theta_b + \left(K_{cd} A'_{cd} + 4 K_{bc} + 4 K_{cf}\right) \theta_c \quad \ldots\ldots\ldots \quad (35b)$$

$$+ 2 K_{cf} \theta_f - K_{cd} C_{cd} c_{cd} \frac{\Delta_{ab}}{L_{cd}} = 0 \quad \ldots\ldots \quad (35c)$$

$$2 K_{cf} \theta_c + \left(K_{ef} A'_{ef} + 4 K_{cf}\right) \theta_f - K_{ef} C_{ef} c_{ef} \frac{\Delta_{ab}}{L_{ef}} = 0 \quad \ldots\ldots \quad (35d)$$

and

$$\frac{K_{ab}}{L_{ab}} C_{ab} c_{ab} \theta_b + \frac{K_{cd}}{L_{cd}} C_{cd} c_{cd} \theta_c + \frac{K_{ef}}{L_{ef}} C_{ef} c_{ef} \theta_f$$

$$- \left(\frac{K_{ab}}{L_{ab}^2} C_{ab} c'_{ab} + \frac{K_{cd}}{L_{cd}^2} C_{cd} c'_{cd} + \frac{K_{ef}}{L_{ef}^2} C_{ef} c'_{ef} \right.$$

$$\left. - \frac{P_{ab}}{L_{ab}} - \frac{P_{cd}}{L_{cd}} - \frac{P_{ef}}{L_{ef}} \right) \Delta_{ab} = H = 0 \quad \ldots\ldots\ldots \quad (35e)$$

As in the previous case, a trial-and-error procedure directed toward the determination of H may be employed. Trial values for the column loads are assumed, and the coefficients in the four equations are evaluated. Setting Δ_{ab} equal to unity, the three joint equilibrium equations are solved for the joint rotations. These values, together with the unit value of Δ_{ab}, are now substituted into the last equation, and the value of H determined. As in the previous case, if H is positive, the assumed column loads exceed their critical values. If, however, H is negative, the loads are less than their critical values. If H vanishes, the loads are equal to their critical values.

If the number of joints is not large, the joint equilibrium equations may be solved easily for the joint rotations by any of the conventional algebraic methods

including Gauss' substitution and elimination procedure, Cramer's determinant method, or Crout's algorithm. If the number of joints is too large to permit the convenient use of these procedures, and if a computer program is not available, the joint equations may be solved by a step-by-step procedure.

Independently Braced Frame.—Frames sometimes exist which are braced against sidesway independently of other frames by structure that may be considered to be external to the frame. This bracing may be in the form of sheathing, wall panels or diagonal tie-rods in the plane of the frame, or, by an eave girt that extends to solid anchorages before and behind the plane of the frame.

In certain cases, support may be provided to a critically loaded frame by adjacent frames that are lightly loaded. This support is transmitted through the bracing system. Such may be the case, for instance, in an industrial building that contains an overhead traveling crane carried by the frames of the building. Obviously, the crane can be in the plane of only one frame at any time, and thus, only this frame could be critically loaded at that time. The other frames, being less than critically loaded, may be able to support the critically loaded frame against sidesway buckling.

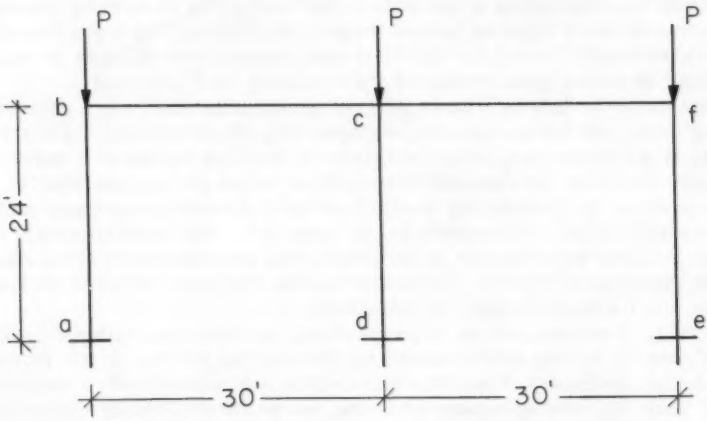

FIG. 8.—REPRESENTATION OF AN INDEPENDENTLY BRACED FRAME

Such bracing often may be represented by a linear spring, as shown in Fig. 8, which also shows the fictitious supporting force, H.

For purposes of illustration, the two-bay frame of the previous section is considered with additional and external bracing represented by the spring shown at joint b.

The three joint equilibrium equations are identical with the first three of Eqs. 35. If k is the stiffness or rate of the spring, then the term $k\Delta_{ab}$ is the spring force. This force acts upon the frame in a direction opposite to the displacement Δ_{ab}, and, for the assumed direction of the displacement, the spring force acts in the positive direction of the fictitious force, H. Consequently, the term $k\Delta_{ab}$ must be added to the fictitious force on the right-hand side of Eq. 35e. Upon transposing this term, the shear equation for the frame becomes

$$\frac{K_{ab}}{L_{ab}} C_{ab}\, c_{ab}\, \theta_b + \frac{K_{cd}}{L_{cd}} C_{cd}\, c_{cd}\, \theta_c + \frac{K_{ef}}{L_{ef}} C_{ef}\, c_{ef}\, \theta_f \quad \ldots\ldots \quad (36a)$$

$$-\left(\frac{K_{ab}}{L_{ab}^2} C_{ab} c'_{ab} + \frac{K_{cd}}{L_{cd}^2} C_{cd} c'_{cd} + \frac{K_{ef}}{L_{ef}^2} C_{ef} c'_{ef} - \frac{P_{ab}}{L_{ab}} - \frac{P_{cd}}{L_{cd}} - \frac{P_{ef}}{L_{ef}} + k\right)\Delta_{ab} = H = 0 \quad \ldots\ldots \quad (36b)$$

and this equation replaces Eq. 35e. The procedure for determining the critical loads from this revised set of equations is essentially the same as that outlined in the previous section.

Sidesway Buckling of Buildings.—The primary structure of certain types of one-story buildings consists of a number of parallel frames interconnected by a bracing system in the form of a truss lying in a horizontal plane at the elevation of the roof or ceiling. In some cases, the horizontal truss is omitted, and the bracing function may be performed by the roof deck. The bracing system should extend over the entire length of the building and be supported by shear walls or by braced frames at the ends of the building or at interior planes. In the absence of shear walls or braced frames, the frames, which are themselves less than critically loaded so that their own independent collapse is not possible, may be called upon to support the critically loaded frames.

Under these conditions, frames will not buckle individually in a sidesway or lurching mode, but rather a general collapse will occur when the loads are sufficiently large, unless a symmetrical mode of buckling occurs at a lower load. A collapse involving the complete structure is called general instability.

The problem of determining whether or not a complete one-story building structure will buckle when a given set of loads is applied simultaneously to all columns includes the elements of the theory that was mentioned previously. In addition, the coupling between the frames and the coincident effect of the frames upon the bracing system must be considered.

One may, of course, arrive at an estimate, or somewhat rational guess, of the stiffness or spring rate provided by the bracing system to the critically loaded frame or frames. When this can be done with satisfactory accuracy, the critical loads of a spring-supported frame can be determined by application of the theory of sidesway buckling for independently braced frames as described previously. However, results obtained by treating the frames independently are not likely to be correct. Although it is a simple matter to obtain a conservative approximation to the critical loads with this approach, the degree of conservatism is difficult to evaluate and may lead to an uneconomical design. A safe estimate for the upper bounds on the critical loads is also difficult to define, and consequently, the designer or analyst may have a wide range from which he must extract the correct values of the critical loads.

The problem of determining the critical loads for a complete one-story structure consisting of a number of parallel frames and a horizontal bracing system is amenable to solution by reasonably simple methods.

For clarity, consider the structure shown in Fig. 9. The structure is assumed to be separated, as shown in the figure, into frames and bracing system. If each frame is loaded in excess of a critical loading, the supporting force H, shown in Fig. 6 and computed by an equation having the character of Eq. 35d, will act to the left on the frame if Δ is a unit displacement to the right. The

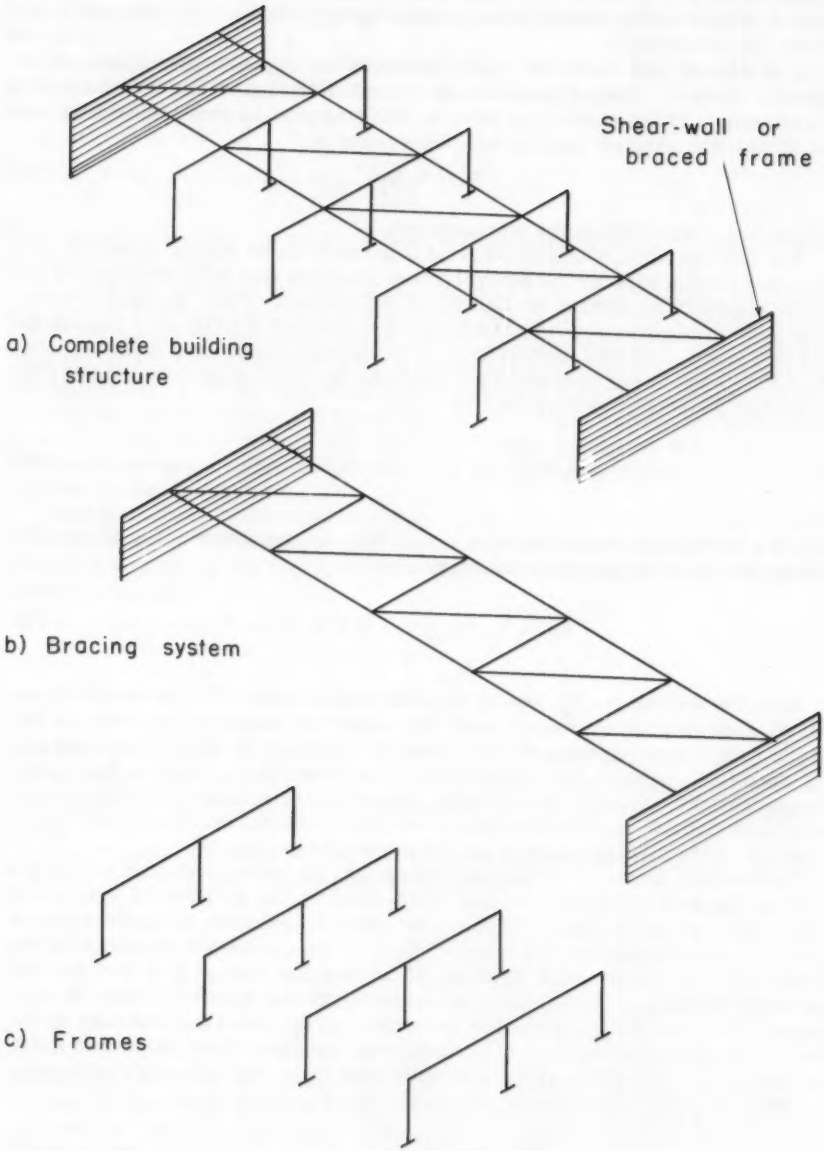

FIG. 9.—COMPLETE STRUCTURE AND ITS COMPONENTS

actual force will be directly proportional to the displacement, and the magnitude of H may be interpreted as a negative spring rate for the unbraced frame under the given loads.

The frames will therefore exert forces in the opposite direction upon the bracing system. Thus, if y_j is actual lateral deflection at the top of the j-th frame, and H_j is the supporting force at that frame per unit displacement, then the total force exerted upon the bracing system is

$$F_j = H_j y_j \quad \ldots\ldots\ldots\ldots\ldots\ldots \quad (37)$$

acting in the direction of the displacement.

The bracing system may be treated separately as an elastic structure, and influence coefficients for the several frame locations may be determined by any of the standard techniques for computing deflections. These influence coefficients are designated a_{ij} and are defined as the lateral deflection at the i-th location due to a unit load applied at the j-th location. Since each frame must be supported, each frame will exert a force upon the bracing system, and the total deflection at the i-th location will be

$$y_i = \sum_{j-1}^{r} F_j a_{ij} \quad (i = 1, 2, \ldots, r) \ldots\ldots\ldots\ldots \quad (38)$$

where r is the number of critically loaded frames. Substituting Eq. 37 into Eq. 38 yields the set of simultaneous equations

$$\sum_{j=1}^{r} a_{ij} H_j y_j = y_i \qquad (i = 1, 2, \ldots, r) \ldots\ldots\ldots\ldots \quad (39)$$

Since the stiffnesses, H_j, depend upon the column loads of the several frames, Eq. 39 defines a set of column loads for which the complete structure is just stable with respect to the sidesway mode of buckling. If the column loads are not specified, a priori, the equations form an eigenvalue problem that yields the permissible values of these loads. However, the relation between the column loads and the frame stiffnesses is so transcendental that the direct determination of the column loads by Eq. 39 is not practical.

Fortunately, from an engineering standpoint, the problem of determining the critical loads of the structure may be replaced by the question of whether or not a specified set of loads will cause the frame to collapse. An answer to this question can be obtained with relative ease, if the question is replaced by the problem of determining the stiffness of the bracing system that will prevent sidesway buckling of the complete structure under the specified loads. In particular, it is desired to determine the factor, μ, by which the stiffness of the bracing system must be multiplied to prevent buckling of the structure under the specified loads. If the stiffness is multiplied by μ, the influence coefficients for deflection are decreased by this factor and Eq. 39 becomes

$$\sum_{j=1}^{r} \frac{a_{ij}}{\mu} H_j y_j = y_i \quad \ldots\ldots\ldots\ldots\ldots\ldots \quad (40a)$$

or

$$\sum_{j=1}^{r} a_{ij} H_j y_j = \mu y_i \quad \ldots\ldots\ldots\ldots\ldots\ldots \quad (40b)$$

The relative values of the y's which satisfy Eqs. 40 can be found by an iterative procedure. After the iterative process has converged, the value of μ can be determined.

One may note that, if the frames are identical and identically loaded, H_j will be the same for all frames and may be replaced by the single value, H. Eq. 40 then may be replaced by

$$\sum_{j=1}^{r} a_{ij}\, y_j = \frac{\mu}{H}\, y_i \qquad \ldots\ldots\ldots\ldots\ldots\ldots (41)$$

This equation, however, is not to be used if the frames differ or if the loadings on the frames differ.

In using the iterative procedure, one assumes a set of y's which preferably are normalized or scaled so that a selected one of the y's has a magnitude of unity. These values are substituted into the left-hand sides of Eqs. 40 or 41. This yields a new and ordinarily more correct set of numbers proportional to the deflections of the bracing system at each frame location. With both the initial set and computed set normalized to unity at the same point, the deflections of the two sets are compared point by point. If the agreement is satisfactory, the magnitude of μ may be computed. If the agreement is not satisfactory, the process should be repeated.

When convergence has been obtained, any of the final set of y's may be used to compute μ. In particular, if $y_i^{(n)}$ represents the values substituted into the left-hand side of Eq. 40, and $y_i^{(n+1)}$ is the value of the right-hand side before normalizing, then

$$\mu = \frac{y_i^{(n+1)}}{y_i^{(n)}} \qquad \ldots\ldots\ldots\ldots\ldots\ldots (42)$$

in which, of course, the same frame location, i, is used in both numerator and denominator. The term μ may be recognized as the "normalizing factor," the quantity by which the output must be divided in order to normalize these quantities.

If the frames are identical and identically loaded so that Eq. 41 may be used in place of Eq. 40, then Eq. 42 may be replaced by

$$\frac{\mu}{H} \quad \frac{y_i^{(n+1)}}{y_i^{(n)}} \qquad \ldots\ldots\ldots\ldots\ldots\ldots (43)$$

Frequently, one wishes to determine the critical loads, under the condition of identical frames and identical loads on all frames, that a given system will support without sidesway collapse. For a given system under these conditions, μ must be taken as unity in Eq. 43, and the criterion for stability becomes

$$H \leq \frac{y_i^{(n)}}{y_i^{(n+1)}} \qquad \ldots\ldots\ldots\ldots\ldots\ldots (44)$$

This equation, however, is to be used only under the conditions stated previously.

The magnitude of μ is the amount by which the stiffness of the bracing system must be multiplied to provide precisely the support that is necessary to prevent sidesway buckling of the complete structure under the imposed loads. Consequently, the computed value of μ serves as a criterion of stability since for stability $\mu \leq 1$, whereas for instability $\mu > 1$.

Several examples will serve to illustrate the methods that have been presented. The reader will recognize that certain simplifications are possible. For example, when the entire structure is composed of the same material and is operating in the elastic range throughout, it may be convenient to divide all constants by the modulus and perhaps by certain dimensional factors. When portions of the structure are operating at different stress levels so that the modulus is different for different members, a reference modulus may be divided out, for example, the elastic modulus. In the interest of clarity, these simplifications are not made in the following examples.

ILLUSTRATIVE EXAMPLES

Symmetrical Buckling of Two-Bay Frame.—In this example the following data is given: the girders are 8 WF 31, the area is 9.12 sq in., $I = 109.7$ in.^{4}; the columns are 8 H 34.3, the area is 10.00 sq in., $I = 35.1$ in.^{4}, and $Q = 10^8$ in.-lbs per radian. For each column

$$P_e = \frac{\pi^2 E I}{L^2} = 125{,}303 \text{ lbs}$$

$$K_{ab} = \frac{30 \times 10^6 \times 35.1}{24 \times 12} = 3.656 \times 10^6 \text{ in.-lbs}$$

$$K_{bc} = \frac{30 \times 10^6 \times 109.7}{30 \times 12} = 9.142 \times 10^6 \text{ in.-lbs}$$

and

$$\frac{Q}{K_{ab}} = \frac{10^8}{3.656 \times 10^6} = 27.35$$

In the symmetrical mode of buckling, $\Delta = 0$, $\theta_c = 0$. Therefore, Eqs. 24a, 25a

$$M_{bc} = K_{bc} \ (4) \ \theta_b \quad \ldots\ldots\ldots\ldots\ldots\ldots \quad (45a)$$

or

$$\left(K_{ab} A'_{ab} + 4K_{bc}\right) \theta_b = 0 \quad \ldots\ldots\ldots\ldots\ldots\ldots \quad (45b)$$

are significant.

Hence, stability criterion becomes

$$A'_{ab} = -4 \frac{K_{bc}}{K_{ab}} = -4 \ \frac{9.142}{3.656} = -10.00$$

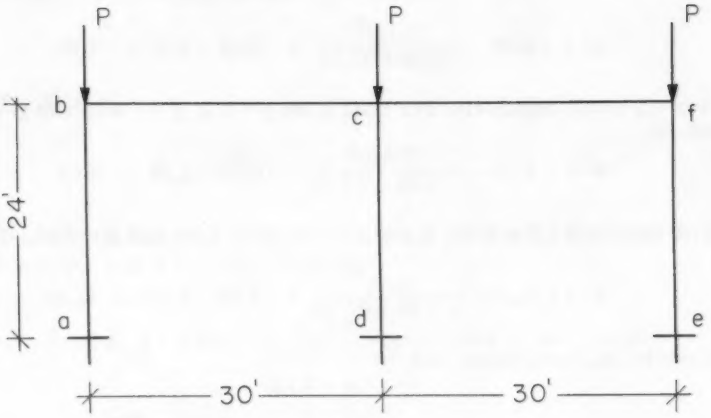

FIG. 10.—ILLUSTRATIVE EXAMPLE TWO BAY FRAMES

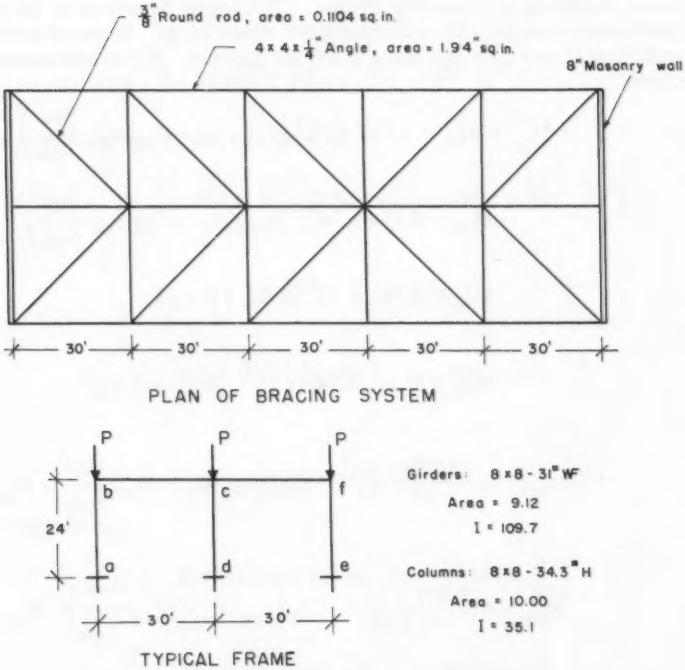

FIG. 11.—ILLUSTRATIVE EXAMPLE—COMPLETE STRUCTURE

for trial 1, for $\rho = 3.0$, A = -5.03 and B = 7.12 from Table 1. Therefore,

$$A' = -5.03 - \frac{(7.12)^2}{-5.03 + 27.35} = -5.03 - 2.27 = -7.30$$

which is too small negatively. For trial 2, for $\rho = 3.1$, A = - 6.05 and B = 7.96. Therefore,

$$A' = -6.05 - \frac{(7.96)^2}{-6.05 + 27.35} = -6.05 - 2.98 = -9.03$$

which is too small. For trial 3, for $\rho = 3.2$, A = - 7.30 and B = 9.02. Therefore,

$$A' = -7.30 - \frac{(9.02)^2}{-7.30 + 27.35} = -7.30 - 4.06 = -11.36$$

By interpolation, for critical load

$$\rho = 3.142$$

and

$$P_{cr} = 3.142\ P_e = 3.142\ (125{,}303) = 393{,}700 \text{ lbs}$$

Sidesway Buckling of Two-Bay Frame.—The same frame is to be used as in the previous example. All columns have equal loads. Mode of buckling is anti-symmetrical and $\theta_f = \theta_b$; also, $\Delta = 0$ for girders. The following equations are derived.

$$M_{ba} = M_{fe} = 3.656 \times 10^6 \left(A'_{ab}\,\theta_b - C_{ab}\,c_{ab}\frac{\Delta_{ab}}{L_{ab}}\right)$$

$$M_{cd} = 3.656 \times 10^6 \left(A'_{cd}\,\theta_c - C_{cd}\,c_{cd}\frac{\Delta_{ab}}{L_{cd}}\right)$$

$$M_{bc} = 9.142 \times 10^6 \left(4\,\theta_b + 2\,\theta_c\right)$$

$$M_{cb} = M_{cf} = 9.142 \times 10^6 \left(4\,\theta_c + 2\,\theta_b\right)$$

$$S_{ab} = -\frac{3.656 \times 10^6}{24 \times 12}\ C_{ab}\left(c_{ab}\,\theta_b - c'_{ab}\frac{\Delta_{ab}}{L_{ab}}\right) - P_{ab}\frac{\Delta}{L_{ab}}$$

and

$$S_{cd} = -\frac{3.656 \times 10^6}{24 \times 12}\ C_{cd}\left(c_{cd}\,\theta_c - c'_{cd}\frac{\Delta_{ab}}{L_{cd}}\right) - P_{cd}\ \frac{\Delta}{L_{ab}}$$

The first two equations are derived from Eq. 13 and the last two from Eq. 14. Since columns are identical and equally loaded, coefficients are the same.

Also, Δ may be taken equal to unity in the final computation.

Joint equilibrium equations are Eqs. 25a and

$$M_{cd} + 2M_{cb} = 0 \quad \ldots\ldots\ldots\ldots\ldots\ldots (46)$$

Also Eq. 34 c or

$$2S_{ab} + S_{cd} = - H = 0 \quad \ldots\ldots\ldots\ldots\ldots\ldots (47)$$

exist.

For trial 1 the following data is obtained: $\rho = 0.9$; P = 0.9 (125,303) = 112,773 lbs; A = 2.645; and B = 2.404. From Eqs. 12

$$A'_{ab} = 2.645 - \frac{(2.404)^2}{2.645 + 27.35} = 2.645 - .193 = 2.838$$

$$C_{ab} = 2.645 + 2.404 = 5.049$$

$$c_{ab} = 1 - \frac{2.404}{2.645 + 27.35} = 1 - .080 = .920$$

and

$$c'_{ab} = 2 - \frac{2.645 + 2.404}{2.645 + 27.35} = 2 - .168 = 1.832$$

The joint equilibrium equations become

$$3.656 \times 10^6 \left(2.838\ \theta_b - 5.049 \times .920\ \frac{\Delta}{L_{ab}}\right)$$

$$+ 9.142 \times 10^6\ (4\ \theta_b + 2\ \theta_c) = 0$$

and

$$3.656 \times 10^6 \left(2.838\ \theta_c - 5.049 \times .920\ \frac{\Delta}{L_{ab}}\right)$$

$$+ 2 \times 9.142 \times 10^6\ (4\ \theta_c + 2\ \theta_b) = 0$$

These reduce to

$$46.944\ \theta_b + 18.284\ \theta_c = 16.9824\ \frac{\Delta}{L_{ab}}$$

and

$$36.568\ \theta_c + 83.512\ \theta_c = 16.9824\ \frac{\Delta}{L_{ab}}$$

which have the solution

$$\theta_b = .34065 \frac{\Delta}{L_{ab}}$$

and

$$\theta_c = .05419 \frac{\Delta}{L_{ab}}$$

Substituting these values into Eq. 14 yields

$$S_{ab} = \frac{-3.656 \times 10^6}{288} 5.049 \quad (.920 \times .34065 - 1.832) \frac{\Delta}{L_{ab}}$$

$$-112,773 \frac{\Delta}{L_{ab}} = -15,414 \frac{\Delta}{L_{ab}}$$

and

$$S_{cd} = \frac{-3.656 \times 10^6}{288} 5.049 \quad (.920 \times .05419 - 1.832) \frac{\Delta}{L_{ab}}$$

$$-112,773 \frac{\Delta}{L_{ab}} = 1,443 \frac{\Delta}{L_{ab}}$$

and, consequently,

$$H = (15,414 - 1,443 + 15,414) \frac{\Delta}{L_{ab}} = 29,385 \frac{\Delta}{L_{ab}}$$

Since H is positive for positive values of Δ, the frame is unstable under the assumed loads.

For trial 2 the following data is obtained: $\rho = 0.8$; P = 0.8 (125,303) = 100,243 lbs; A = 2.816; and B = 2.346. The equations, therefore, are

$$A'_{ab} = 2.816 - \frac{(2.346)^2}{2.816 + 27.35} = 2.634$$

$$C_{ab} = 2.816 + 2.346 = 5.162$$

$$c_{ab} = 1 - \frac{2.346}{2.816 + 27.35} = 1 - .078 = .922$$

and

$$c'_{ab} = 2 - \frac{2.816 + 2.346}{2.816 + 27.35} = 2 - .171 = 1.829$$

The joint equilibrium equations, Eqs. 25a and 46 become

$$3.656 \times 10^6 \left(2.634\ \theta_b - 5.162 \times .922\ \frac{\Delta}{L_{ab}}\right)$$

$$+ 9.142 \times 10^6\ (4\ \theta_b + 2\ \theta_c) = 0$$

and

$$3.656 \times 10^6 \left(2.634\ \theta_c - 5.162 \times .922\ \frac{\Delta}{L_{ab}}\right)$$

$$+ 2 \times 9.142 \times 10^6\ (4\ \theta_c + 2\ \theta_b) = 0$$

and reduce to

$$46.198\ \theta_b + 18.284\ \theta_c = 17.4002\ \frac{\Delta}{L_{ab}}$$

and

$$36.568\ \theta_b + 82.766\ \theta_c = 17.4002\ \frac{\Delta}{L_{ab}}$$

These have the solution

$$\theta_b = .35562\ \frac{\Delta}{L_{ab}}$$

and

$$\theta_c = .05311\ \frac{\Delta}{L_{ab}}$$

The shears become

$$S_{ab} = \frac{-3.656 \times 10^6}{288}\ 5.162\ (.922 \times .35562 - 1.829)\ \frac{\Delta}{L_{ab}}$$

$$- 100{,}243\ \frac{\Delta}{L_{ab}}$$

and

$$S_{cd} = \frac{-3.656 \times 10^6}{288}\ 5.162\ (.922 \times .05311 - 1.829)\ \frac{\Delta}{L_{ab}}$$

$$- 100{,}243\ \frac{\Delta}{L_{ab}}$$

or

$$S_{ab} = (98{,}359 - 100{,}243)\ \frac{\Delta}{L_{ab}} = -1{,}884\ \frac{\Delta}{L_{ab}}$$

and

$$S_{cd} = (116{,}641 - 100{,}243)\frac{\Delta}{L_{ab}} = 16{,}398\frac{\Delta}{L_{ab}}$$

Consequently,

$$H = -(-1{,}884 + 16{,}398 - 1{,}884)\frac{\Delta}{L_{ab}} = -12{,}630\frac{\Delta}{L_{ab}}$$

The sign of H shows that the frame is stable under the assumed loads. Comparison with the previous trial indicates that critical loads lie between the magnitudes assumed for the two trials. By interpolating between these two cases, the critical loads may be found to correspond to $\rho = 0.83$ or $P_{cr} = 0.83 \times 125{,}303 = 104{,}000$ lbs on each column.

It should be noted that the axial loads on the three columns need not be equal. A similar method of analysis would apply as long as the axial loads on the two outer columns were equal and the frame was symmetrical. If the axial load on the center column differs from that on each of the outer columns, or if the properties of the center column differ, the coefficients and constants will, of

TABLE 2.—INFLUENCE[a] COEFFICIENTS, a_{ij}

Location of Deflection, i	Location of Unit Load, j			
	Frame 1	Frame 2	Frame 3	Frame 4
Frame 1	127,266	98,200	67,279	46,180
Frame 2	98,200	194,440	135,584	67,279
Frame 3	67,279	135,584	197,415	117,885
Frame 4	46,180	67,279	117,885	127,885

[a] The influence coefficients are in units of 10^{-6} in per lb.

course, be different for this column. However, only two joint equilibrium equations will still suffice. If the loadings of all three columns differ, or if the frame is not symmetrical, it will be required to write and solve simultaneously three joint equilibrium equations in the three rotations.

Sidesway Buckling of Complete Frame.—In this example, a complete structure, comprising four parallel frames and a bracing system as shown in Fig. 11, is considered. The frames are identical with those used in the previous examples, and the columns are assumed to be restrained elastically as in the previous examples. The bracing system is supported at its ends by masonry walls.

By conventional techniques for computing deflections, such as the Maxwell-Mohr method, the deflections of the bracing system due to unit loads applied at each frame location have been computed and are listed in Table 2.

Substituting the numerical values of the a_{ij} into Eq. 40 gives for the displacements of the bracing system at each of the frame locations

$$127.266\,H_1y_1 + 98.200\,H_2y_2 + 67.279\,H_3y_3 + 46.180\,H_4y_4 = 10^6\,\mu\,y_1$$

$$98.200\,H_1y_1 + 194.440\,H_2y_2 + 135.584\,H_3y_3 + 67.279\,H_4y_4 = 10^6\,\mu\,y_2$$

$$67.279\,H_1y_1 + 135.584\,H_2y_2 + 197.415\,H_3y_3 + 117.885\,H_4y_4 = 10^6\,\mu\,y_3$$

and

$$46.180\ H_1y_1 + 67.279\ H_2y_2 + 117.885\ H_3y_3 + 127.885\ H_4y_4 = 10^6\ \mu\ y_4$$

To determine whether a given set of loads will or will not cause the structure to buckle in the sidesway mode, one first computes H for each frame by the method previously described in connection with the discussion of sidesway or anti-symmetrical buckling of independent frames that is illustrated in the previous example. These numerical values are then substituted into the previous set of equations, (those derived from Eq. 40) and iterations are performed upon these equations to obtain the mode shape of the buckled structure. Finally, the value of μ is found by use of Eq. 42 and the inequalities for stability conditions are applied to determine whether the frame is stable or unstable.

TABLE 3.—ITERATED VALUE OF DEFLECTIONS

	y_1	y_2	y_3	y_4
Second Cycle	271.5	428.6	448.1	296.3
Normalized	0.606	0.956	1.000	0.661
Third Cycle	268.8	425.4	445.7	294.7
Normalized	0.603	0.954	1.000	0.661
Fourth Cycle	268.2	424.8	445.3	294.4
Normalized	0.602	0.954	1.000	0.662
Fifth Cycle	268.1	424.7	445.3	294.5
Normalized	0.602	0.954	1.000	0.661
$y^{(5)}/y^{(4)}$	445.3	445.2	445.3	445.5

The case of identical loads on all frames is considered first. Each of the previous set of equations is divided through by the common factor H and become

$$127.266\ y_1 + 98.200\ y_2 + 67.279\ y_3 + 46.180\ y_4 = 10^6\ \frac{\mu}{H}\ y_1$$

$$98.200\ y_1 + 194.440\ y_2 + 135.584\ y_3 + 67.279\ y_4 = 10^6\ \frac{\mu}{H}\ y_2$$

$$67.279\ y_1 + 135.584\ y_2 + 197.415\ y_3 + 117.885\ y_4 = 10^6\ \frac{\mu}{H}\ y_3$$

and

$$46.180\ y_1 + 67.279\ y_2 + 117.885\ y_3 + 127.885\ y_4 = 10^6\ \frac{\mu}{H}\ y_4$$

Relative values of the y's are found by iteration starting with arbitary initial values. Suppose that initial values 0.700, 1.000, 1.000, and 0.700 are used; upon substituting into the left-hand side of the first equation, the following result is obtained:

$$127.266\ (0.700) + 98.200\ (1.000) + 67.279\ (1.000) + 46.180\ (0.700) = 286.9$$

Substituting the initial values into the remaining three equations yields values of 445.9, 462.6, and 307.0, respectively. It is convenient to normalize these

numbers by dividing by the magnitude of one of the quantities, usually the largest. On this basis, the normalized results become 0.620, 0.964, 1.000, 0.664. Evidently, these values do not agree with the initially assumed values and must be used as the basis for a second cycle of computations. This process is repeated until convergence is obtained, requiring about five cycles in the present example.

Although the iterations were carried through the fifth cycle, it is evident that the results of the third cycle have sufficient accuracy for practical purposes. However, using the final results for y_3 and Eq. 44, and recalling that the right-hand sides of the deflection equations were $10^6\, y_i\, \mu/H$,

$$10^{-6} H = \frac{1}{445.3}$$

in which μ has been taken as unity to indicate that no additional stiffening is contemplated. This yields a value of H of 2246 lbs.

Comparing the results of the third cycle before normalizing with the normalized values of the second cycles, that may be interpreted as input for the third cycle, yields the ratios 443.5, 445.0, 445.7, and 445.8 at the four locations. It can be shown by rigorous mathematical process, that the correct value of $10^6\, \mu/H$ lies at, or between, the limiting values of this range; that is,

$$443.5 \leqq 10^6\, \mu/H \leqq 445.8$$

or, with μ taken equal to unity

$$2243 \leqq H \leqq 2255 \text{ lbs}$$

The range, and therefore the maximum possible error, is about 0.5 % so that it is likely that the results of the third cycle would have been sufficiently accurate for practical purposes.

It is now necessary to find the magnitudes of the column loads that when applied to the frame will produce an H of this magnitude.

The columns of each frame are taken, by the conditions of the problem, to be equally loaded. For a first trial, a value of $\rho = 2.2$ is assumed for each column. The trial value of the load is

$$P = 2.2\, P_e = 2.2\, (125{,}303) = 275{,}667 \text{ lbs}$$

From Table 1, for $\rho = 2.2$, $A_{ab} = -0.519$, and $B_{ab} = 3.901$. Also,

$$C_{ab} = 3.382$$

$$A'_{ab} = -0.519 - \frac{(3.901)^2}{-0.519 + 27.35} = -1.086$$

$$c_{ab} = 1 - \frac{3.901}{-0.519 + 27.35} = 0.8546$$

$$c'_{ab} = 2 - \frac{3.382}{-0.519 + 27.35} = 1.8739$$

and

$$C_{ab}\, c_{ab} = 2.8903$$

The formulas for relevant moments are, by Eqs. 1 and 13,

$$M_{ba} = 3.656 \times 10^6 \left(- 1.086\ \theta_b - 2.8903\ \frac{\Delta}{L} \right)$$

$$M_{bc} = 9.152 \times 10^6 \left(4\ \theta_b + 2\ \theta_c\right);\ M_{cb} = 9.152 \times 10^6 \left(4\ \theta_c + 2\ \theta_b\right)$$

and

$$M_{cd} = 3.656 \times 10^6 \left(- 1.086\ \theta_c - 2.8903\ \frac{\Delta}{L} \right) = M_{cf}$$

The joint equilibrium equations, Eqs. 25a and 34a, become, upon reduction,

$$8.916\ \theta_b + 5.001\ \theta_c = 2.8903\ \frac{\Delta}{L}$$

and

$$10.002\ \theta_b + 18.918\ \theta_c = 2.8903\ \frac{\Delta}{L}$$

and their solution is

$$\theta_b = 0.3390\ \frac{\Delta}{L}$$

and

$$\theta_c = - 0.0265\ \frac{\Delta}{L}$$

The column shears obtained by use of Eq. 14, are,

$$S_{ab} = S_{ef} = \frac{- 3.656 \times 10^6 \times 3.382}{288} \left(.8546 \times .3390\ \frac{\Delta}{L} - 1.8739\ \frac{\Delta}{L} \right)$$

$$- 275{,}667\ \frac{\Delta}{L} = - 207{,}653\ \frac{\Delta}{L}$$

and

$$S_{cd} = \frac{- 3.656 \times 10^6 \times 3.382}{288} \left(- .8546 \times .0265\ \frac{\Delta}{L} - 1.8739\ \frac{\Delta}{L} \right)$$

$$- 275{,}667\ \frac{\Delta}{L} = - 194{,}245\ \frac{\Delta}{L}$$

With $\Delta = 1$ and $L = 288$

$$H = - S_{ab} - S_{cd} - S_{ef} = 2{,}116 \text{ lbs}$$

This value is slightly below the value of 2246 lbs that was found to define the limit of stability. Therefore, the assumed trial value of the column loads is too low. A slightly greater load should be chosen for a second trial, if the critical load is to be established.

Following the above procedure, and with an assumed load corresponding to $\rho = 2.4$, or $P = 2.4\ (125{,}303) = 300{,}727$ it may be determined that $H = 2351$ lbs. By interpolation it is found that, for $H = 2246$ lbs, $\rho = 2.311$, which determines the critical load to be $P_{cr} = 2.311\ (125{,}303) = 289{,}575$ lbs.

Sidesway Buckling with Unequally Loaded Frames.— The theory and general procedure are applicable to cases in which the frames are not identical or not identically loaded. As an example, the frame of the previous problem is checked for stability for loads equal to 2.4 ρ on the third frame and 2.2 ρ on the remaining frames.

Since the bracing system is unchanged from the previous problem, the table of influence coefficients is also unchanged. Eqs. 40 become

$$127.266 \times 2116\ y_1 + 98.200 \times 2116\ y_2 + 67.279 \times 2351\ y_3 + 46.180 \times 2116\ y_4 = 10^6\ \mu y_1$$

$$98.200 \times 2116\ y_1 + 194.440 \times 2116\ y_2 + 135.584 \times 2351\ y_3 + 67.279 \times 2116\ y_4 = 10^6\ \mu y_2$$

$$67.279 \times 2116\ y_1 + 135.584 \times 2116\ y_2 + 197.415 \times 2351\ y_3 + 117.885 \times 2116\ y_4 = 10^6\ \mu y_3$$

and

$$46.180 \times 2116\ y_1 + 67.279 \times 2116\ y_2 + 117.885 \times 2351\ y_3 + 127.885 \times 2116\ y_4 = 10^6\ \mu y_4$$

These reduce to

$$0.26929\ y_1 + 0.20779\ y_2 + 0.15817\ y_3 + 0.09772\ y_4 = \mu y_1$$

$$0.20779\ y_1 + 0.41144\ y_2 + 0.31876\ y_3 + 0.14236\ y_4 = \mu y_2$$

$$0.14236\ y_1 + 0.28690\ y_2 + 0.46412\ y_3 + 0.24944\ y_4 = \mu y_3$$

and

$$0.09772\ y_1 + 0.14236\ y_2 + 0.27715\ y_3 + 0.27060\ y_4 = \mu y_4$$

For starting the iterative process, initial relative deflections are selected arbitrarily and substituted into the left-hand sides of the preceding equations.

The computed values of μy_i are then normalized and again substituted into the above equations. The process, repeated until convergence is obtained, is recorded in the Table 4.

Evidently, the third cycle has converged and can serve as an accurate basis for determining the stiffness factor. By Eq. 42, using the values for y_3,

$$\mu = \frac{0.981}{1.000} = 0.981$$

Since this quantity is less than unity, the structure is stable under the assumed loads. In fact, the loads may be increased somewhat before the structure would buckle in the sidesway mode. It may be noted that the same result would be obtained by using the values at any of the other frames. It is also worthy of mention that the lower and upper limits based upon the results of the second cycle are

$$0.977 \leq \mu \leq 0.984$$

Thus, if the process were stopped at this point and the average value of μ were used, it would be known to be correct to within $\pm$ 0.3%.

TABLE 4.—ITERATED VALUES OF DEFLECTIONS

	y_1	y_2	y_3	y_4
Initial	0.600	0.900	1.000	0.650
First Cycle	0.570	0.906	0.970	0.640
Normalized	0.588	0.934	1.000	0.659
Second Cycle	0.575	0.919	0.980	0.646
Normalized	0.587	0.938	1.000	0.659
Third Cycle	0.576	0.920	0.981	0.646
Normalized	0.587	0.938	1.000	0.659

In order to establish the magnitudes of the critical loads, the stability of the structure under a second set of assumed heavier loads may be investigated. If, however, it is only desired to obtain a fairly dependable estimate of the critical load on the third frame when the loads on the columns of the remaining frames are 2.2 times the Euler loads, such an estimate may be obtained by an extrapolation based upon the present and the previous example.

To implement this approach, one may note from the previous problem that, under identical loads on all frames, it was established that

$$10^6 \frac{\mu}{H} = 445.3$$

and also that H = 2116 lbs when $\rho = 2.2$. Consequently, at this loading

$$\mu = 445.3 \times 2116 \times 10^{-6} = 0.942$$

Extrapolation based upon $\mu = 0.942$ when $\rho_3 = 2.2$, and $\mu = 0.981$ when $\rho_3 = 2.4$, yields $\mu = 1.000$ when $\rho_3 = 2.497$. Hence, when the axial loads on the columns of frames 1, 2, and 4 are 275,677 pounds per column, the axial loads on the columns of frame 3 are 2.497 x 125,303 = 312,882 lb.

Journal of the
STRUCTURAL DIVISION
Proceedings of the American Society of Civil Engineers

LONG SPAN PRESTRESSED CONCRETE FOLDED PLATE ROOFS[a]

By John C. Brough, Jr.,[1] M. ASCE, and B. H. Stephens, Jr.,[2] A. M. ASCE

SYNOPSIS

The design and construction of long span prestressed concrete folded plate structures are presented herein. The economics of such design is indicated by including actual construction costs of four roof structures. A simplified design procedure is outlined and a typical case presented. Field experience with construction methods utilized and recommendations for field inspections are included based on the authors' observations.

INTRODUCTION

The design and construction methods utilized for creating low cost, long span, fire resistant roof structures are presented. It is generally agreed that building costs must be reduced to the minimum, yet the continuing demand for longer spans usually results in pushing cost ever upward.

It has also been recognized that in order to obtain longer span construction, the shape of the structure becomes a dominant factor. The proper utilization of shape for economical usage of material can and does result in enhancing the esthetic value. The full utilization of the structural shape eliminates the addition of superfluous embellishment that can become quite expensive.

Note.—Discussion open until March 1, 1961. To extend the closing date one month, a written request must be filed with the Executive Secretary, ASCE. This paper is part of the copyrighted Journal of the Structural Division, Proceedings of the American Society of Civil Engineers, Vol. 86, No. ST 10, October, 1960.

[a] Presented at the March 1960 ASCE Convention in New Orleans, La.

[1] Cons. Engr., Memphis, Tenn.

[2] Assoc., John C. Brough, Jr., Cons. Engrs. Struct., Memphis, Tenn.

The folded plate shape of roof structure has come into wide usage because of its low cost of construction for long span, high load carrying capacity, rigidity, and because it furnishes esthetic interest. Selection of concrete for the shell material furnishes a high degree of fire resistivity, ease of molding to the desired alinement and profile, a great degree of permanence, and low construction and maintenance costs.

The decision for utilizing concrete narrows is the remaining problem to that of obtaining the most economical usage of materials that will provide the required loading capacity. The profile of the folded plate roof has an important bearing on the economy of the structure. This corrugated configuration can, however, have many variations to accomplish the requirements of the construction. Each must meet the needs of its span conditions, that is simple span or multiple span with varying conditions of continuity.

Let us consider, for example, a simple span of $62\frac{1}{2}$ ft in which we shall arbitrarily assume a column spacing along the ends of this longer span of, say, 23 ft. The slope of each plate will be assumed to be $3\frac{1}{2}$-on-12, vertical to horizontal (Fig. 1). A trial analysis will indicate this corrugated configuration to be unsuitable for conventionally reinforced concrete due to the very small area of concrete available at the ridge, causing high compressive stresses and a very high percentage of steel reinforcement necessary. This can primarily be attributed to the shallow ratio of depth from ridge to valley for the long span of $62\frac{1}{2}$ ft and the absence of sufficient concrete area in the ridge.

Several remedies for this condition become readily apparent. These could be (1) to steepen the slope of the plate and add a third plate horizontally at the ridge to provide sufficient concrete area to reduce the high compressive stresses, (2) to steepen the slope of the plates in order to provide a deeper section from ridge to valley, (3) to provide a combination of each of those stated in (1) and (2), or (4) prestress the structure to utilize all of the concrete area as a homogeneous section.

This paper shall advance a method of analysis for the design of post-tensioned prestressed concrete folded plate structures. The entire cross-sectional area of concrete of each plate will thus be utilized for flexure as a homogeneous section.

The design of the structure is more easily understood with the assumption of one individual leaf isolated from the others (Fig. 2). Consider the plate oriented in its working position and compute its section properties about the horizontal axis extending through its center of gravity.

Notation.—The letter symbols adopted for use in this paper are defined where they first appear, in the illustrations or in the text, and are arranged alphabetically, for convenience of reference in the Appendix.

DERIVATION OF FORMULA UTILIZED

Fig. 2 indicates the terms used in the following presentation. The formulas used in the design will be derived.[3] The moment of inertia of an inclined plate on a horizontal axis taken thru c. g. of section is derived as follows:

$$d_A = t\ d_x \quad \ldots\ldots\ldots\ldots\ldots\ldots \quad (1a)$$

$$d_Y = a/12\ d_x \quad \ldots\ldots\ldots\ldots\ldots\ldots \quad (1b)$$

[3] "Design of Prestressed Concrete Structures," by T. Y. Lin.

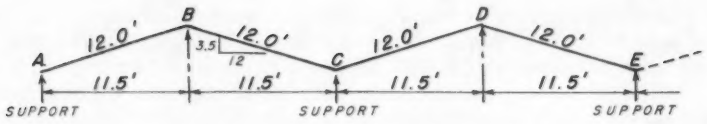

FIG. 1.—TYPICAL CROSS SECTION THRU MULTIPLE FOLDS

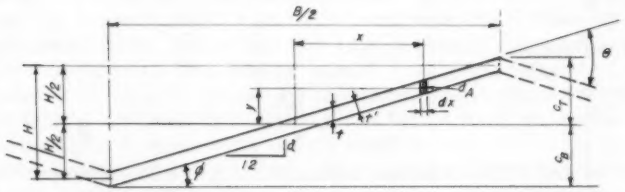

FIG. 2.—SECTION PROPERTIES OF ONE FOLDED PLATE.

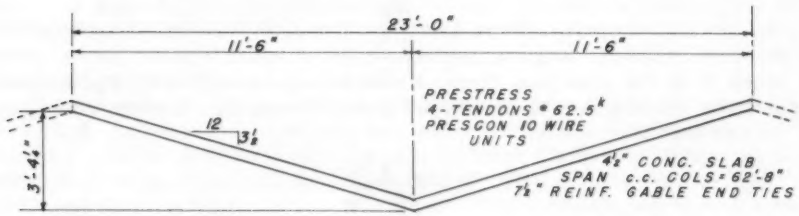

FIG. 3.—RICHLAND ELEMENTARY SCHOOL—MEMPHIS, TENNESSEE

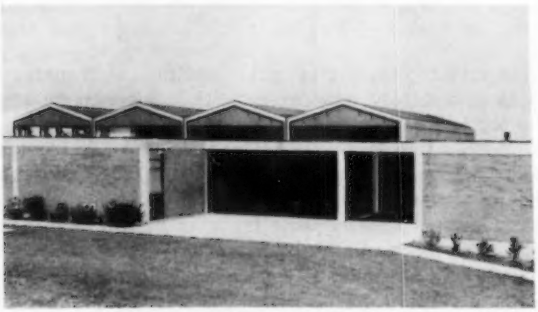

FIG. 4.—FRONT ELEVATION OF RICHLAND ELEMENTARY SCHOOL

$$d_x = 12/a\ d_y \quad \ldots\ldots\ldots\ldots\ldots\ldots (1c)$$

$$I = \int_{-H/2}^{+H/2} y^2\, t\, dx = \int_{-H/2}^{+H/2} y^2 \left(t\,\frac{12}{a}\right) dy = \frac{12\,t}{a} \int_{-H/2}^{+H/2} y^2\, dy \quad \ldots\ldots (2a)$$

and

$$I = \frac{12t}{a}\left[\begin{matrix}+H/2 \\ \\ -H/2\end{matrix}\ \frac{y^3}{3}\right] = \frac{12\,t}{a}\left[\frac{\left(\frac{H}{2}\right)^3}{3} + \frac{\left(\frac{H}{2}\right)^3}{3}\right] = \frac{12\,t}{a}\left[\frac{H^3}{24} + \frac{H^3}{24}\right] \quad \ldots\ldots (2b)$$

from which we obtain

$$I = \frac{t}{a}\,H^3 \quad \ldots\ldots\ldots\ldots\ldots\ldots (3)$$

in which t′ is the slab thickness normal to slope, a is the slope rise on 12, t is the vertical thickness of slab, and H refers to the height valley to ridge center to center.

The tensioning force required for zero stress in the bottom under working load, midspan is

$$F = \frac{M_{tl}}{e + k_t} \quad \ldots\ldots\ldots\ldots\ldots\ldots (4)$$

in which F is the prestress force, e refers to the eccentricity of prestress force from the c. g. and k_t is the kern point. The top fiber stress, mid-span at working load is

$$f_{ct} = \frac{F\,H}{A_c\,C_b} \quad \ldots\ldots\ldots\ldots\ldots\ldots (5)$$

in which f_c is the allowable concrete unit stress, H is the vertical height of the section valley to the ridge, and A_c is the area of the concrete. The bottom fiber stress at initial condition at transfer

$$f_{cb} = \frac{F_i}{A_c}\left[1 + \frac{e - \left(M_{dl}/F_i\right)}{k_t}\right] \quad \ldots\ldots\ldots\ldots (6)$$

in which the subscript i indicates the condition at transfer of prestress.

The section is completely supported in this position by adjoining leaves connected at the top and bottom of the plate under consideration.

The stress distribution acting axially along the longitudinal axis is the same as for any homogeneous beam, that is, rectangular in shape. The top surface will be in compression, the bottom in tension under gravity loads. Application of a sufficient prestressing force at a suitable distance below the center of gravity of the section can eliminate the tension stresses. This is the same principle utilized in all prestressed concrete.

The transverse direction of the plate is analysed as a continuous slab of length equal to the width of the plate and supported at the fold lines of the ridges and valleys. These spans being quite short thus require only nominal

steel reinforcing as dictated by slab thickness and bending moment. Distribution bars are provided in the longitudinal direction in an amount ordinarily utilized for temperature steel.

The prestressing tendons extending in the longitudinal direction of the plate are draped parabolically to locate the center of force at or above the lower kern point at the ends of the span. This will prevent the occurrence of top tension in the concrete at the ends of the span.

The eccentric force application by the prestressing-steel cambers the section along its longitudinal axis, offsetting the deflection normally present in conventionally reinforced concrete. The resulting camber supports the plate in its geometrical position, thus eliminating critical secondary stresses caused by rotation of the ends at the supports that would be inevitable with deflections encountered in conventionally reinforced concrete. Reductions of the plate action deflections along the ridges and valleys permit analysis of the transverse slab by moment distribution with a reasonable degree of accuracy.

The ends of the plates behind the anchorage are thickened to provide for distribution of the concentrated force applied by the tendons. Additional reinforcing in the form of transverse and tie steel is provided in the area immediately behind the tendon anchorages to resist the bursting of the concrete created by the prestress force.

The end leaves of a transverse section through the structure must be provided with tension ties to resist the horizontal force component. This may be accomplished by providing a tie beam, gable wall or other means, at or near the supports, that is adequate for resistance of the horizontal reaction.

Construction methods utilized for forming, steel placement, concrete placement, curing and protection, tendon tensioning, and grouting follow the normal construction techniques.

The authors have four projects completed to date (1960), utilizing post-tensioned, prestressed, cast-in-place concrete folded plate designs. The earliest was a roof structure for the Richland Elementary School for the Memphis, Tenn., Board of Education (Fig. 3). This building was designed in 1956, and constructed in 1957. A photograph of the complete building is shown in Fig. 4. An addition, including additional folds to the prestressed concrete folded plate roof over the cafetorium is under construction (1960).

The Memphis Art Academy also utilized the methods described in this presentation (Figs. 5 and 6). The prestressed folded plate roof covers the third floor and is located approximately 50 ft above the first floor. Shoring had to be provided for the entire height in order to construct this structure in place. At some future date this project will be enlarged to approximately four times its present completed size. The addition will extend the folded plate roof from its present size of 69 ft by 98 ft-4 in. to proposed dimensions of 320 ft by 98 ft-4 in. and cover an entire fine arts center.

The Holiday Inn in Sarasota, Fla., utilizes a prestressed folded plate roof over the one story private club facilities (Fig. 7). A different exterior appearance was achieved as the ends of the roof folds were cantilevered beyond the end walls, the gables are open and glazed, and thrust being taken by tension ties between supporting columns located approximately 3 ft below the low point of the valleys. The valley frequency of 15 ft is appreciably shorter than the other projects being described.

The most recently completed project to be described is the Richland Junior High School (Figs. 8-10) for the Memphis Board of Education. This project provides the largest area covered (to 1960) by means of the methods described

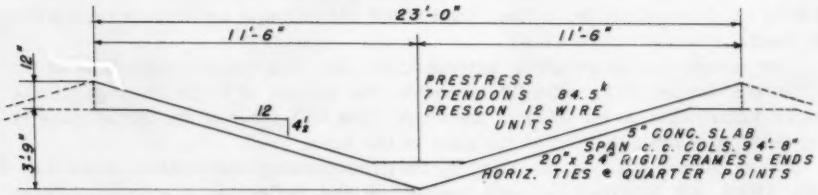

FIG. 5.—MEMPHIS ACADEMY OF ARTS—MEMPHIS, TENNESSEE

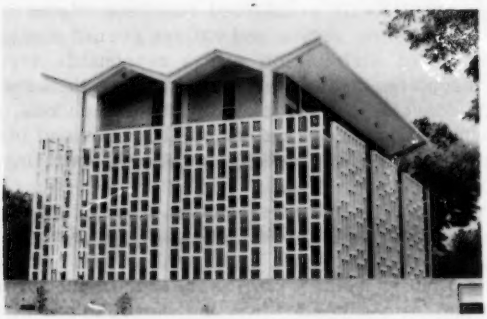

FIG. 6.—MEMPHIS ART ACADEMY

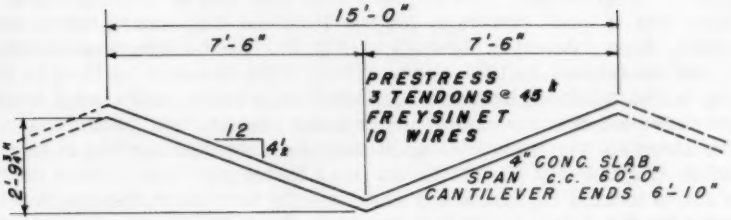

FIG. 7.—HOLIDAY INN, SARASOTA, FLORIDA

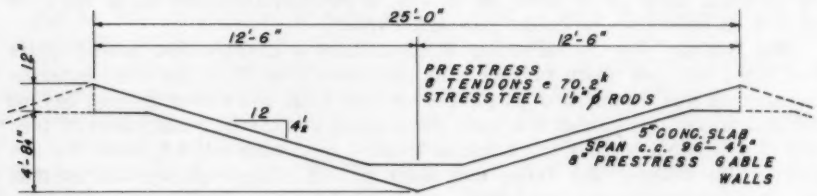

FIG. 8.—RICHLAND JUNIOR HIGH SCHOOL—MEMPHIS, TENNESSEE

FIG. 9.—EXTERIOR VIEW OF FOLDED PLATE ROOF UPON COMPLETION OF CONCRETE PLACING. RICHLAND JUNIOR HIGH SCHOOL.

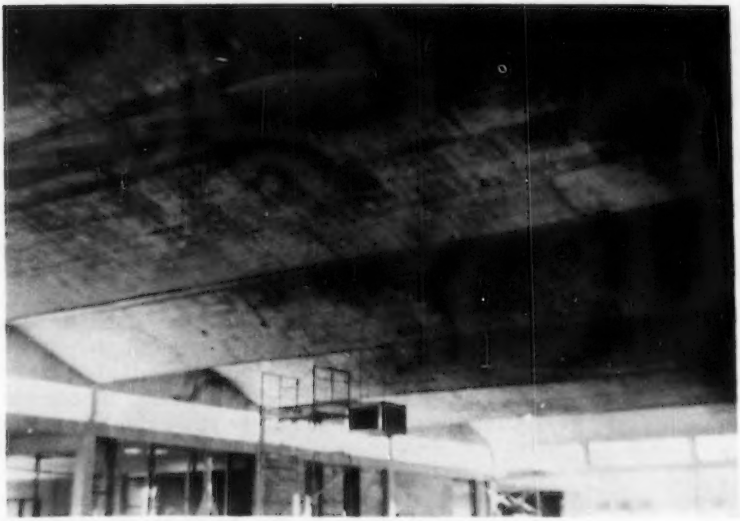

FIG. 10.—INTERIOR VIEW OF UNDERSIDE OF FOLDED PLATE ROOF IMMEDIATELY AFTER FORM REMOVAL. RICHLAND JUNIOR HIGH SCHOOL.

in this presentation. This roof structure encloses a gymnasium and a cafetorium. The span is $96\frac{1}{2}$ ft and slab thickness of 5 in. was necessary for the valley frequency of 25 ft.

Insulation of the folded plate roof slabs on each of the four projects described in this paper was accomplished by means of welded wire mesh reinforced vermiculite cast-in-place concrete. An excellent insulating coefficient was obtained by using a mix proportion of one part portland cement to six parts of vermiculite aggregate.

Rooifing materials for the Richland Elementary School and Holiday Inn was of the conventional type having a five-ply built-up asphalt and felt, with gravel surfacing. Roofing for the Memphis Art Academy and the Richland Junior High School projects was "Cocoon," which is a vinyl-plastic sprayed on finish. Color selected was white.

Ceilings within each of the structures were finished vermiculite acoustical plastic applied directly to the bottom surfaces of the concrete slab. Thus, a pleasing esthetic value was achieved which was proven to have very excellent acoustic absorbsion characteristics. The total completed structures accomplished very economical and attractive enclosures for very large areas with long clear spans.

CONSTRUCTION METHODS

Forming was accomplished by utilizing steel scaffolding of the demountable type. For shoring to the ground, wood trussed rafters were placed on top of this scaffolding (Fig. 11). The trussed rafters simplified the erection of the straight gable shape of each bay. The deck was placed, using $\frac{3}{4}$ in. plywood applied directly to the top of the wood trussed rafters. The design considerations for dimensioning the structure to use full size sheets of plywood realized maximum economy in forming.

Reinforcement-placing was handled in the conventional manner with variation in placing sequence. Bottom layer reinforcement was the longitudinal distribution steel, supported on slab bolsters extending from valley to ridge. The slab's positive moment reinforcement, extending transversely, was placed on top of the distribution steel. The prestressing tendons were placed directly on top of the bottom steel and tied to the bottom mat at the correct location in the leaf. Tendons were draped in parabolic curves (Fig. 12) spaced 3 in. on center at the center of the long span and raised to locate the center of prestress force at the bottom kern point at the ends. The bottom tendon extended straight through at the valley. After all tendons were placed, the end bearing plates were substantially anchored to the end form. All cable sheaths were carefully examined to repair any separation or indentation that could permit leakage of cement mortar and hamper elongation of the prestress reinforcement. The reinforcing bars for slab negative moments at the valleys and ridges, stirrup ties and grids for resistance of bursting of concrete at the end anchorages were placed last. Fig. 13 shows the placement of prestress tendons, anchorage plates, and conventional reinforced steel at a valley support location.

Prestressing tendon couplers that were necessary for the long cables were arranged in a staggered pattern as shown in Fig. 14. Concrete placing was accomplished with concrete slumps ranging from 2 in. to 3 in. Vibration was

FIG. 11.—SCAFFOLD SUPPORT OF FORMING FOR RICHLAND JUNIOR HIGH SCHOOL

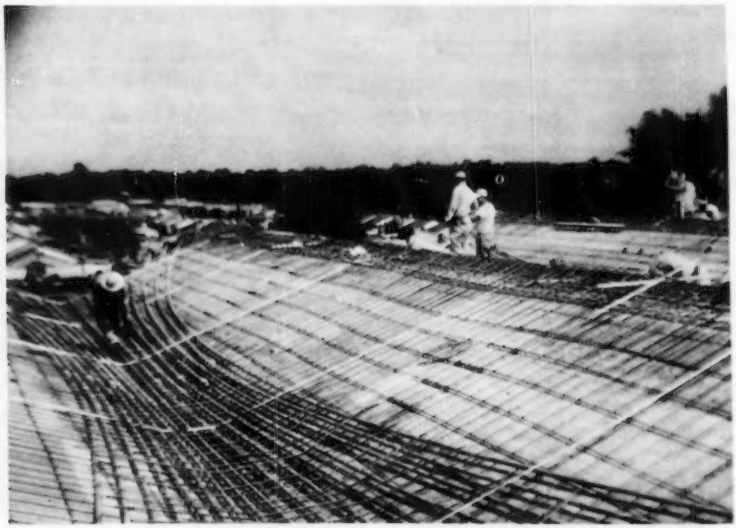

FIG. 12.—PRESTRESS TENDONS AND REINFORCING FOR FOLDED PLATE ROOF OF RICHLAND JUNIOR HIGH SCHOOL

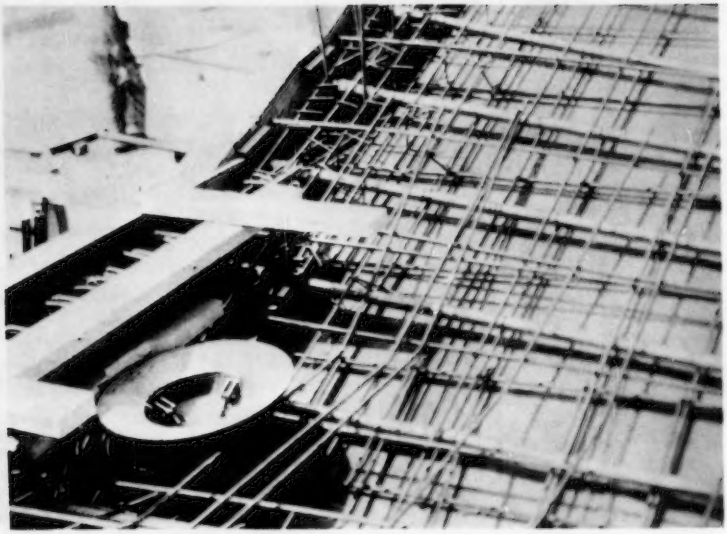

FIG. 13.—VALLEY OF FOLDED PLATE ROOF AT SUPPORTING COLUMN SHOWING ROOF DRAIN IN COLUMN—RICHLAND JUNIOR HIGH SCHOOL

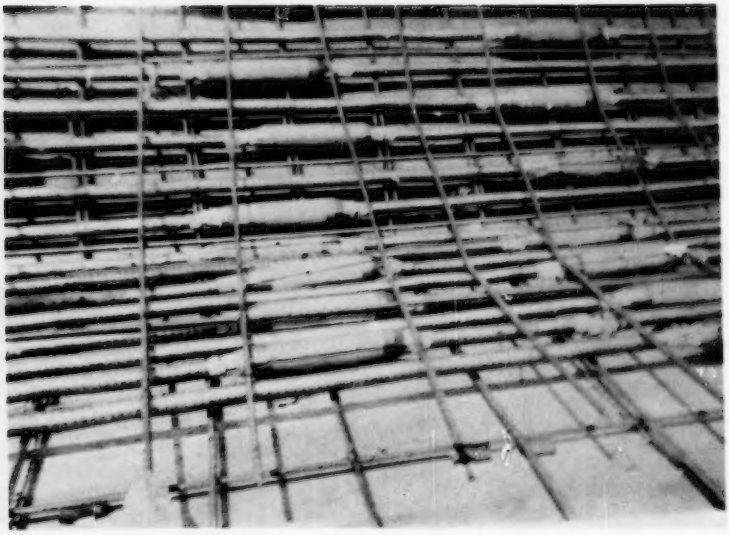

FIG. 14.—VALLEY OF FOLDED PLATE ROOF NEAR CENTER OF 97 FT. SPAN SHOWING STRESS-STEEL TENDON CQUPLERS IN PLACE—RICHLAND JUNIOR HIGH SCHOOL

handled carefully and no difficulty was experienced in consolidating the material. Finishing requires more labor than the conventional level surfaces and particular care must be exercised in screed placement to yield the desired straight lines to the ridges and valleys. Concrete placement in the vicinity of the prestress tendon anchorages and bearing plates must be performed most carefully as the high bearing stresses will not permit any poor concrete or honeycomb.

The tensioning of prestress reinforcement was deferred until the field cylinders verified the specified minimum strength concrete. A sequence of tensioning cables was selected to keep the center of prestress forces as near to the center of gravity of the final prestress force as possible. Each leaf had identical tendons tensioned prior to starting the next cable sequence. Tensioning was performed by jacking from both ends simultaneously to reduce, as much as possible, the differential stress along the tendon created by friction within the conduits. Experience has demonstrated that most formulas for estimating the amount of over-tensioning necessary to overcome friction are inadequate.

Selection of a friction coefficient of approximately twice that recommended by the manufacturer seems to come closer to indicating the necessary additional force. Very little difference in frictional resistance could be observed between tendons having large drape and angle change as compared with the straightest tendon. It is concluded that the wobble of the conduit along its placed position is much more responsible for creating the frictional resistance than is the angular change of the parabolic drape of the tendon. The delay created by the time required for the frictional slippage of each tendon to take place within the flexible metal conduit was reduced by tensioning each cable to the maximum initial force permissible to keep the end bearing stresses within the maximum allowable. All cables were then retensioned to obtain the total required elongation. The two-step tensioning necessitated some bookkeeping to record the measured elongation at each end of each tendon. A check of final force actually furnished in each tendon is also available as a by-product of this operation.

Grouting of the tendons was accomplished on each job by means of different types of grout equipment. The "Moyno" pump for the pumping of the portland cement grout was very efficient and positive in its action (Fig. 15), whereas other types of pumps became inoperative when speed was most necessary.

ECONOMICS

Contractors costs for these four projects are summarized in Table 1.

DESIGN PROCEDURE

Assume a slab thickness and compute the moment of inertia of the cross section for the inclined position to the vertical axis in which it is to perform. This moment of inertia of one plate is derived by Eq. 3 with a slab thickness of $4\frac{1}{2}$ in. normal to the slope, and a slope of plate 3.5 vertical to 12 horizontal.

FIG. 15.—GROUTING OF POST-TENSIONED CABLES

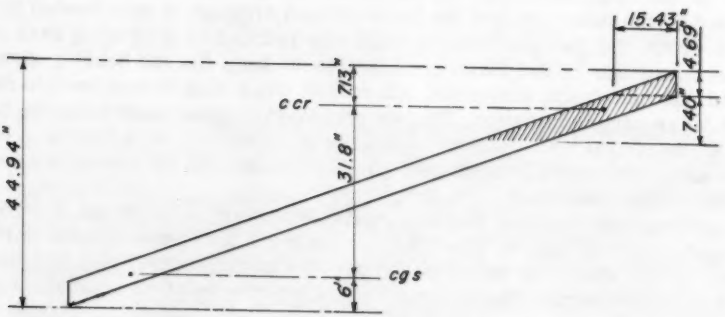

FIG. 16.—ULTIMATE MOMENT STRESS CONDITION

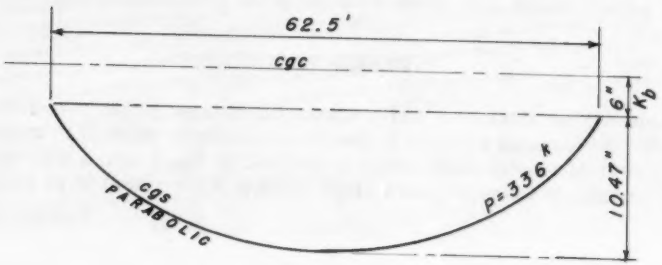

FIG. 17.—LOCATION OF PRESTRESS FORCE ARRANGED IN PARABOLIC CURVE

Thus,

$$t = \frac{t'}{\cos \phi} = \frac{4.5}{.98} = 4.6875 \text{ in.}$$

$$I = \frac{4.6875}{3.5} (40.25)^3 = 87{,}300 \text{ in.}^4$$

Area = 4.6875 (11.5-by-12) = 647 in.^{2} (cross section of one plate)

$$r^2 = \frac{87{,}300}{647} = 135: \; c_t = c_b = \frac{H+t}{2} = \frac{44.94}{2} = 22.47 \text{ in.}$$

and

$$k_t = k_b = \frac{r^2}{c} = \frac{135}{22.47} = 6.0 \text{ in.}$$

in which k is the kern point and r is the radius of gyration.

Assume center of gravity of tendons as being e′ above bottom of section at midspan. Prestress force eccentric arm is therefore:

$$e = c - e' = 16.47 \text{ in. Max. (Assume } e' = 6.0 \text{ in.)}$$

Compute the longitudinal bending moments acting on the section for the dead load of the slab, the applied dead loads such as the roofing, insulation and ceiling, and the live load for which the structure shall be designed. The following values shall be used as an illustrative example.

The dead load for a $4\frac{1}{2}$ in. slab is

$$\frac{4.5}{12} = \frac{w'}{144} = 54 \text{ psf/Cos } \phi = \frac{54}{0.96} = 56.25\text{-by-}11.5 = 646 \text{ plf}$$

The additional applied dead load consists of the built up roofing (5.5), the applied 2 in. vermiculite concrete insulation (6.5), and the $\frac{1}{2}$ in. acoustical plaster (1.7), producing a total additional applied dead load of 13.7 psf. The live load was 25 psf.

$$13.7 \cos \phi = 14.25 \text{ psf}$$
$$14.25 \; (11.5) = 164 \text{ plf}$$

and

$$25.0 \; (11.5) = 287.5 \text{ plf}$$

The total load then (95.5 psf 11.5 ft) equals 1.1 kip per ft.

M_{dl} Slab $= .646 \left(\frac{62.5^2}{8}\right) = 315.5$ ft-kip

M_{dl} Applied $= .164 \left(\frac{62.5^2}{8}\right) = 80.1$ ft-kip

$M_{ll} = .287.5$ by $\left(\frac{62.5^2}{8}\right) = 140.4$ ft-kip

M_{tl} 1.0975 536.0 ft-kip

TABLE 1.—CONSTRUCTION COSTS

RICHLAND ELEMENTARY SCHOOL[a]
MEMPHIS, TENNESSEE

ITEM	QUANTITY	UNIT COSTS		COST		TOTAL
		LABOR	MATERIAL	LABOR	MATERIAL	
3750 psi Concrete	90 cu yd	4.72	12.12	$ 425.70	$ 1,091.70	$ 1,517.40
Concrete Finishing	6112 sq ft	0.03	—	188.38	—	188.38
Curing & Protection	6112 sq ft	0.01	0.01	61.12	61.12	122.24
Concrete Forms & Shoring	6232 sq ft	0.40	0.20	2,492.80	1,246.40	3,739.20
Intermediate Grade Reinforcing Steel	19129 lbs	0.02	0.09	382.58	1,721.61	2,104.19
Prestress Reinforcing	2050 linear ft	0.294	1.24	602.57	2,550.00	3,152.57
Sub-totals				$ 4,153.15	$ 6,670.90	$10,824.05
Sales Tax 3% Material						124.59
F.O.A.B., SS & Insurance 10% Labor						667.07
Net Cost						$11,615.73

Area Covered = 63.63 ft by 93.0 ft Horiz. Proj. = 5,917.6 sq ft
Cost per square foot = $1.963

RICHLAND JUNIOR HIGH SCHOOL[b]
MEMPHIS, TENNESSEE

ITEM	QUANTITY	UNIT COSTS		COST		TOTAL
		LABOR	MATERIAL	LABOR	MATERIAL	
3750 psi Concrete	393 cu yd	3.00	$15.30	$ 1,179.00	$ 6,012.90	$ 7,191.90
Concrete Finishing	20,371 sq ft	0.03	—	611.13	—	611.13
Concrete Curing & Protection	20,371 sq ft	0.01	0.01	203.71	203.71	407.42
Concrete Forms & Shoring	24,007 sq ft	0.371	0.20	8,906.60	4,801.40	13,708.00
Intermediate Grade Reinforced Steel	57,077 lbs	0.02	0.085	1,141.54	4,851.55	5,993.09
Prestress Reinforced Stress Steel	11,746 linear ft	0.153	0.60	1,802.94	7,061.52	8,864.46
Sub-totals				$13,844.92	$22,931.08	$36,776.00
Sales Tax 3% Material						687.93
F.O.A.B.; SS & Insur. 11% Labor						1,522.94
Net Cost						$38,986.87

Horizontal Projection
Area Covered = 97.71 ft by 175.6 ft = 17,193 sq ft.
Average Net Cost per square foot = $2.27

MEMPHIS ART ACADEMY[c]
MEMPHIS, TENNESSEE

ITEM	QUANTITY	UNIT COSTS		COST		TOTAL
		LABOR	MATERIAL	LABOR	MATERIAL	
Slab 3750 psi Concrete	153 cu yd	3.00	15.50	$ 459.00	$ 2,372.00	$ 2,831.00
Columns 3000 psi Concrete	8 cu yd	5.00	14.00	40.00	112.00	152.00

TABLE 1.—CONTINUED

ITEM	QUANTITY	UNIT COSTS LABOR	UNIT COSTS MATERIAL	COST LABOR	COST MATERIAL	TOTAL
Concrete Finishing	6,687 sq ft	0.03	—	$ 201.00	$ —	$ 201.00
Concrete Rubbed Finish	3,688 sq ft	0.15	—	553.00	—	553.00
Columns & Beam Forms	2,485 sq ft	0.75	0.35	1,864.00	870.00	2,734.00
Slab Forms and Shoring	6,000 sq ft	0.45	0.25	2,700.00	1,500.00	4,200.00
Intermediate Grade Reinforced Steel	29,610 lbs	0.02	0.0885	592.20	2,619.50	3,211.70
Post-tensioned tendons	4,250 linear ft	0.13	1.46	553.00	6,248.00	6,801.00
				$ 6,962.20	$13,721.50	$20,683.70
Sales Tax						225.50
Labor, Tax & Insurance						836.00
Job Equipment & Supervision						1,084.00
Net Cost						$22,829.20

Horiz. Projection Covered = 98.33 ft by 69.0 ft = 6,785 sq ft = $3.36 per square foot

HOLIDAY INN[d]
SARASOTA, FLORIDA

ITEM	QUANTITY	UNIT COSTS LABOR	UNIT COSTS MATERIAL	COST LABOR	COST MATERIAL	TOTAL
3750 psi Concrete	92 cu yd	4.25	16.00	$ 391.00	$ 1,472.00	$ 1,863.00
Concrete Finishing	6,660 sq ft	0.10	—	666.00	—	666.00
Concrete Protection and Cure	6,660 sq ft	0.01	0.005	66.00	33.00	99.00
Forms, Shoring and Removal	7,214 sq ft	0.415	0.18	2,993.81	1,298.52	4,292.33
Intermediate Grade Reinforcing Steel	16,650 lbs	0.25	0.07	416.25	1,165.50	1,581.75
Post-Tensioned Tendons	1,765 linear ft	0.184	1.15	324.00	2,027.04	2,351.04
Sub-totals				$ 4,857.06	$ 5,996.06	$10,853.12
Hoisting Crame Rental						408.00
Sales Tax 3.25% Material						192.10
Insurance, SS, F.O.A.B., Etc.						1,087.98
Net Cost						$11,997.23

Horiz. Area Covered = 73.17 ft by 84 ft = 6150 sq ft = $1.95 per square foot

[a] Roof over cafetorium spanning 62 ft-8 in., slab thickness 4 1/2 in., valley frequency 23 ft o. c.; slope 3 1/2-on-12; 7 1/2 in. thick reinforcing gable end wall ties included. Post-tensioning tendons 4 per leaf @ 62.5[k] ea.; "Prescon" 10G2 Cables.

[b] Roof over gymnasium and cafetorium, span 96 ft-4 1/2 in., slab thickness 5 in., valley frequency 25 ft o. c.; slope 4 1/2-on-12; 8 in. thick reinforcing and prestressed concrete gable walls included. Post-tensioning cables 8 per leaf @ 70.2[k] ea. Stressteel Corp. 1 1/8 Rod Tendons; Cable ties 7/8 in. Rod Tendons.

[c] Roof over third floor of art school spanning 94 ft-8 in., slab thickness 5 in., valley frequency 23 ft o. c.; slope 4 1/2-on-12. Thrust of end leaves resisted by tensors across ridges located at quarter points and by 20 in-by-24 in. concrete rigid frame supports at ends of span. Post-tensioning tendons 7 per leaf @ 84.5[k] Prescon 12G2 Cables.

[d] Roof over club; span 60 ft; slab thickness 4 in., valley frequency 15 ft o. c.; slope 4 1/2-on-12; 8 in.-by-16 in. tensor ties @ 3 ft below valley. Post-tensioned cables 3 per leaf @ 45 kips each Prescon 6G2 Cables.

Having established the section properties and the load moments, use the conventional methods for computing the required prestressing force to furnish zero stress in the bottom at midspan with total load moment.

$$F = \frac{M_{tl}}{e + k_t} = \frac{536.\ x\ 12{,}000}{16.47 + 6.0} = 286 \text{ kip}; \quad F = \frac{286}{.85} = 336 \text{ kip}$$

Using, say, four cables requires F = 71.5 kip per tendon; F_i = 82 kip per tendon. The initial tensioning force required for each cable should be increased adequately for overcoming tendon friction and wobble of conduit.

Solving for the several stresses occurring in the section due to moment, prestress force, and eccentric arm we have the following:

Under total load; unit stresses at midspan will be

$$F_{top} = \frac{F\ h}{A_c\ c_b} = \frac{286\ (44.94)}{647\ (22.47)} = 884 \text{ psi top compression}$$

0 psi bottom compression

in which h is the vertical distance above or below the c. g. of the concrete section and c is the vertical distance from c. g. of rection to the top or bottom surface;

Under slab load only, the unit stresses at the time of transfer or prestress force will be;

$$F_{bot} = \frac{F_i}{A_c} = \left[1 + \frac{e - \frac{M_{dl}}{F_i}}{k_t}\right] = \frac{336}{647}\left[1 + \frac{16.47 - \frac{315.5}{336}}{6.0}\right]$$

$$\frac{336}{647}\ (1.866) = 968 \text{ psi compression}$$

Using the allowable steel and concrete stress[4]

Prestressing Steel f'_s = 240,000 psi f'_{sy} = 210,000 psi

temporary $f'_s = .70\ f'_s$ = 168,000 psi

at design loads = $.60\ f'_s$ = 144,000 psi

Concrete f'_c = 3,750 psi

temporary compression $0.55\sqrt{f_c}$ = 2,060 psi

temporary tension w/reinf. $6\sqrt{f'_c}$ = psi

at design loads - compression $0.45\ f'_c$ = 1,688 psi

at design loads - tension $3\ f'_c$ = 183 psi

anchorage bearing $f_{cp} = 0.6\ f'_c\ 3\sqrt{A_c/A_b}$ $\left(f'_c = 3{,}750\right)$

The position of the prestressing steel can be varied throughout the length by draping the tendons in either a parabolic, circular or tangential pattern and reducing the eccentricity at the ends of the span. Locating the center of the prestressing force at the kern point at the ends will prevent tensile stress in the top at the end supports.

---

[4] Joint Committee 323 ACI - ASCE for Prestressed Concrete for Tensioned Members.

The ends of the span require additional thickness in order to have sufficient bearing area for transfer of the concentrated forces exerted by the end-bearing plates of the prestressing tendons. The stresses occurring at the bearing plate are usually the most critical concrete stresses that will be encountered in the folded plate section and particular attention should be given this area. The jacking forces required to stress the tendons to initial stress will need to be increased to overcome friction and wobble effect. Most manufacturers' standard end bearings are designed for use with 5,000 psi concrete in lieu of the 3,750 psi concrete sufficient for all other requirements of the section. Additional thickness is easily obtained by tapering the end-4 ft uniformly in the form of a symmetrical haunch above and below the slab to the additional thickness required.

Determine the area of prestress steel required as being

$$A_s = \frac{F}{f_s} = \frac{286{,}000}{144{,}000} = 2.0 \text{ sq in.}$$

Check the shear unit stresses:

$$V = 1.1 \times \frac{62.5}{2} = 34.4 \text{ kip}$$

Assume tendons placed in parabolic curve:

$$c - k = e \quad \ldots\ldots\ldots\ldots\ldots\ldots \quad (7)$$

22.47 in. - 6.0 in. = 16.45 in. above bottom at ends.

The center of gravity of midspan is 6.0 in. above the bottom at midspan. The function h = 10.45 in. = 0.87 ft L (the length of span c to c of supports principal span) out to out tendons equals 64 ft.

$$V_s = 4\frac{F\,h}{L} = \frac{4 \times 286. \times 0.87}{64} = 15.5^{k} \quad I = 87{,}300 \text{ in.}^4$$

$$V_c = V - V_s = 34.4 - 15.5 = 18.9 \text{ kip} \quad b = 15.4 \text{ in. or } 4.5 \text{ in.}$$

$$v_c = \frac{V_c\,Q}{I_b} = \frac{19.1 \times 3207}{87{,}300 \times 4.5} = 156 \text{ psi} \quad Q = 16.71 \times 2.19.34 + 287.\ 5 \times 8.89$$

$$Q = 647 + 2560 = 3207$$

and

$$f_c = \frac{286{,}000}{647} = 442 \text{ psi}$$

in which v is the unit shear, Q is the moment of the area and b is the horizontal projection of the plate width.

The principal tensile stress is determined as follows:

$$S = n^2 + \frac{(fc)^2}{(2)} - \frac{f_c}{2}$$

$$S = (156)^2 + \frac{(442)^2}{(2)} - \frac{442}{2}$$

$$S = 24{,}300 + 48{,}900 - 221$$

$$S = 271 - 221 = 50 \text{ psi (ok allowable = 112 psi)}$$

and

$$S_t = 300 \text{ psi}$$

The shear is then checked for ultimate load;

$$2 \text{ TL } V_{ult} = 2 \times 34.4 = 68.8 \text{ kip}$$

$$v_c = 68.8 - 15.5 = 53.3$$

$$V_{ult.} = \frac{53.3 \times 3207}{87{,}300 \times 4.5} = 436 \text{ psi}$$

$$S_t' = (436)^2 + 48{,}900 - 221$$

and

$$S_t' = 190{,}000 + 48{,}900 - 221$$

$$S_t' = 374 - 221 = 153 \text{ psi ok}$$

The section is checked for cracking moment. Assume the modulus of rupture of the concrete equals $0.14\ f'_c$ $(0.14\ 3750) = 525$ psi $M_s = F(e + k_t) = 286$

$(16.47 + 6.0) = 286 \times \frac{22.47}{12} = 536$ ft - kip $M_c = \frac{F_c\ I}{c_b} = \frac{525 \times 87{,}300}{22.47 \times 12} = M_c$

$= \frac{170 \text{ ft - kip}}{706 \text{ ft - kip}}$

The factor of safety against cracking $= \frac{706}{536} = 1.32$ times TL

The factor of safety against live load cracking is determined as

$$\frac{706 - 395.6}{140.4} = \frac{310.4}{140.4} = 2.21 \text{ times LL plus DL}$$

The section is then checked for ultimate moment. The ultimate tensile force is determined as

$$f'_c\ A_s = 240{,}000 \times 2.0 = 480 \text{ kip}$$

This force is resisted by f'_c (average) (See Fig. 16)

$$0.85\ f_c = .85 \times 3750 = 3190 \text{ psi}$$

Total A_c under compression $= \frac{480.}{3.19} = 150.5$ sq in.

The ultimate center of compressive resistance below the top fiber is then located.

Compute equivalent width as: $(12/3.5)\ 4.5$ in. $= 15.43$ in.

Compute Area of top triangle $= (4.69/2)\ 15.43 = 36.2$ sq in

Additional portion of stem necessary $= 150.5 - 36.2 = 114.3$ sq in.

Additional required vertical depth $= 114.3/15.43 = 7.40$ in. therefore, the center of concrete resistance is

$$ccr = \frac{36.2\ (2/3\ (4.69)\ ) + 114.3\ (7.40/2 + 4.69)}{150.5} = 7.13 \text{ in. below top}$$

Ultimate lever arm $= 44.94 - (6.0 + 7.13) = 31.8$ in.

Ultimate M - 480^k $(31.8/12) = 1272$ ft -kip

Therefore the factor of safety for TL $= 1272/536 = 2.83$ times total load, whereas the factor of safety for LL $= \frac{1272 - 395.6}{140.4} = 6.25$ times (LL + DL)

The transverse bending in successive plates is analyzed by the conventional moment distribution methods utilized for continuous structures. The span length is the slope length from valley to ridge. The valley and ridge serve as support for the slab. This being a short span, 11 ft -6 in. in the example, moments will be no greater than would be encountered in a level slab with supports at the same frequency (Fig. 1).

For example, assume fixed and negative moments at the valley and ridge of $\frac{w\ l^2}{12}$ and midspan positive moments of one half this value. Compute stiffness and distribution factors in the usual manner and compute the maximum and minimum moments for each span. End leaves deserve special consideration and need provision for support by means of columns, edge beams, upturned leaf or wing or thickened to provide stiffness to the cantilever beyond the last valley or ridge.

Analysis of a 1-ft wide strip transverse to the main span is derived by the following means (Fig. 1):

$W_{dl} = (4.5/12)\ 144 = 54$ lbs $W_{ll} = 25\ (\text{Cos}\ \phi) = 24.5$ lbs

$W_{dl} = 14$

$W_{dl} = \overline{68}$ psf $W^{tl} = 68 + 24.5 = 92.5$ lbs

$FEM_{dl} = 68 \times \frac{(12)}{12} 2 = .816$ ft . kip $FEM^{tl} = 92.5 \times \frac{(12)^2}{12} = 1.11$ ft - kip

$I = 91.2$ in.^{4}

$K = I/L = \frac{91.2}{12} = 7.6$

Distribution factors = 1.0; 0.43; 0.56; 0.50; 0.50

	A	B		C		D		E		E
D.F	1.0	.43	.57	.50	.50	.50	.50	.50	.50	.50
FEM_{dl}	-.816	-.816	-.816	-.816	-.816	-.816	-.816	-.816	-.816	
FEM_{tl}	-1.11	+0.56	-1.11	-1.11	+.56	-1.11	-1.11	+.56	-1.11	-1.11	-1.11	-1.11
Dist.	-0.13	+0.13	-0.56	-0.15	+.12	-0.17	-0.15	+.11	-0.15	-0.15	-0.15	-0.15
Add	-1.24	+0.40	-1.67	-1.26	+.13	-1.28	-1.26	+.11	-1.26	-1.26	-1.26	-1.26
C.O.	+1.24	+0.18	-0.23									
Dist. M.	0	+1.09	-1.49	+0.81	-1.27	+.78	-1.26	+.78	-1.26			
Min. A_s		+0.216	-.296	+0.161	-.252	+.155	-.250	+.155	-.25			

No. 3 @ 6 in. oc No. 3 @ 4½ in. oc No. 3 @ 8 in. oc No. 3 @ 5 in. oc No. 3 @ 8¾ in. oc No. 3 @ 5 in. oc.

Distribution Steel Longitudinal = (0.0025) (4.5) (12) = No. 3@10 in. o.c.
Average Steel per square foot = 0.337 sq in = 1.15 psf

The end leaf is unopposed. Therefore, a tie must be provided to resist the horizontal component. Thus, the vertical Load of end leaf = 1.11 (31.25) = 34.7 kip, and the horizontal component = 34.7 x 12/3.5 = 119 kip. This can be

resisted by a prestress force of this amount or reinf. steel = $\frac{119}{20}$ = 5.95 in 2, say, 6 - No. 9 Bars.

Analysis of stress distribution and variation may be computed in the manner described by H. Simpson.5

DEFLECTION

The moment due to prestress (Fig. 17) is computed as

M due to prestress = p e = 336 x 6/12 = 168 ft uniform

plus 336 x $\frac{10.47}{12}$ = 293 ft kip parabolic

M_{dl} Slab = 315.5 ft -kip

M_{dl} Applied = 80.1 ft -kip

M_{ll} = 140.4 ft -kip

Instantaneous upward deflection due to prestress is

$$\left(\frac{168 \text{ ft. kip}}{8} + \frac{5 \times 293}{48}\right) \frac{62.5^2 \times 12^2 \times 12{,}000}{3{,}500{,}000 \times 87{,}300} = 1.14 \text{ in. initial;}$$

$$0.85 \times 1.14 = .965 \text{ in. after losses}$$

Downward deflection due to M Slab:

$$\frac{(5 \times 315.5)}{48} \frac{62.5^2 \times 12 \times 12{,}000}{3{,}500{,}000 \times 87{,}300} = 0.73 \text{ in. (1.27 in. assuming } 2.0 \times 10^6 \text{E)}$$

Hence, immediate upward deflection at transfer = 1.14 - 0.73 = 0.41 in.

Added DL deflection = $\frac{80.1}{315.5}$ x 0.73 = 0.19 in.

= (.965 - .73 - .19) 2 = .09 in.
after loss of initial prestress and effect of creep.

Instantaneous downward deflection due to live load moment is

$$\frac{140.4}{315.5} \times .73 = 0.325 \text{ in.}$$

ACKNOWLEDGMENTS

The Richland Elementary and Junior High Schools in Memphis, Tenn., and the Memphis Art Academy were designed by Mann and Harrover, Architects of Memphis. The Holiday Inn of Sarasota, Fla., was designed by William Bond, Architect of Memphis. The schools were built by the S&W Construction Co., Inc., of Memphis. The Art Academy was built by the Whitsitt Construction Co. of Memphis, while the Holiday Inn was build by Allen Brothers and O'Hara, Inc.

---

5. "Design of Folded Plate Roofs," by Howard Simpson, Proceedings, ASCE, Vol. 84, No. ST 1, January, 1958.

APPENDIX - NOTATION

a = slope rise on 12;
A_c = area of concrete;
A_s = area of steel;
B = spacing of valleys;
b = horizontal projection of plate width;
c = vertical distance from c.g. of section to top or bottom surface;
c.g. = center of gravity;
e = eccentricity of prestress force from the c.g.;
e' distance from surface to center of prestress force;
F- = prestress force after losses;
F_i = prestress force at time of transfer;
f_c = allowable concrete unit stress:
f'_c = design concrete strength;
f_s = allowable steel unit stress;
f'_s = ultimate strength of steel:
H = vertical height of section valley to ridge;
h = vertical distance above or below c.g. of concrete section;
I = moment of inertia of section;
i = subscript indicating condition at transfer of prestress;
k = kern point;
K = stiffness factor;
L = length of span center to center of supports principle span;
M = bending moment;
Q = moment of area;
r = radius of gyration;
S = principle tensile stress;
S' = principle tensile stress for ultimate;
T = thickness of slab normal to section;
T' = thickness of slab vertically;
ult. = ultimate;
V = shear;

v = unit shear;

W = total load on section for span considered;

w = unit load per sq ft;

x = distance from support to point under consideration;

ω = width of plate along the surface;

ϕ = angle of intersection of plate slope with the horizontal;

TL = total load;

LL = live load; and

DL = dead load.

Journal of the
STRUCTURAL DIVISION
Proceedings of the American Society of Civil Engineers

FREEZING AND THAWING EFFECTS ON PRESTRESSED CONCRETE[a]

By M. J. Gutzwiller,[1] M. ASCE, and F. E. Musleh,[2] A.M. ASCE

SYNOPSIS

Freeze and thaw tests were conducted on 48 specimens representing strength levels of 5,000 psi and 3,000 psi. Some of the beams with a 5,000 psi strength were post-tensioned throughout the test. Significant improvement in the durability was found to result from post-tensioning of the beams. Post-tensioned concrete specimens made of a rich mix showed better durability than unstressed concrete made of the same mix and also better durability than unstressed concrete made of a leaner mix.

INTRODUCTION

In the United States, the use of prestressed concrete has developed to the point that detailed information concerning its physical characteristics is urgently needed by engineers.

Prestressed concrete offers many advantages and has many new and important applications in civil and structural engineering. The fine cracks that develop in conventional reinforced concrete cannot be avoided, but with the use of prestressed concrete, the absence of cracks as a permanent feature can be assured up to maximum design loading. Prestressed concrete members having large span-to-depth ratios can be used. This means a saving in the volume of concrete to be used in a given structure. The prestressing steel used is a high-strength grade of steel resulting in a smaller weight of steel.

Note.—Discussion open until March 1, 1961. To extend the closing date one month, a written request must be filed with the Executive Secretary, ASCE. This paper is part of the copyrighted Journal of the Structural Division, Proceedings of the American Society of Civil Engineers, Vol. 86, No. ST 10, October, 1960.

[a] Presented at the March 1960 ASCE Convention in New Orleans, La.

[1] Assoc. Prof. of Struct. Engrg., Purdue Univ., Lafayette, Ind.
[2] Design Engr., Pierce, Gruber and Beam, Inc., Indianapolis, Ind.

The difference in the cost ratio of materials to labor in the United States, as compared to some European countries, has influenced the direction of the development of this new use of materials. With the birth of this new era of prestressed concrete, a field has been opened for research to study the physical characteristics of this new combination of high-strength steel and prestressed concrete.

The effect of freezing and thawing on ordinary concrete has been investigated extensively. Among the leading researchers in this field are D. W. Lewis,[3] F. F. Bartel,[4] L. C. Pendley,[5] J. G. Higgs,[6] S. Walker and D. L. Bloem,[7] F. H. Jackson,[8] and L. O. Hansen.[9] In 1949, Pendley reported a study wherein beams restrained from expansion were subjected to freezing and thawing. Although his arrangement did not directly involve prestressing as we know it, he found that restraint of concrete decreased deterioration caused by exposure. He suggested that the increase in durability of restrained beams was apparently due to the prevention of cracking perpendicular to the longitudinal axis of the beam. The cracking pattern in the restrained beams was parallel to the beam axis as compared to a random pattern in unrestrained beams.

An acceptable explanation of concrete failure under repeated cycles of freezing and thawing was the hypothesis presented by T. C. Powers.[10] This hypothesis presents the action of frost as being the cause of hydraulic pressure that tends to cause the deterioration of concrete. This hydraulic pressure depends on many factors, the most important of which is the permeability of the material through which the water must flow to escape from the saturated regions on the surface of the test specimen during the cooling cycle. The degree of saturation and the absorptivity of the test specimens were emphasized as important factors in discussing freezing and thawing of concrete.

Prediction of the durability of concrete to be used in a structure by means of a laboratory test is practically impossible. The problem of trying to get precisely the same concrete in a test specimen as you would in a structure and then being able to subject this specimen to the same temperature changes, moisture gradients, and load conditions as the structure in service make the task more difficult than ever. The only true test would be to observe the actual structure in service. Many tests have been conducted with

---

[3] "Research as Related to Aggregate Specifications," by D. W. Lewis and K. B. Woods, Proceedings, 35th Annual Road School Extension Series No. 69, Purdue Univ., pp. 155-173, 1949.

[4] "Effect of Air Entrainment on Resistance to Freezing and Thawing of Concrete Made with Questionable Aggregates," by F. F. Bartel, Circular 31, Natl. Sand and Gravel Assoc., March, 1949.

[5] "The Effect of Restraint on the Durability of Concrete Aggregates," by L. C. Pendley, Thesis, submitted to Purdue Univ. in partial fulfilment of the requirements for the degree of Master of Science in Civ. Engrg., June, 1949.

[6] "Influence of Fine Aggregates on Concrete and Mortar Durability," by J. G. Higgs, Thesis, submitted to Purdue Univ. in partial fulfilment of the requirements for the degree of Master of Science in Civ. Engrg., February, 1950.

[7] "Study of Sands in Concrete Subjected to Freezing and Thawing," by S. Walker and D. L. Bloem, Circular 34, Natl. Sand and Gravel Assoc., August, 1949.

[8] "Resistance of Concrete to Frost Action as Affected by the Water-Cement Ratio," by F. H. Jackson, Proceedings, Highway Research Bd., Vol. 11, Part I, p. 227, 1931.

[9] "Wheathering Tests on Concrete," by L. O. Hansen, Proceedings, Highway Research Bd., Vol. 14, p. 303, 1934.

[10] "A Working Hypothesis for Further Studies of Frost Resistance of Concrete," by T. C. Powers, Proceedings, A. C. I., Vol. 41, p. 245, 1945.

the hope that the information obtained would help in the development of a standard freezing and thawing test capable of yielding information that will indicate the potential frost resistance of concrete in service. At the present time there are four different tentative methods recommended by the American Society for Testing Materials (ASTM) as means of predicting the possible deterioration of concrete. However, none of these methods were intended to be used for predicting the deterioration of prestressed concrete. The ASTM Specification C291-52T was used as a guide in the execution of this work.

PURPOSE AND SCOPE

The purpose of this research was threefold:

1. To study the durability of prestressed concrete under repeated cycles of freezing and thawing;
2. To compare the freezing and thawing effects on prestressed concrete and ordinary concrete for specimens made of the same mix giving an ultimate strength of 5,000 psi or better after 28 days;
3. To compare the effect of freezing and thawing on prestressed concrete having an ultimate strength of 5,000 psi and ordinary concrete specimens made with a leaner mix given an ultimate strength of about 3,000 psi after 28 days.

The freezing and thawing machine that was available for these tests could accommodate a reasonable number of beams as large as 3-in.-by-4-in.-by-16-in. A post-tensioning arrangement was used in order to develop the desired force throughout the full length of the prestressed specimens.

Two series of tests were conducted in this study. Two different mix designs were included in each series. One mix design was used for three batches and the other for one batch. Six 3-in.-by-4-in.-by-16-in. beams (and three 6-in.-by-12-in. compression test cylinders) were made from each batch of concrete, resulting in twenty-four beams for each series. The results of freezing and thawing tests on a total of forty-eight beams are thus reported in this study.

Series I and II were identical in all respects except for the time of curing. Series I was cured for 28 days and Series II was cured for 14 days. In each series, mix designs A, B, and C were the same and were intended to have a minimum ultimate compressive strength of 5,000 psi. Mix design D in each series was intended to have a minimum ultimate compressive strength of 3,000 psi.

MATERIALS

The coarse aggregate used was a glacial gravel. The gravel has been used extensively and has a fairly good field performance record. The gravel was separated into four gradations: 1 in. to 3/4 in., 3/4 in. to 1/2 in., 1/2 in. to 3/8 in., and 3/8 in. to No. 4. Equal weights of each gradation were used.

The sand was divided into two parts, with 66% of the mix design weight passing a No. 16 sieve and 34%, by weight, retained on the No. 16 sieve. Type I portland cement was used in all mixes. Darex was used as the air entraining agent in all mixes. The post-tensioning steel bars were 5/8-in. round high

strength steel bars. End plates and nuts were used on each of the post-tensioned beams.

EQUIPMENT

The equipment used in this study was available in the Joint Highway Research Project and the Purdue University Materials Testing and Structural Engineering Laboratories. This equipment consisted of the concrete mixer, vacuum saturating unit, and the freezing and thawing apparatus. A new 60-ton capacity Simplex hydraulic jack with 3 in. of travel was employed in the post-tensioning of the beams. A certified gage calibration was furnished with the jack and this calibration was checked by the use of a 120,000-lb Baldwin Universal Testing Machine. This positive check on the applied load permitted the use of a rather simple jacking arrangement. The jacking unit in operation is shown in Fig. 1.

The steel forms normally used for 3-in.-by-4-in.-by-16-in. freeze-thaw specimens were used with some minor alterations. New sliding end plates were prepared with 11/16 in. holes drilled in their centers. Two C-clamps on the ends of the forms maintained the proper dimensions of the beams. The molds were covered with a light film of oil before the concrete was placed. The Stressteel bars were placed through the holes in the end plates and coated with a lubricant to prevent the development of bond between the steel and the concrete. A typical form used to mold the beams and a completed beam are shown in Fig. 2. The cyclic range of the freezing and thawing apparatus was between 0° F and 40° F. Approximately seven freeze-thaw cycles were obtained for each 24 hr period. The time to complete one cycle was in accordance with the timing suggested in ASTM C291-52T.

The natural frequency measuring unit in these experiments was composed of a variable frequency oscillator, a variable frequency driving unit to induce controlled frequency vibrations in the specimen, and a milliammeter to measure the current flow from the pickup. When the induced vibration is the same frequency as the natural frequency of the beam, resonance occurs and is detected by a sudden increase in the milliammeter reading. Thus, the maximum current flow occurs at the fundamental frequency of vibration of the specimen. The frequency of the induced vibration can be read directly on the oscillator dial. The frequency measuring unit is shown in Fig. 3.

RESEARCH PROCEDURE

The concrete mix designs A, B, and C were the same and were designed for a strength of 5,000 psi after 28 days. Mix D was designed for a strength of 3,000 psi after 28 days. Detailed information concerning the mixes is shown in Table 1.

Each mix provided enough concrete for three 6 in.-by-12 in. compression test cylinders and six 3 in.-by-4 in.-by-16 in. beams. The beams of Series I were cured for 28 days and Series II for 14 days in a saturated lime solution at about 70° F.

At the end of the curing period the specimens were removed from the lime solution, washed, dried, and weighed. They were assigned and marked with a letter-number designation as shown in Table 2.

All specimens designated by letters A, B, or C followed by numbers 1 or 2 were tested for the fundamental frequency that corresponded to the zero cycle

FIG. 1.—SIXTY-TON HYDRAULIC JACKING UNIT AND SPECIMEN IN POSITION FOR POST-TENSIONING

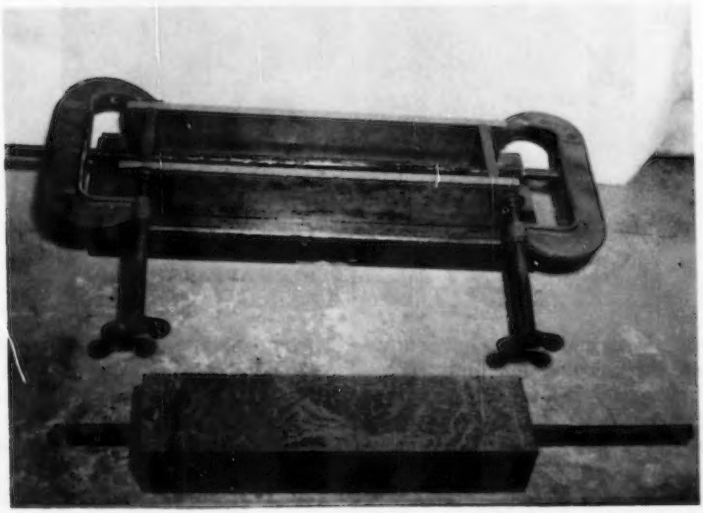

FIG. 2.—A TYPICAL CONCRETE FORM

and 100% relative modulus of elasticity. These specimens were meant to represent an ordinary concrete beam made of a rich mix. There was a total of six of these beams for each of the two series. The beams were tested for the fundamental frequency about every twenty freeze-thaw cycles and were weighed. Each beam had a steel bar in its center.

All specimens designated by letters A, B, or C followed by numbers 3 or 4 were tested for fundamental frequency and were weighed, thus giving the zero cycle readings. Then these beams were post-tensioned with a net average stress of 2,000 psi on the cross-sectional area. This is the recommended

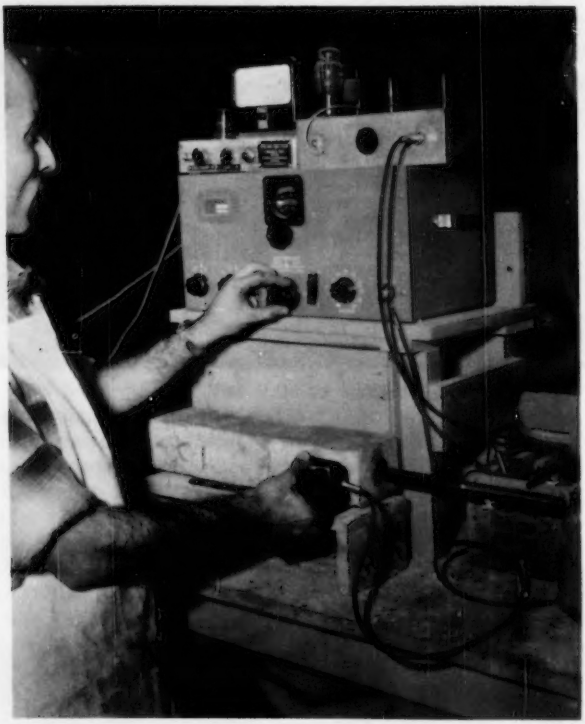

FIG. 3.—THE NATURAL FREQUENCY APPARATUS AND SPECIMEN IN POSITION FOR TESTING

value of 0.4 f'_c used in design practice. These beams were then placed in the freezing and thawing machine. The post-tensioning force was released each time, before the beam was weighed and tested for its fundamental frequency. The original post-tensioning force was reapplied before the beam was put back into the freezing and thawing apparatus. The beams were tested about every 20 cycles.

Specimens designated by letters A, B, and C followed by numbers 5 or 6 were post-tensioned to 2,000 psi before any readings were taken. This force was left on the beams throughout the entire test period. After the initial force

TABLE 1.—MIX DESIGN DATA[a]

Mix Designation (1)	Compressive Strength[b] PSI (2)	Water/Cement (3)	Sack/cu yd (4)	Air Content, Percent (5)	Slump, Inches (6)
1A	6,420	.450	6.76	2.5	2.5
1B	5,540	.457	6.74	2.7	3.5
1C	5,110	.514	6.61	2.3	5.5
1D	3,740	.695	4.36	1.7	2.5
IIA	7,000	.420	6.77	2.5	1.8
IIB	5,600	.445	6.74	2.0	3.0
IIC	5,800	.452	6.69	2.5	3.8
IID	3,730	.622	4.24	5.2	3.0

[a] All mixes were designed initially by the b/bo method.
[b] Standard 6 in. by 12 in. cylinders—28 days.

TABLE 2.—SPECIMEN MARKINGS AND TEST SUMMARY

3,000 PSI CONCRETE	5,000 PSI CONCRETE		
Plain Concrete Steel Bar in Center	Plain Concrete Steel Bar in Center	Prestressing Force Released During Testing	Permanently Prestressed Concrete
	A1 A2	A3 A4	A5 A6
	B1 B2	B3 B4	B5 B6
	C1 C2	C3 C4	C5 C6
D1 D2 D3 D4 D5 D6			
6	6	6	6

was applied, these beams were weighed and tested for the fundamental transverse frequency. They were tested periodically about every 20 cycles.

The six beams designated by the letter D and numbers 1 through 6 represented concrete made of a leaner mix for comparison purposes. The beams were cast with a steel bar in the center similar to the other specimens. They were tested periodically for weight and fundamental transverse frequency at about every 20 cycles of freezing and thawing.

RESULTS AND ANALYSIS

The test procedure consisted of determining the natural fundamental frequency and weight of each beam at intervals of about 20 cycles of freezing and thawing. A relationship exists between the fundamental transverse frequency of a concrete specimen and its modulus of elasticity. This relationship appears in ASTM Specification C215-58T and can be expressed as follows

$$E = C\,W\,n^2 \quad \ldots\ldots\ldots\ldots\ldots\ldots \quad (1)$$

in which E is Young's dynamic modulus of elasticity, in pounds per square inch; W denotes the weight of specimen, in pounds; n is the fundamental transverse frequency, in cycles per second; and C refers to a constant for any given specimen.

An absolute value of the modulus of elasticity could be obtained by Eq. 1. However, for comparing the durability of various specimens, it is only necessary to obtain relative values. The ASTM specifications permit the assumption that C and W remain constant throughout the durability test, although disintegration of the specimen probably tends to change these values.

Basically, a change in Young's modulus as a result of alternate freezing and thawing cycles can be assumed to represent deterioration of the concrete specimen. Hence, relative value of Young's modulus computed from frequency readings obtained during the testing process would indicate the effects of freezing and thawing on the durability of a given type of concrete. Considering the initial fundamental transverse frequency of a specimen to represent Young's modulus at 100% relative value, the subsequent frequency readings can be related by the formula

$$P_c = \frac{n_c^2}{n_o^2}\ 100 \quad \ldots\ldots\ldots\ldots\ldots\ldots \quad (2)$$

in which P_c is the relative modulus of elasticity, in percent, after c cycles of freezing and thawing; n_c denotes the fundamental transverse frequency after c cycles of freezing and thawing, in cycles per second; and n_o is the fundamental transverse frequency at zero cycles of freezing and thawing, in cycles per second.

The relative moduli of elasticity were computed for each specimen following a measurement of natural frequency. The weights of the specimens were recorded throughout the experiment. Excessive pitting and pop-outs during the experiment, even at early stages, rendered weight analysis meaningless.

The durability factor was computed by the formula (ASTM C291-52T)

$$DF = \frac{P\,N}{M} \quad \ldots\ldots\ldots\ldots\ldots\ldots \quad (3)$$

in which DF is the durability factor of a certain test specimen; P denotes the relative dynamic modulus of elasticity at N cycles, in percent; N is the number of cycles at which P reaches the specified minimum value for discontinuing the test or the specified number of cycles at which the exposure is to be terminated, whichever is less; and M refers to the specified number of cycles at which the exposure is to be terminated. For the purpose of this research, the testing of any specimen was to be terminated at 300 freeze-thaw cycles or at the time when the modulus of elasticity dropped to 50% of its initial value.

A curve showing the variation in the relative modulus of elasticity with the number of cycles of freezing and thawing was plotted for each specimen.

Fig. 4 shows the results obtained for each individual beam in mix II-A. Since these six beams were divided into three groups of similar specimens, only three legends appear on the graph. The circled figure at the end of each line indicates the number of the specimen. Similar graphs were plotted for mixes I-A, I-B, I-C, II-B, and II-C.

Fig. 5 is a plot of the average effect of freezing and thawing on the modulus of elasticity of similar specimens from mix II-A. It should be noted that each curve represents the average result from two similar specimens. Similar graphs were plotted for specimens from I-A, I-B, I-C, II-B, and II-C.

Fig. 6 summarizes the results of Series I. The values of the relative moduli of elasticity of each six similar specimens were averaged. Likewise, average results from the six similar specimens of mix D in Series I were computed and plotted on the same graph for purposes of comparison and evaluation. Fig. 7 shows the results of Series II in a similar manner. When a specimen was withdrawn from the experiment, its contribution to the average of the group was dropped, and the average for the remaining similar specimens only was computed. To show this on the graphs, a vertical line was drawn through the appropriate curve at the last average point taken before the withdrawal of the beam. This will explain the abrupt change in some of the curves.

Table 3 shows the values of the durability factors for the individual beams of Series I at 300 cycles of freezing and thawing. The average durability factor for each six similar beams is given.

Table 4 summarizes the results of Series II in a similar manner.

TYPES OF CONCRETE FAILURE

The decrease in the dynamic modulus of elasticity was measurable in all the specimens tested. In the case of beams numbered 3 and 4 of mixes A, B, and C where the initial prestressing force was applied after each test of the beam, failure came at an early stage. In the beams numbered 5 and 6, a greater number of freeze-thaw cycles was required to produce failure. In the latter case, the initial prestressing force was applied before the beginning of the test and was maintained permanently throughout the study. As the experiment proceeded, creep took place and the initial prestressing force dropped significantly. A typical failure of a prestressed concrete beam is shown in Fig. 8.

In addition to the decrease in the dynamic modulus of elasticity, three major classifications of deterioration in concrete are recognized as the result of unsound aggregates. These are (a) pitting and pop-outs, (b) D-line deterioration, and (c) map cracking.

Pitting is the gradual disintegration of deleterious pieces of aggregates near the surface of the specimens due to frost. Pop-outs usually take a conical

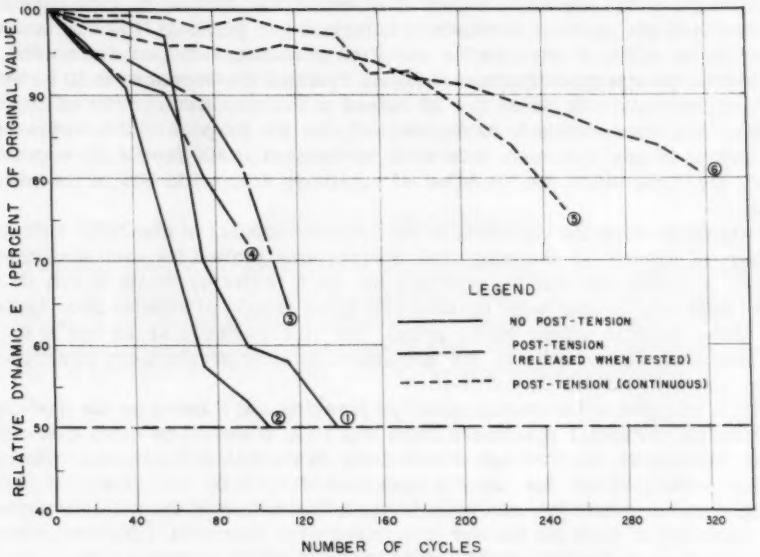

FIG. 4.—THE EFFECT OF FREEZING AND THAWING ON THE DYNAMIC MODULUS OF ELASTICITY (MIX II A)

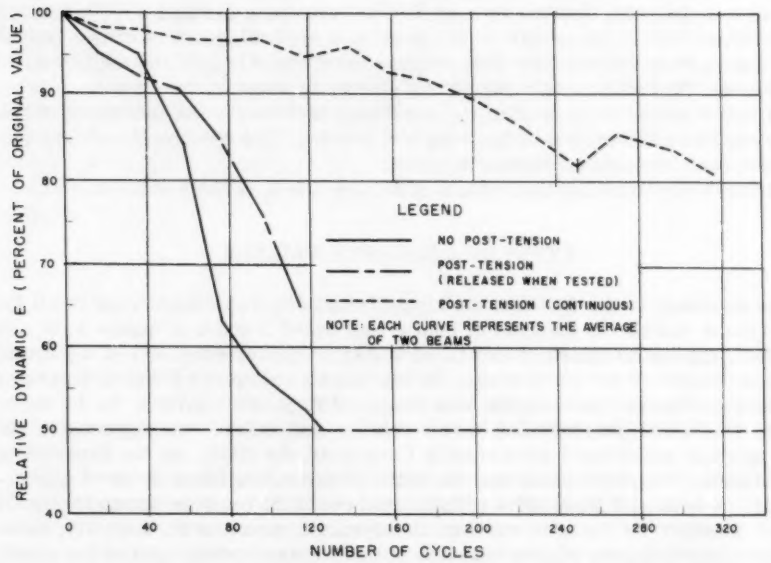

FIG. 5.—THE EFFECT OF FREEZING AND THAWING ON THE DYNAMIC MODULUS OF ELASTICITY (MIX II A)

shape with the apex at an aggregate particle. These are caused by rapid disruption of a saturated piece of deleterious aggregate. Pitting and pop-outs were frequent during the experiment. They were mainly caused by the limonite particles in the aggregates.

D-line cracking is a tensile failure in the matrix. D-lines first appear as fine cracks along the free edges of the specimen. These were noted on some of the specimens.

TABLE 3.—DURABILITY FACTORS OF SERIES I BEAMS AT 300 CYCLES

MIX	BEAM	3,000 PSI PLAIN CONCRETE	5,000 PSI CONCRETE		
			Plain Concrete	Prestressing Force Released During Testing	Permanently Prestressed Concrete
A	1		27.5		
	2		28.2		
	3			67.6	
	4			54.3	
	5				84.6
	6				60.5
B	1		31.2		
	2		34.7		
	3			79.1	
	4			57.1	
	5				87.9
	6				72.4
C	1		25.7		
	2		24.3		
	3			65.8	
	4			20.1	
	5				60.5
	6				46.1
D	1	67.8			
	2	14.1			
	3	71.0			
	4	86.0			
	5	91.6			
	6	69.5			
AVERAGE		66.7	28.6	57.3	68.7

Map cracking is a form of disintegration in which random cracks develop over the entire surface. This kind of failure was not observed in this study. Fig. 9 shows samples of pitting (C), pop-outs (B), and D-line cracking (A).

ANALYSIS OF RESULTS

In the analysis of the results of any laboratory freezing and thawing test, certain facts should be kept in mind.

1. No generally accepted freezing and thawing test has been developed up to this time. The ASTM specifications list four tentative methods for such tests.

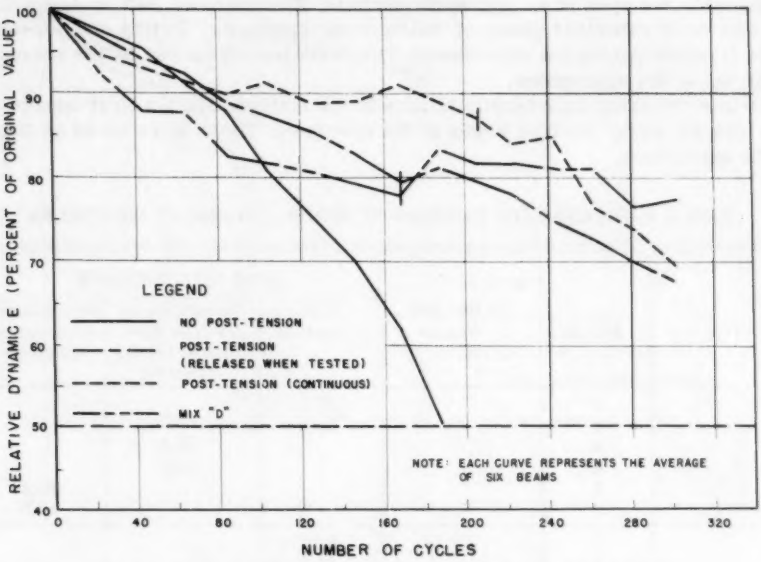

FIG. 6.—THE EFFECT OF FREEZING AND THAWING ON THE DYNAMIC MODULUS OF ELASTICITY (SERIES I)

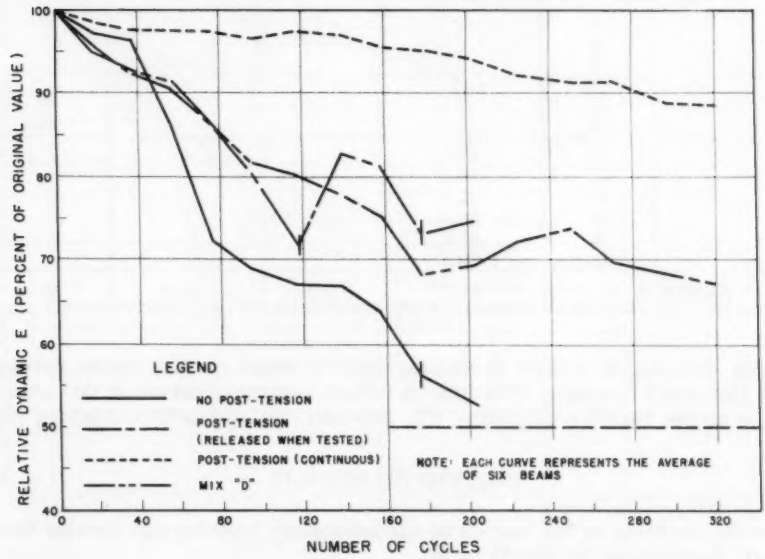

FIG. 7.—THE EFFECT OF FREEZING AND THAWING ON THE DYNAMIC MODULUS OF ELASTICITY (SERIES II)

2. The freezing and thawing test cannot establish quantitative information to determine the length of actual performance of concrete in the field. The test is expected to give a general idea about the qualitative behavior of the concrete exposed to the natural weathering conditions.

3. At best, the results to be obtained from a freezing and thawing test are comparative data on the durability of the test specimens.

4. The accelerated freezing and thawing tests that are performed in the laboratory are generally considered to be very severe tests.

5. Vacuum saturation of the aggregate makes it particularly vulnerable to attack by freezing and thawing.

TABLE 4.—DURABILITY FACTORS OF SERIES II BEAMS AT 300 CYCLES

MIX	BEAM	3,000 PSI PLAIN CONCRETE	5,000 PSI CONCRETE		
			Plain Concrete	Prestressing Force Released During Testing	Permanently Prestressed Concrete
A	1		50.0		
	2		18.0		
	3			30.1	
	4			28.0	
	5				83.2
	6				82.0
B	1		12.7		
	2		23.3		
	3			33.4	
	4			28.4	
	5				82.0
	6				91.3
C	1		77.0		
	2		63.3		
	3			35.5	
	4			37.3	
	5				95.1
	6				98.0
D	1	61.0			
	2	84.0			
	3	72.0			
	4	55.4			
	5	37.3			
	6	68.0			
AVERAGE		63.0	40.7	32.1	88.6

Freezing and thawing tests specified by the ASTM are meant to be performed on homogeneous beams of concrete. The test used for plain concrete specimens was adopted in this research. The steel bars that were inserted at the center of the beam did not influence the results obtained in this study for the following reasons:

1. The steel bars were used on all beams tested. Thus, the comparative results obtained are considered valid.

2. Bond was not developed between the steel and the concrete. A sample beam was tested for its fundamental frequency with the bar in its center, and

FIG. 8.—A TYPICAL FAILURE OF A POST-TENSIONED BEAM SPECIMEN C-3 SERIES I

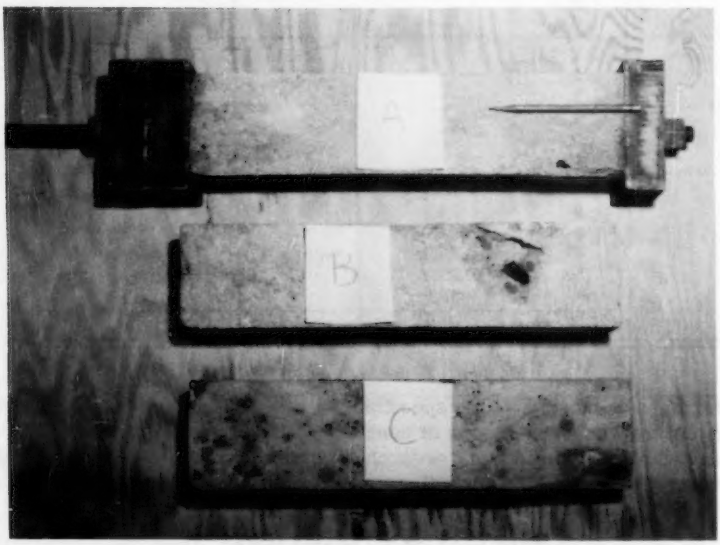

FIG. 9.—CONCRETE FAILURE CAUSED BY DELETERIOUS MATERIAL

then the same beam was tested again with the bar removed. The fundamental frequencies measured in both cases were identical. This check was repeated frequently during the various stages of the experiment and similar results were obtained in every check. Therefore, the fundamental frequency of the concrete was not affected by the unstressed steel bar.

Beams numbered 5 and 6 of mixes A, B, and C of both series were tested for the fundamental frequency in a post-tensioned condition. The loading arrangement adopted consisted of a non-bonded steel bar placed axially in the center of the beam and post-tensioned, distribution plates being used at the ends of the beam to transmit the load to the concrete. Steel nuts on the outer side of each end plate maintained the post-tensioning force. This arrangement provided a self-contained system that was tested dynamically in a manner similar to that used for the unstressed concrete. In this case, the fundamental frequency of the stressed system was about half the value obtained for the same beam with end plates removed. About 5% of the reduction was due to the stress, the remaining reduction was due to the mass of the end plates and nuts. This is in agreement with the detailed theoretical analysis given by Elvery and Furst.[11] When these beams were subjected to the repeated cycles of freezing and thawing, the fundamental frequency of the system dropped. This indicated the deterioration that occurred in the post-tensioned beams. The deterioration occurred in the concrete and the post-tensioning of the concrete did influence the rate and the nature of the deterioration.

CONCLUSIONS

Based on the results obtained and with the limitation of the variables studied in this experiment, the following conclusions are drawn:

1. The post-tensioning of concrete improves its effective durability against cyclic freezing and thawing.
2. Continuously post-tensioned concrete, having a minimum ultimate strength of 5,000 psi after 28 days is effectively more durable than unstressed concrete having minimum ultimate strength of 3,000 psi after 28 days.
3. Continuously prestressed concrete is effectively more durable than intermittently stress-released concrete of the same mix. Furthermore, in four out of the six cases observed, the latter is apparently more durable than unstressed concrete of the same mix.

ACKNOWLEDGMENTS

The research reported in this paper has been conducted in the Joint Highway Research Laboratory at Purdue University. This research work was sponsored by the Joint Highway Research Project.

The authors are grateful to Messrs. J. L. Waling and J. F. McLaughlin for their comments and suggestions in conducting the investigation.

---

[11] "The Effect of Compressive Stress on the Dynamic Modulus of Concrete," by R. H. Elvery and M. Furst, Magazine of Concrete Research, Vol. 9, No. 27, p. 145, November, 1957.

The authors are grateful to the Stressteel Corporation for their donation of the steel and the steel accessories used in this study, and to the Western Indiana Sand and Gravel Co. for the concrete aggregates.

ADDITIONAL READING REFERENCES

1. "A Method of Porportioning Concrete for Strength, Workability, and Durability," by A. T. Goldbeck, and J. E. Gray, Bulletin No. 11, Natl. Crushed Stone Assoc., 1953.
2. "Recommended Practice for Selecting Proportions for Concrete," Proceedings, American Concrete Inst., Vol. 50, p. 105, 1954.
3. "Tentative Recommendations for Prestressed Concrete," ACI-ASCE Joint Committee 323, Proceedings, Journal A.C.I., Vol. 54, January, 1958.
4. "The Effects of Crushed Stone and Heavy Media Separation on the Durability of Concrete Made with Indiana Gravel," by R. D. Walker, Thesis, submitted to Purdue Univ. in partial fulfillment of the requirements for the degree of Master of Science in Civ. Engrg., June, 1955.
5. "The Effects on Freezing and Thawing on Prestressed Concrete," by F. E. Musleh, Thesis, submitted to Purdue Univ. in partial fulfillment of the requirements for the degree of Master of Science in Civ. Engrg., January, 1959.

Journal of the
STRUCTURAL DIVISION
Proceedings of the American Society of Civil Engineers

FLOW GRAPHS IN STRUCTURAL ANALYSIS

By Kurt H. Gerstle,[1] M. ASCE

SYNOPSIS

The relation of flow graphs to the analysis of physical systems is presented. The algebra of flow graphs, including two methods of solution of these graphs, is treated. The setting up and solution of flow graphs is illustrated in terms of several problems from the field of indeterminate structural analysis.

INTRODUCTION

The behavior of any physical system can be expressed in terms of a set of simultaneous equations corresponding to restraints imposed on the system. In particular, the analysis of statically indeterminate structures is usually performed by means of a series of simultaneous equations expressing conditions of geometry which must be satisfied. Thus, for the fixed beam of Fig. 1, these conditions are

$$\Sigma \theta_A = 0 : M_A \delta_{AA} = -M_B \delta_{AB} - P \delta_{AP} = 0 \quad \ldots\ldots\ldots \quad (1a)$$

and

$$\Sigma \theta_B = 0 : M_A \delta_{BA} = -M_B \delta_{BB} - P \delta_{BP} = 0 \quad \ldots\ldots\ldots \quad (1b)$$

in which M_A and M_B are redundant moments, P is the applied load, and δ_{ij} are influence coefficients.

Note.—Discussion open until March 1, 1861. To extend the closing date one month, a written request must be filed with the Executive Secretary, ASCE. This paper is part of the copyrighted Journal of the Structural Division, Proceedings of the American Society of Civil Engineers, Vol. 86, No. ST 10, October, 1960.

[1] Assoc. Prof. of Civ. Engrg., Univ. of Colorado, Boulder, Colo.

Eqs. 1 indicate a functional dependence between the independent variable P, and the dependent variables, in this case the moments M. Eq. 1a, for instance, expresses the fact that the moment M_A is a function of the dependent variable M_B and the independent variable P. The coefficients in the expression, $-\delta_{AB}/\delta_{AA}$ and $-\delta_{AP}/\delta_{AA}$, are sometimes called "dependences."

Another way of expressing this functional dependence is pictorially by means of "flow graphs." This system was originated by S. J. Mason and has been applied in electronic and feedback theory.[2,3] In many cases, this method of representation has been of advantage in several respects. Often, it enables the analyst to keep in better touch with the physical aspects of the problem, thus enabling him to make appropriate simplifications, and to maintain a certain confidence with respect to the rationality of the approach. Moreover, methods have been established for the direct solution of the problem from the flow graph. Thus, the formal writing down of the system of equations is completely bypassed, and the relation between the dependent and independent variables may be obtained from the pictorial representation of the various dependences.

This paper intends only to present the basic techniques of the approach. For mathematical proofs and further details and extensions of the theory and use of flow graphs, the reader is referred to several works in the electrical engineering literature.[2,3,4,5] Example problems presented here refer to the field of structural analysis; applications to other branches of applied mechanics, such as vibration theory and kinematics, could be cited.

PROPERTIES OF FLOW GRAPHS

A flow graph illustrates the functional dependence between several variables. Thus, the expression

$$A = a\,x + b\,y \quad \ldots\ldots\ldots\ldots\ldots\ldots \quad (2)$$

is represented by the flow graph of Fig. 2. Here, x and y are the independent variables, A is the dependent variable, a and b are the dependences. Each variable is expressed by directed branches and arrow heads define the direction. The effect of any variable upon another is equal to the value of the first variable multiplied by the dependence of the branch connecting the nodes representing the two variables. The value of the variable represented by any node is equal to the sum of all effects entering that node. The value of the variable represented by any node is carried by all branches leaving that node.

A more comprehensive example is given in the flow graph of Fig. 3, representing the system of equations

$$A = b\,C + a\,x \quad \ldots\ldots\ldots\ldots\ldots\ldots \quad (3a)$$

$$B = c\,A + d\,B \quad \ldots\ldots\ldots\ldots\ldots\ldots \quad (3b)$$

and

$$C = e\,A + f\,B + g\,C \quad \ldots\ldots\ldots\ldots\ldots\ldots \quad (3c)$$

---

[2] "Feedback Theory—Some Properties of Signal Flow Graphs," by S. J. Mason, Proceedings, I.R.E., Vol. 41, September, 1953.

[3] "Automatic Feedback Control System Synthesis," by J. G. Truxal, McGraw-Hill, 1955.

[4] "Feedback Theory—Further Properties of Signal Flow Graphs," by S. J. Mason, Proceedings, I.R.E., Vol. 44, July, 1956.

[5] "Theory and Applications of Flow Graphs," by C. S. Lorens, M. I. T. Thesis, 1956.

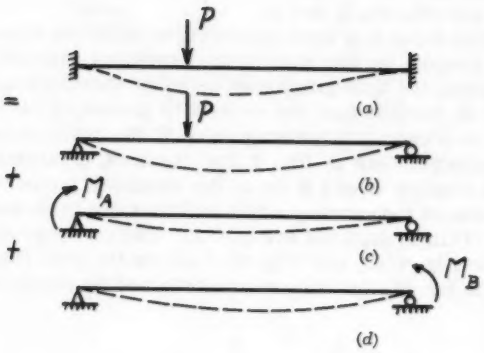

FIG. 1

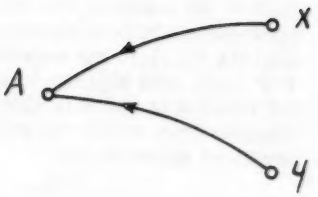

FIG. 2

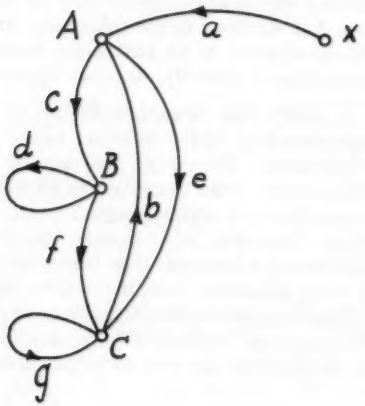

FIG. 3

in which x is an independent variable and A, B, C, are dependent variables. In any flow graph, a sequence of branches starting and ending at the same node is called a "loop." In Fig. 3, the branches A-B-C-A and A-C-A form two loops. Loops touching only one node are called self-loops. In Fig. 3, there are self-loops at nodes B and C. The product of the transmittances of all branches of any loop is called the "loop product;" accordingly, in Fig. 3 loop products corresponding to the named loops are cfb, eb, d, and g.

The method would be of limited value it it were necessary to write the equations prior to drawing the flow graphs, as was done in the preceding example. In applying it to a physical problem, the flow graph may be drawn directly from the physical interrelations. It is obvious that the necessary prerequisite to the efficient use of the method is a complete understanding of the problem on part of the analyst. For the beam problem of Fig. 1, for instance, a rational approach might be to equate the rotation of end A due to the redundant moment, $M_A\left(M_A\ \delta_{AA}\right)$, to the negative sum of the corresponding rotations due to causes $P\left(P\ \delta_{AP}\right)$, and $M_B\left(M_B\ \delta_{AB}\right)$. This is depicted in Fig. 4(a). The corresponding relation at end B is shown in Fig. 4(b), and Fig. 4(c) shows the total flow diagram from which the solution for M_A and M_B can be obtained by methods explained subsequently.

OPERATIONS ON FLOW GRAPHS

The operations of this section may be performed on flow graphs without changing their significance. All of these rules can be derived by consideration of the algebraic equations which are represented by the graphs. As example of a typical proof, rule 3 is derived in the following; the validity of the other rules can easily be demonstrated in an analogous fashion. For complete derivations, or demonstrations of validity, another source should be consulted.[2]

1. Elimination of a node: Two branches in series may be replaced by a single branch, the dependence of which is equal to the product of the dependences of the original branches. Thus Fig. 5(a) equals Fig. 5(b).

2. Elimination of a branch: Two branches in parallel may be replaced by a single branch, the dependence of which is equal to the sum of the dependences of the original branches. Thus Fig. 6(a) equals Fig. 6(b).

3. Shift of the head end of a branch: The terminal end of a branch may be shifted from one node to an adjacent node, if the flow diagram is changed in an appropriate manner. This manner is best illustrated by reference to Fig. 7(a), showing part of a flow diagram. Branch FB, of dependence f, is to be shifted from the old terminal node, B, to the new terminal node, C. This can be done in two steps:

   a. Branch FB is transferred to Node C, and its dependence is multiplied by the dependence of the branch flowing from the old to the new terminal node, BC.

   b. The starting node, F, is connected to all nodes receiving branches from the old terminal node, with the exception of the new terminal node. The dependences of these new branches are equal to the dependence of the shifted branch, f, multiplied by the dependence of the branch connecting the old terminal node, B, with the node corresponding to each new branch. Thus, the new branch, FE, of dependence fd, is introduced.

The result of these two operations is shown in Fig. 7(b). A proof of the validity of this operation follows. The relations shown in Fig. 7(a) represent the alge-

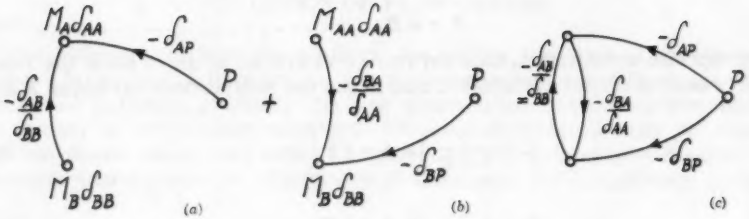

FIG. 4

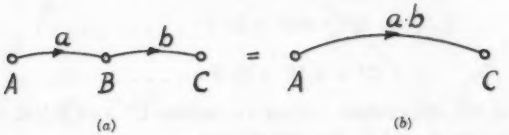

FIG. 5

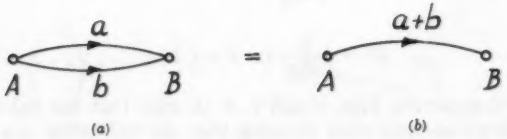

FIG. 6

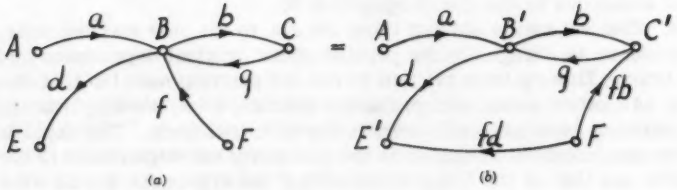

FIG. 7

braic dependences of the set of equations

$$B = a\,A + g\,C + f\,F \quad \ldots\ldots\ldots\ldots\ldots\ldots \quad (4a)$$

$$C = b\,B \quad \ldots\ldots\ldots\ldots\ldots\ldots\ldots\ldots \quad (4b)$$

and

$$E = d\,B \quad \ldots\ldots\ldots\ldots\ldots\ldots\ldots\ldots \quad (4c)$$

By appropriate substitution, this set can be rewritten so as to show the relation between the output variables C and E and the independent variables A and F

$$C = \frac{b}{1-b\,g}\,(a\,A + f\,F) \quad \ldots\ldots\ldots\ldots\ldots\ldots \quad (5a)$$

and

$$E = \frac{b}{1-d\,g}\,(a\,A + f\,F) \quad \ldots\ldots\ldots\ldots\ldots\ldots \quad (5b)$$

The relations of Fig. 7(b) can be written as

$$B' = aA + gC' \quad \ldots\ldots\ldots\ldots\ldots\ldots\ldots \quad (6a)$$

$$E' = dB' + fd\,F \quad \ldots\ldots\ldots\ldots\ldots\ldots\ldots \quad (6b)$$

and

$$C' = b\,B' + fb\,F \quad \ldots\ldots\ldots\ldots\ldots\ldots\ldots \quad (6c)$$

Again rewriting the dependent output variables C' and E' in terms of the independent variables A and F, the quantities

$$C' = \frac{b}{1-bg}\,(a\,A + f\,F) \quad \ldots\ldots\ldots\ldots\ldots\ldots \quad (7a)$$

and

$$E' = \frac{d}{1-bg}\,(a\,A + f\,F) \quad \ldots\ldots\ldots\ldots\ldots\ldots \quad (7b)$$

are obtained. Comparing Eqs. 5 and 7, it is seen that the values of C and C', and E and E' are identical, thus showing that the operation does not change the meaning of the graph.

4. Shift of the tail end of a branch: The starting end of a branch may be shifted from one node to an adjacent node if the flow diagram is changed in a manner analogous to the one of operation 3:

a. The tail end is shifted from the old to the new starting node, and its dependence is changed to the product of its original dependence and that of the branch flowing from the new to the old starting node (in that direction).

b. All other nodes, except the new starting node, sending branches to the old starting node are connected to the terminal node. The dependences of these new branches are equal to the product of the dependence of the shifted branch and that of the branch connecting the appropriate node with the old starting node.

Fig. 8 shows an example of this operation. Branch AD of Fig. 8(a) is to be transferred to Node B.

5. Removal of self loop: Any self loop can be removed if the dependences of all branches entering the node in question are divided by the quantity (1 - dependence of self loop). This operation is exemplified in Fig. 9.

SOLUTION OF FLOW GRAPHS

Two different methods are available for solving a system of equations expressed in terms of a flow graph. The first one makes use of the prior named operations to reduce gradually the flow graph to one (or more, depending on the number of independent variables) branch indicating directly the relation between cause (input) and effect (output). This step by step reduction corresponds to a successive elimination of unknowns in the algebraic process.

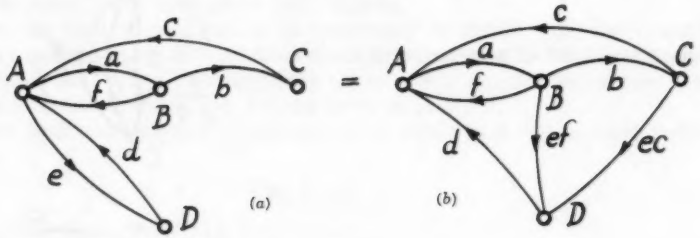

FIG. 8

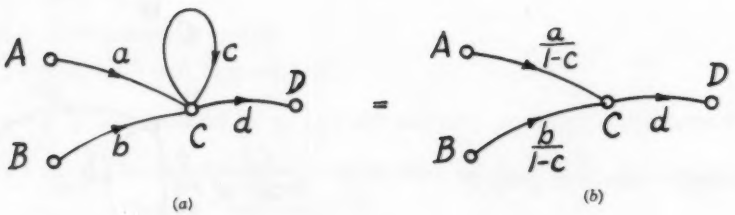

FIG. 9

Its use will be demonstrated in the following; no definite rules can be given, however. Often rule 5 is applied first, rules 1 or 2 subsequently, and rules 3 and 4 are used only after other possibilities are exhausted. With some experience, the solution can be performed quite rapidly.

The system represented by the flow graph of Fig. 3, and again shown in Fig. 10(a), will be solved by this method. Figs. 10(b) to 10(f) show the successive steps used in the solution.

From Fig. 10(f), the value of A is obtained in terms of the independent variable x as

$$A = \frac{a(1-g)}{(1-g) - b\,c\,f/(1-d) - e\,b}\ x \qquad \ldots\ldots\ldots\ldots\ldots (8)$$

(a)

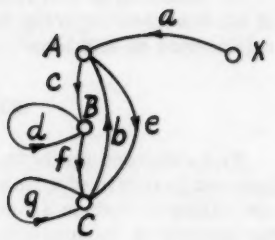

(b) ELIMINATE SELF LOOP AT B AND g (RULE 5)

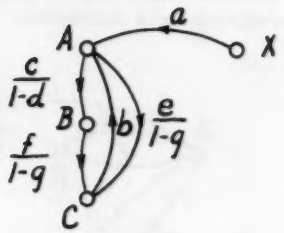

(c) ELIMINATE NODE AT B

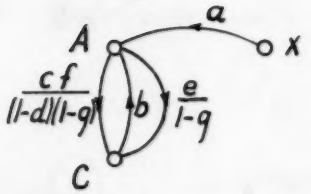

(d) ELIMINATE BRANCH AC (RULE 2)

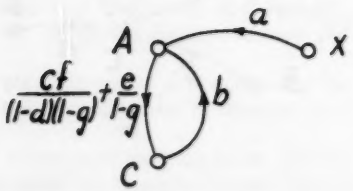

(e) ELIMINATE NODE C (RULE 1)

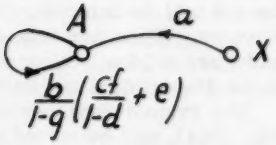

(f) ELIMINATE SELF LOOP AT A (RULE 5)

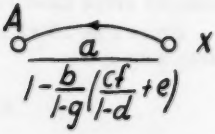

FIG. 10

Variable B can be found from Fig. 10(b):

$$B = \frac{c}{1-d} A = \frac{c\ a(1-g)}{(1-d)\ [(1-g) - b\ c\ f/(1-d) - e\ b]}\ x \quad \ldots\ldots\ (9)$$

Fig. 10(d) yields the dependent variable C as

$$C = \left[\frac{c\ f}{(1-d)(1-g)} + \frac{e}{(1-g)}\right] A = \left(\frac{c\ f}{1-d} + e\right)\left[\frac{a}{(1-g) - \frac{b\ c\ f}{1-d} - e\ b}\right] x \quad \ldots\ (10)$$

The second method used for the solution of flow graphs is a more formal one, making use of certain relations between the properties of flow graphs and the theory of determinants. The so called "Loop Rule" used in this method, and its proof, have been given by S. Mason.

Before stating this rule, it is necessary to define "disjoint loops." Two loops are said to be disjoint from one another if they do not have any nodes in common. Fig. 3, for instance, does not have any disjoint loops, except the self loops at B and C which are disjoint from each other.

The loop rule states that between two variables A and x, there is the relation

$$A = T_{xA}\ x \quad \ldots\ldots\ldots\ldots\ldots\ (11)$$

where the dependence T_{xA} is given by

$$T_{xA} = \frac{\sum_n \left[(\text{Loop product of } n^{th} \text{ path between x and A})\ \Delta_n\right]}{\Delta} \quad \ldots\ldots\ (12)$$

In Eq. 12,

Δ = Determinant of system

$= \prod_n (1 - n^{th}$ self loop product)

$- \sum_1 \left[(\text{Loop product 1})\ \prod_n (1 - n^{th}\ \text{Self loop product disjoint from 1})\right]$

$+ \sum_{(lm)} \left[(\text{Loop product 1})\ (\text{Loop product m})\ \prod_n (1 - n^{th}\ \text{self loop product disjoint from 1 and m})\right]$

$- \sum_{(lmn)} \left[(\text{Loop product 1})\ (\text{Loop product m})\ (\text{Loop product n})\ \prod_n (1 - n^{th}\ \text{Self loop product disjoint from 1, m, n})\right]$

$+ \ldots\ldots$

In this expression, the loop products l, m, n, are disjoint from each other. The series is continued until all disjoint loops in the system are multiplied by each other. The term $\prod_n x_n$ is the product of all quantities $x_1, x_2, \ldots x_n, \ldots$ in a set; Δ_n = co-factor of n^{th} path between x and A; and Δ_n = determinant of part of system disjoint from n^{th} path between x and A.

To demonstrate the use of the loop rule, the value of the dependent variable C in Eqs. 3 is calculated in terms of x. Referring to Fig. 3, there are two paths between x and C, acf, and ae. The determinant becomes

$$\Delta = (1-d)(1-g) - [(cfb)\ 1 + (be)(1-d)] \quad \ldots\ldots\ldots\ (13)$$

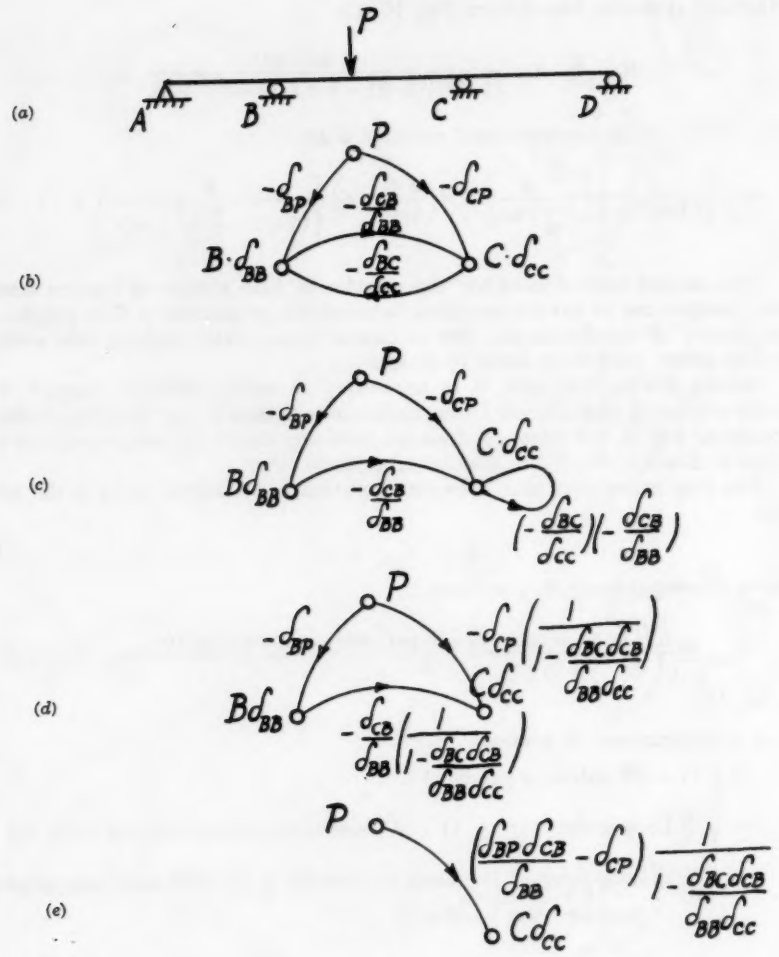

FIG. 11

There are no paths from x to C disjoint from each other; next, co-factors for paths acf and ae are, respectively,

$$\Delta_{acf} = 1 \quad \ldots\ldots\ldots\ldots\ldots\ldots \quad (14)$$

$$\Delta_{ae} = (1-d) \quad \ldots\ldots\ldots\ldots\ldots\ldots \quad (15)$$

and

$$\therefore T_{xC} = \frac{acf + ae\,(1-d)}{(1-d)(1-g) - cfb + be(1-d)} \quad \ldots\ldots\ldots\ldots \quad (16)$$

and therefore

$$C = \frac{acf + ae(1-d)}{(1-d)(1-g) - cfb + be(1-d)} \quad x \quad \ldots\ldots\ldots\ldots (17)$$

checking the previously obtained value.

APPLICATIONS

A regular scheme can be set up for elastic structures of any degree of indeterminacy. A typical model can be set up in terms of a continuous beam

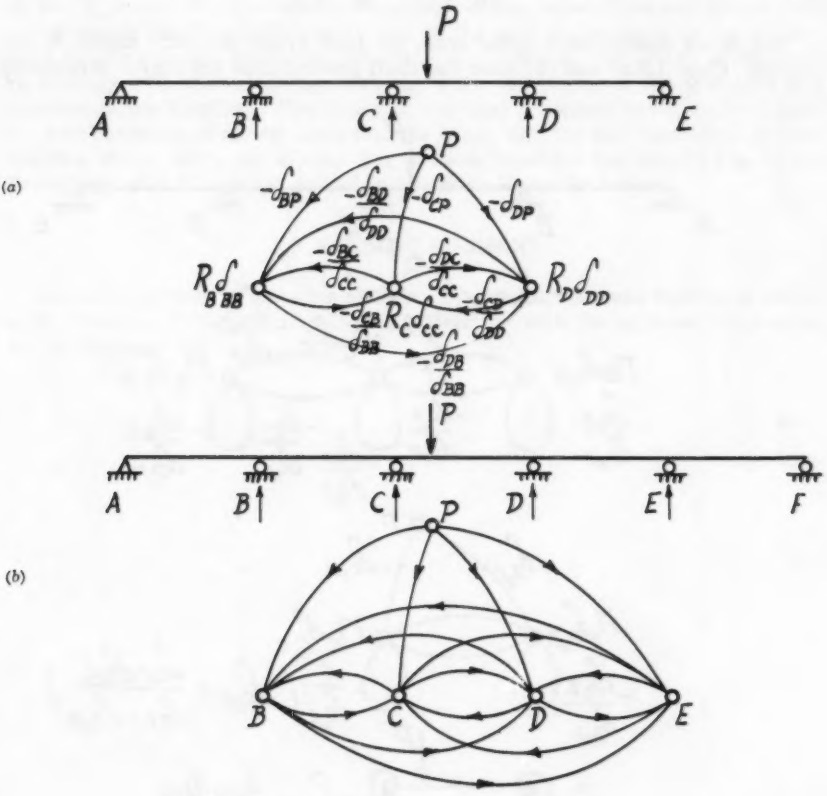

FIG. 12

with a number of redundant reactions to the degree of indeterminacy considered. A reasoning very similar to the one of the example of Fig. 4 may be used. For the two times indeterminate beam of Fig. 11(a), the interior reactions may be considered as redundants. At point B, for instance, the deflection of the primary structure due to the redundant reaction, B $(B\ \delta_{BB})$, is set equal to the negative value of the deflection due to the applied load $(P\ \delta_{BP})$ and that due to the redundant C $(C\ \delta_{BC})$. Following this reasoning one is led

to the flow graph of Fig. 11(b). To solve the system, the step-by-step process is used in Figs. 11(c) to (e). By inspection of Fig. 11(e), the value of the redundant C is written as

$$C = \frac{-\delta_{CP}\,\delta_{BB} + \delta_{BP}\,\delta_{CB}}{\delta_{BB}\,\delta_{CC} - \delta_{BC}\,\delta_{CB}}\,P \quad \ldots\ldots\ldots\ldots \quad (18)$$

and, making use of the relations of Fig. 11(b), the value of the redundant B is determined to be

$$B = \frac{-\delta_{BP}\,\delta_{CC} + \delta_{CP}\,\delta_{BC}}{\delta_{BB}\,\delta_{CC} - \delta_{BC}\,\delta_{CB}}\,P \quad \ldots\ldots\ldots\ldots \quad (19)$$

For more complicated structures, the flow graph can very easily be expanded. Figs. 12(a) and (b) show the most general flow graphs for structures

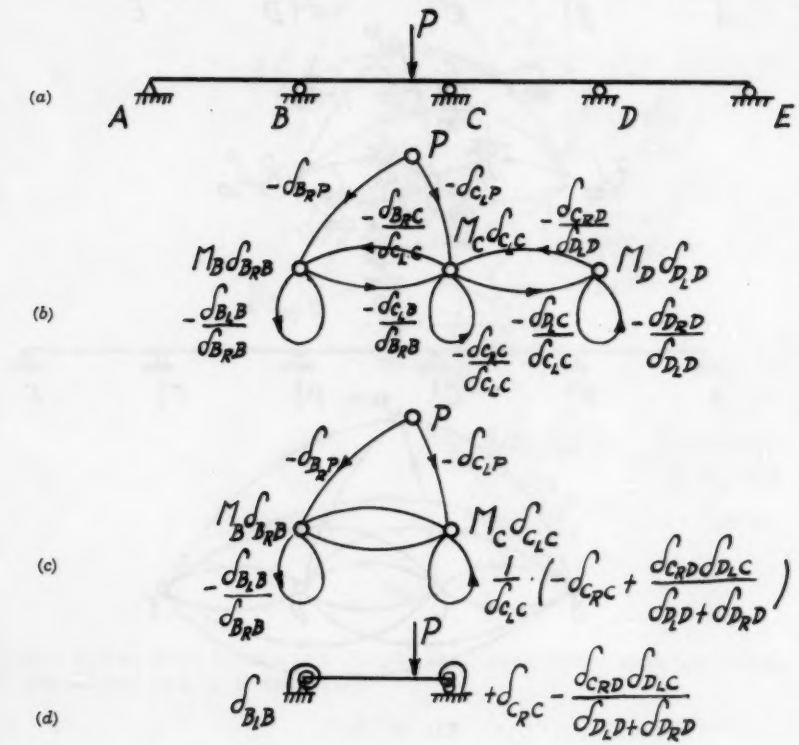

FIG. 13

of three and four degrees of indeterminacy. Due to coupling effects between all redundants, there are branches connecting every variable to every other variable.

Often, the analyst has the choice of the forces to be considered as redundants. For instance, it is well known that consideration of the support mom-

ents of a continuous beam as redundants will lead to a quicker solution than the previously utilized scheme. This also can be illustrated handily by use of flow graphs. Fig. 13(b) shows the flow graph obtained by equating rotations on both sides of each interior support due to the various possible causes. Here, $\delta_{B_R C}$, for instance, denotes the rotation of the beam end to the right of support B due to a unit moment at end C of the same beam. Redundant moments are considered positive as shown in the figure, and positive rotations are clockwise. It is obvious that a reduction of the flow graph of Fig. 13(b) may be accomplished quicker than of the corresponding graph of Fig. 12(a). Additional spans can easily be accounted for by extending the scheme shown.

Useful results can be deduced in the course of reduction of the graph of Fig. 13(b). It should be noted that the numerator of the value of the self loop at node D represents the flexibility coefficient of the part of the beam to the right of point D. Now, in the course of reduction, the graph of Fig. 13(c) is obtained. By analogy with the foregoing, here again the numerator of the self loop at C represents the rotational flexibility of the total structure to the right of point C. For purposes of stress analysis, the beam with the end restraints of flexibilities shown in Fig. 13(d) may thus be substituted for the beam of Fig. 13(a). Reductions of this type are useful in influence line calculations.

ACKNOWLEDGMENT

Acknowledgment is extended to Nolan Frederick, National Bureau of Standards, Boulder, Colo., for acquainting the author with the approach elaborated on in this paper.

Journal of the
STRUCTURAL DIVISION
Proceedings of the American Society of Civil Engineers

DISCUSSION

Note.—This paper is a part of the copyrighted Journal of the Structural Division, Proceedings of the American Society of Civil Engineers, Vol. 86, No. ST 10, October, 1960.

ELASTI-PLASTIC ANALYSIS OF CONTINUOUS FRAMES AND BEAMS[a]

Closure by Lawrence P. Johnson, Jr. and Herbert A. Sawyer, Jr.

LAWRENCE P. JOHNSON, Jr.[1] M. ASCE and HERBERT A. SAWYER, Jr.,[2] F. ASCE.—Mr. Augusti used influence lines and integration to illustrate the error of the approximation in assuming that a distributed plastic curvature is concentrated at the point of maximum moment. Actually, as stated in the paper, for any given span, including non-prismatic and curved spans, the location of this concentration for exact results is at the centroid of the distributed curvature. This principle is based on the linear relationship between the location of any angle change and the end-moment or force caused by the angle change. This linearity is expressed for the general case by the first terms of the equations at the top of Fig. 3 (Y_o being a linear function of K_b), and it is also expressed by Mr. Augusti's influence lines, which must always be linear.

Therefore, the error discussed by Mr. Augusti is simply the error in assuming the centroid of curvature at the point of maximum moment, and it can usually be dismissed by inspection. As the paper stated, to eliminate this error "for extremely asymmetrical curvature diagrams, the actual location of the centroid can be computed." Although this error was insignificant and thus tolerated for the illustrative examples, the authors would certainly agree with Mr. Augusti that this error may occasionally be significant.

Mr. Renzulli's analytical determination of the $M - \phi$ relationship for a rectangular section of an ideal material, being outside the scope of the paper, will not be commented on here. References were listed in the paper for work in this area for steel and reinforced concrete. Mr. Renzulli's expressions for plastic angles, his Eqs. (6) and (7), are identical to those in Fig. 2 of the paper for $k_2 = 0$.

Mr. Renzulli's Eq. (8), the general equation for joint continuity, is interesting as a mathematical expression of the problem to be solved. To be completely general, terms expressing the joint angles from sway should be added to this equation. As the discusser stated, direct solution of the system of non-linear simultaneous equations obtained by writing this equation for all joints is practically impossible. He therefore recommends that the non-linear terms be estimated using an assumed set of moments, and that the resulting linear system of equations then be solved for the moments and sways. Generally, the moments and sways so obtained will not agree with the assumed moments and sways, and new trials based on new sets of assumed moments will be necessary. Actually, this algebraic procedure is equivalent to the numerical procedure of the paper, the only important difference being that in the latter the

---

[a] December, 1958, by Lawrence P. Johnson, Jr. and Herbert A. Sawyer, Jr.

[1] Special Design Engr., Water Bureau, Metro. Dist. Comm., Hartford, Conn.
[2] Prof. of Civil Engrg., Univ. of Connecticut, Storrs, Conn.

moments of each trial are obtained by a moment distribution rather than by solution of simultaneous equations. The superiority of moment distribution over an algebraic method is well known (although with electronic computers this superiority is reduced). For example, for the algebraic solution of Example 2, each trial would involve the solution of 22 equations for 22 unknowns, whereas the corresponding solution by moment distribution occupies four or five horizontal lines of Fig. 6(b).

On the other hand, the interesting alternative approach to the problem suggested by Dr. Rosenblueth, involving assumption of elastic hinges at the plastic regions, is like the method of the paper in that it uses moment distribution for each trial. To the authors, however, an important point of difference is that the spring constants of the elastic springs change with each trial, necessitating a recalculation of the fixed-end-moments, relative stiffnesses, and carry-over factors of all hinged spans for each trial. These elastic quantities remain constant for the method of the paper.

The design of a structure usually involves analyses for several loading conditions, and several moment-distributions are required for each elasti-plastic analysis. Because of this repetition, the authors recommended and illustrated use of unit-moment distribution factors as the most efficient method of moment distribution. The authors agree with Dr. Rosenblueth that the advantages of this method diminish as the number of joints increase. However, this method is optional, and the usual method of moment distribution may be reverted to at any time in the design process without affecting the over-all operation of the method.

Both Mr. Renzulli and Dr. Rosenblueth present interesting simplifications of the general method of the paper, the former a method in which the elastic deformations are neglected, Fig. 8(b), and the latter a method following Baker in which there is a sudden and complete transition from elasticity to plasticity without strainhardening, Fig. 8(c). Both of these methods are compromises between the general elasti-plastic method of the paper and the well-known simple rigid-plastic theory, and the potential value of these compromises is that they may, unlike simple plastic theory, account for deformations, and that this accounting may be accurate enough for design purposes without resorting to the more complex elasti-plastic methods.

The authors cannot agree that Mr. Renzulli's approximation involving neglect of elastic strains is generally good for "homogeneous and reinforced concrete sections". The ratio of total elastic to total plastic angle change for any member with a linear moment diagram is equal to the ratio of the elastic to plastic areas below the level of M of the $M - \phi$ diagram, authors' Fig. 1(a). For the $M - \phi$ diagram derived and presented by Mr. Renzulli in his Eqs. (1) and (2) and his Fig. 2, using his "ideal" stress-strain relationship with $\epsilon_r = 3\epsilon_0$, this ratio has been calculated to be about 5 for $M = M_u$, and it approaches infinity as M approaches M_e. Elastic strains seem to be equally important for reinforced concrete. As an example, for the $M - \phi$ relationship used in Example 2, based on tests of reinforced concrete, the minimum ratio of elastic angle to plastic angle for a linear moment diagram is 3.8. Certainly the major source of strain cannot be neglected in a strain analysis. Therefore, the approximation of Fig. 8(b) should not be used for reinforced concrete.

As for steel, tests recently conducted by one of the authors at the University of Connecticut yielded, for rolled steel sections with linear moment diagrams, minimum ratios of elastic angle to plastic angle of from 0.09 to 0.70. (Since sections with rather slender elements were used for many of these tests, the

lower of these ratios is probably more representative of the usually-used sections than the higher.) Although these ratios are much lower than those for reinforced concrete, other considerations cause the authors to question the use of the neglect-of-elastic-strain approximation for steel. First, an important purpose of a strain analysis is presumably to detect those structures for which a limiting strain may prevent attainment of the ultimate load indicated by the rigid-plastic theory. Unfortunately, those members with the smallest limiting strain are also the members with the highest ratios of elastic to plastic angles. Hence, the error of this approximation is greatest (and on the unsafe side) for the very members or structures for which a strain analysis may be important. A second, and secondary consideration is that the post-elastic portion of the moment curvature diagram for rolled steel sections, consisting as it does of an essentially horizontal, "true plastic" line and an inclined strain-hardening or "modified plastic" line, as shown in Fig. 1(b), cannot be accurately represented by any single line.

The two other possible purposes of a strain analysis of a steel structure in the plastic range should also be mentioned: one is the determination of the amount that strain-hardening will allow the load on a structure to exceed the fully-plastic ultimate load, and the second is the determination of deflections.

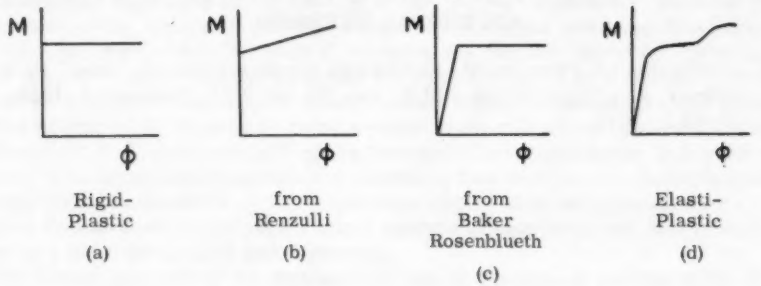

FIG. 8.—COMPARISON OF M - ϕ CURVES

For both of these purposes, the above errors would make the use of the neglect-of-elastic-strain approximation for steel very questionable.

The Baker-Rosenblueth approximation avoids the above errors by accounting for elastic strains, and thus the authors would agree that this approximation is of potential value for reinforced concrete design. Since one of the authors has recently discussed the relationship between this approximation and the elasti-plastic methods in these pages,[15] further discussion will be limited to two observations. One is that the strain-hardening portion of the M - ϕ relationship, neglected in this approximation, is essential for any rational determination of the plastic-region curvatures at the time the limiting strain is attained, and therefore essential for rational determination of ultimate hinge-rotation capacities.[2] Second, the authors believe that this advantage and the other advantages[15] of elasti-plastic methods which result from use of the full M - ϕ relationship do not seem to be outweighed by any increase in computational difficulty. It is primarily a lack of definitive information on M - ϕ relationships which presently discourages use of elasti-plastic methods for reinforced concrete design.

The authors appreciate Dr. Rosenblueth's elaboration on the possibilities, valuable in design, of making structural changes at intermediate stages of a

limit analysis. As Mr. Eremin mentioned, the elastic properties used with an elasti-plastic method are independent of the magnitude, location, or quantity of the plastic regions, so the designer can make adjustments in reinforcing steel without redoing previous computations and without change of procedure for the next trial.

Mr. Eremin's presentation of an alternative graphical method of moment distribution, with its attendent advantage of pictorial clarity, is appreciated.

A word about the relationship of the elasti-plastic methods of this paper and a preceding paper[2] is in order. The method of the preceding paper is analogous to the column analogy or elastic center methods used for elastic solutions, and it should be used for an elasti-plastic solution in any situation for which the column analogy is suitable for an elastic solution. The method of the present paper is analogous to the Cross moment distribution method used for elastic solutions, and it is suitable for elasti-plastic solutions in situations for which moment distribution is suitable for elastic solutions.

The authors thank the discussers for their imaginative and valuable contributions to our knowledge of the elasti-plastic behavior, analysis, and design of structures.

ADDITIONAL REFERENCE

15. Discussion of: "Review of Limit Design for Structural Concrete," by H. A. Sawyer, Jr., Proceedings, ASCE, Vol. 85, No. ST 7, September, 1959, pp. 51-52.

ITALIAN ARCH DAM DESIGN AND MODEL CONFIRMATION[a]

Discussion by K. G. Harding and N. S. Trahair

K. G. HARDING[3] AND N. S. TRAHAIR.[4]—The author is to be congratulated for his paper on arch dams in which he has traced the trends in modern concrete dam design to the double curvature arch dam and has indicated Italian design methods for this type of dam. In Australia there is a growing interest in recent developments of the arch dam by European designers. Without first hand knowledge of the inter-relation of the various innovators of these developments, it appears that the tensile stresses at the base of cantilevers in a single curvature dam gave rise to the concept of the "active" cantilever, which in itself contains the notion of vertical membrane stresses near the foundation. Thence it appears as another step to conceive the "active" dome or the membrane shape, wherein bending moments have been reduced to a minimum. The shapes of the Italian membrane dams derived from mathematical and model studies appear to be similar to those evolved from rubber membrane methods suggested by J. F. Lobo Fialho[5] of the National Civil Engineering Laboratory, Lisbon. The membrane shape should produce a dam with the most efficient use of concrete. The evolution of the shape from experiment and approximate calculation appears now to require a basic analytical approach, and Mr. Oberti's paper is a pioneer work in this direction.

The author has rightly emphasized the use of structural models in the design of arch dams and his descriptions of some of the work carried out by ISMES show clearly how powerful a design tool model studies can be. The method of analysis by model studies is extremely versatile and makes it possible to account for a large number of varying site conditions which are difficult to include in analytical design methods.

Existing theoretical methods of analyzing arch dams are generally only approximate because of the complexity of the design problem and the number of different effects involved. The more sophisticated of these analytical methods are generally very tedious in application. This has discouraged a great many designers and influenced them towards model studies. However, the advent of the electronic computing machine is changing this state of affairs. The trail load method of analysis,[6] once frightening in its complexity and length, has been revised by Mladyenovitch[7] for solution by electronic computing machines and this has resulted in a great saving of time and labour.

---

[a] March, 1960, by Guido Oberti.

[3] Superv. Engr., Dept. of Works, Canberra, Australia.

[4] Engr., Dept. of Works, Canberra, Australia.

[5] "Principios Orientadores do Projecto de Barragens Abobada," by J. F. Lobo Fialho, Memoria No. 67, Bol. Ord. Eng. 4, No. 1, January, 1955.

[6] "Trial Load Method of Analyzing Arch Dams," U. S. Bur. of Reclam.

[7] "The Analysis of Arch Dams by the Solution of Linear Equations," by V. Mladyenovitch, Travaux, No. 290, December, 1958.

Even at the present time, analytical methods play a very important part in the design of arch dams. By the judicious use of these methods initially, a preliminary design may be quickly achieved. The refinement of the design is usually obtained by a trail and error process, each trial being checked either by model studies (if the specialists and laboratory facilities are available) or by a sophisticated analytical method using electronic computing machines.

There is no set method of attack in the design of arch dams and the designer has a number of conflicting factors to resolve and several methods of analysis. A method of design to account for both membrane and bending stresses in arch and cantilever is proposed as follows:

1. Preliminary selection of horizontal arch curvatures. These depend chiefly on the valley widths.
2. Preliminary selection of arch thicknesses. This may be done either by assuming that the horizontal arches carry the total applied loads, or by deriving an equation for uniform strength as indicated by Mr. Oberti.
3. Preliminary selection of the curvature of the central cantilever so that it follows the funicular polygon of the water loads carried by the central cantilever.
4. Graphical analysis of the central cantilever as set out by the author. This changes the total applied water loads H_i to a series of horizontal water loads S_i.
5. Application of the water loads S_i to the dam in a simple arch-cantilever analysis such as that reported by Parme.[8]
6. Modification of the geometry of the dam following the results of step 5.
7. Repetition of steps 4, 5, and 6 until a satisfactory preliminary design is achieved.
8. Analysis of preliminary design by either model studies or a more refined analytical method (in which the water loads S_i would be used).
9. Successive adjustment of the geometry of the dam based on the results of step 8 followed by the repetition of the analysis until a satisfactory final design is achieved.

This proposed method of design should be checked by model studies to determine its accuracy and limits of application.

It is suggested that the papers' value would be increased by the following changes:—

In Fig. 5, Section BB, change $T_C + \frac{\partial T_C}{\partial \phi} d\phi$ to $\left(T_C + \frac{\partial T_C}{\partial \phi} d\phi\right)\left(r + \frac{\partial r}{\partial \phi} d\phi\right) d\theta$.

In Fig. 5, Section BB, change $M_C + \frac{\partial M_C}{\partial \phi} d\phi$ to $\left(M_C + \frac{\partial M_C}{\partial \phi} d\phi\right)\left(r + \frac{\partial r}{\partial \phi} d\phi\right) d\theta$.

In Fig. 5, Section AA, change r to ρ_{Π}. In Fig. 5, Section AA, change $dX = r\, d\phi$ to $dX = r\, d\theta$. In Fig. 5, Section AA, change $d\theta$ to $d\theta \frac{r}{\rho_{\Pi}}$. Change the equation $X = \rho\gamma^3$ (under the heading "Requirements of Similtude") to $X = \rho\lambda^3$. In Eq. 16 change $K_s = \frac{\gamma 1_m}{\gamma}$ to $K_s = \frac{\gamma 1_m}{\gamma 1}$.

---

8 "Arch Dams with Arches of Variable Thickness," by A. L. Parme, Constructional Review, Vol. 21, No. 1, May, 1948.

THE IMPACT OF COMPUTERS ON ENGINEERING EDUCATION[a]

Discussion by Francis E. Swain

FRANCIS E. SWAIN,[8] M. ASCE.—The author has presented an excellent paper which points out the resounding influence which the engineer's new tool, the electronic digital computer, is having upon the engineering profession in general and upon engineering education in particular.

Electronic computers have had a pronounced effect in many areas of the engineering profession, as the author notes. Many organizations, both public and private, have used such equipment for investigative, design, and research studies for 8 years or more. The impact upon engineering educational institutions, other than on those which have been concerned with graduate studies in the research and development of computers for some time, has been felt more recently. Some engineering schools, even now, have not installed or do not have access to electronic computing equipment, while others only recently have acquired such machines. One reason for this delay undoubtedly has been the limited funds available to many schools for the rental or purchase of a computer. Other institutions may have put off the inclusion of computing work in their curricula until definite trends and requirements in what is needed are established. As the author points out, however, the university now finds itself in the position of being forced to respond to the profound effects of the electronic computer. This pressure may, in many instances, be more than slightly discomforting. The manner in which the university responds is of utmost importance if the true functions of the institution are to be carried out in this field.

The author states that the overriding question concerning curricular policy would seem to be a decision as to whether major emphasis shall be placed on educating users of computing equipment or designers of computing equipment. The writer wonders if the paramount question concerning curricula is not so much whether designers or users should be produced, but rather how best can all engineering students be educated in the fundamental overall capabilities and potentialities of computers, regardless of whether they may go on into the development of new machines or use them to solve engineering problems. Many students, such as those taking architectural, chemical, civil, and mechanical engineering, probably would have little interest in the design of computing equipment. Such interest would lie primarily with students of electrical engineering and mathematics, depending upon whether they were interested in the design of computer hardware or the development of the logic for the machine.

The writer concurs, in the main, that no new technical courses dealing exclusively with computers need be added to the curriculum to educate either potential designers or users. There is no more reason to provide special courses

---

[a] April, 1960, by Gordon P. Fisher.

[8] Chf., Automatic Data Processing Branch, Office of Asst. Commr. and Chf. Engr., U. S. Bur. of Reclam., Denver, Colo.

for future computer designers than there is need to have such courses for potential designers of radio, radar, telemetering, or television equipment. A thorough fundamental knowledge in electronics, solid state physics, circuits, and mathematical logic should, as the author notes, suffice for all.

Engineering students can be better fitted for potential users by providing them with a good foundation in fundamentals, particularly in basic sciences and mathematics, including numerical analysis. A progressive faculty interested in and with some knowledge of machine computation is indispensable as the author points out. One important responsibility of all engineering faculties is to impress firmly upon the students that to sit before a desk-type calculator and do hundreds or thousands of computations is not to do professional engineering work. Doctors have medical technicians to run their laboratory tests and lawyers have stenographers and typists to perform the mechanical operations in the preparation of their briefs. Too many engineers have considered too long that depressing key-board buttons and reading calculator dials constituted professional engineering services. When pressed for a reason for so doing, the answer most always is, "This is the way we always have done it." Engineers must be made to know that their profession is going to acquire additional stature and prestige only through the professional use of their technical talents and training. The application of electronic computing equipment as a tool to do routine and repetitive calculations is a big step toward achieving this goal. In some instances this may not be an easy task to perform. Perhaps by constant impressions and suggestions over the longer 5-year undergraduate programs, time-worn traditions and the "way we have always done it" attitude may be changed.

The author presents two important points in his discussion under "Research;" namely, that the computer is no substitute for intelligence, and that the computer cannot formulate problems but only follow detailed logical instructions. Due undoubtedly to catchy phrases and misinformation appearing in the popular press during the early history of computers, many engineers look upon the devices as "magic brains" or "machines that think." They were led to believe that electronic calculators were all powerful in solving all problems, and that to use such machines one had to be a member of that exclusive society which includes Einstein and von Neumann. Engineers in school and those in practice must be made to know the capabilities and the limitations of computers if they are to use the machines intelligently as powerful tools. These engineers must also be made aware that computers are most impartial; they will process nonsense as well as good information.

The writer would like to place emphasis on the author's statement that the university must look beyond the bounds of curriculum adjustment and research programs to its relationship with engineering practice. It has been the writer's experience that many practicing engineers in the field or in small design offices are not making use of computers in any manner because of their complete unfamiliarity with the machines. Remarks are often made in some such form as, "I don't know whether I have any problems that can be solved on a computer because I don't know what such machines can do." The university can fill the need for supplying such information by furnishing or sponsoring short courses, seminars, clinics, and adult education courses in appropriate areas. A true university should be of service to its complete family, not only to those still in attendance within its hallowed halls. Where such instruction can be given by industry, the university should not be called upon to serve, as the author notes.

Company-sponsored classes may not be possible in many instances, however, because of the lack of trained personnel within a given organization.

The author concludes his thought provoking discourse with two important statements; namely, that the influence which digital computers are having and will have on engineering education is one of the most generally significant revolutions ever faced by engineers, and that few persons will deny that engineering education is being impelled into an era of genuine enrichment. The writer believes also that through the intelligent application of the electronic computer, the engineer himself is entering into an era which will be full of both personal and professional enrichment. High-speed computing devices give the engineer a new tool which will permit him to drop the role of numerical technician and to assume the mantle of a truly professional person.

DYNAMIC EFFECTS OF EARTHQUAKE[a]

Discussion by A. A. Eremin

A. A. EREMIN,[23] M. ASCE.—Mr. Clough has shown an interesting analysis of the Building codes for seismic forces and forces computed from the dynamic equations for vibrated structures. The similarity of the seismic force expressions was correctly shown.

The theory of vibration of structures has a wide range of application. Therefore, applying the dynamic equations from the theory of vibration to the seismic force, the design of buildings may be considerably improved.

Generally, in computing critical seismic force, the maximum magnitude of seismic shock is considered. With dynamic equations, greater precision in seismic stresses may result by considering the maximum intensity of seismic shock.

It is well known that the intensity of seismic shock varies not only with the magnitude of the nearest fault line and distance of the fault line to the structure, but also with the geologic properties of the ground at the fault line.

In Fig. 3 the graphs for spectral velocity may be changed by inclusion of the factor $\frac{2\pi}{T}$ in the expression for spectral velocity S_V. More direct graphs for seismic force will result.

The author made a valuable contribution by introducing the dynamic equations for seismic force analysis.

---

[a] April, 1960, by Ray W. Clough.

[23] Assoc. Bridge Engr., Calif. State Highway Dept., Sacramento, Calif.

INFLUENCE OF PARTIAL BASE FIXITY ON FRAME STABILITY[a]

Discussion by Eugene Guillard

EUGENE GUILLARD,[15] F. ASCE.—Mr. Galambos shows for a symmetrically loaded frame, in which he chooses to ignore the primary bending moments normally associated with this type of frame, that as the column base restraint is increased the effective length of the column is reduced, thus increasing the buckling strength of the frame. He also shows that small amounts of restraint result in relatively large reductions in the effective length of the columns. This is interesting, but of little practical value to the designer, confronted with a real structure subjected to a normal loading configuration, until the effect of primary bending moments in the frame can also be evaluated.

The theoretical problem presented by the author has been adequately treated by F. Bleich[2] who cautions that the primary bending moments have not been considered, and further states that, "At present no suitable method is available for determining the critical load of rectangular rigid frames which takes account of the influence of these bending moments on the stability of the structure." A paper by E. Chwalla investigating the problem of lateral stability of a rigid frame subjected to transverse loads has also been reviewed.[2] The paper treats a specific problem and the analytical results indicate that the distortion of the framework prior to buckling, caused by the transverse loading of the horizontal member, reduces the buckling strength of the system only to a rather limited extent. It remains to be proved, however, that this is generally true.

In view of the preceding, the critical load computed in the illustrative problem is subject to some doubt. It, at best, can only be an upper bound to the buckling load of the frame.

In the section on the "Application of the Theory" and the illustrative example in Appendix II there are several assumptions which may be misleading and which tend to credit the normal pinned base with a fixity coefficient which is too large. For example, in the expression for the moment-rotation characteristics of the base plate connection (Eq. 39) it its assumed that there are compressive strains under the entire base plate throughout the range of interest. It is of interest to know if this is true. Also, what value of modulus of elasticity (E_c) should be used? Because, in concrete, strain increases faster than stress and permanent deformation occurs under low stress would it not be more realistic to use a lower value for E_c than that normally associated with the modular ratio? Does not the preceding reasoning also apply with regard to the stress-strain relationship of the soil under the footing?

Considering the stiffness of the base plate connection and the stiffness of the footing in the soil, the statement is made, "Whichever of the two stiffnesses

---

[a] May, 1960, by Theodore V. Galambos.

[15] Res. Engr., Armour Research Foundation of Illinois Inst. of Tech., Chicago, Ill.

yields the least stiffness would be used to determine the coefficient λ and thus the buckling strength of the frame." Would it not be more correct to consider that the two stiffnesses are in series? The end restraint of the column would thus be less and tend more toward the pinned base.

With regard to the illustrative problem if it is assumed that the top cross beam of the frame supports a uniform load, the maximum total load that may be applied to the frame whether the column bases are pinned or fixed, is approximately 40 kips using AISC specifications. Under these conditions the footing assumed in the example appears to be much too large for the pinned base assumption.

As a final plea for conservatism in the evaluation of end restraint of columns the writer makes reference to a paper[16] by F. R. Shanley and quotes therefrom:

> In theory, end restraint has a very simple effect: It merely changes the effective column length. In practice, however, the accurate determination of the effect of end restraint for any column except a pin-ended column is a difficult problem. . . . . It is important to realize that efficiently designed structures cannot be made proportionately stronger by increasing the amount of end restraint. This fact, too, was pointed out by Mr. von Karman when he declared, in effect, that end restraint causes a marked increase in buckling strength only for long slender columns, not for shorter ones.

---

16 "Applied Column Theory," by F. R. Shanley, Transactions, ASCE, Vol. 115, 1950, pp. 698-727.

VARIOUS INSTABILITY MODES OF THE FIXED BASE COLUMN[a]

Discussion by Marvin A. Larson

MARVIN A. LARSON,[3] F. ASCE.—The author is to be commended for the general excellence of his paper. However, the writer feels impelled to offer disagreement on several points.

The mechanism termed by the author "column supporting a roller" should more properly be described as a rocker. This is the terminology used for similar mechanisms when used at the supports of bridges or similar structures. A rocker is fixed through its center of rotation to the supported structure, and rotates but does not move laterally if the support moves horizontally beneath the structure. A roller is interposed between the structure and its support. If the support moves a given distance laterally, the center of the roller will move a distance half as great. If the support is a fixed base column, as in the case under consideration, and the top of the column rotates during buckling, the direction and point of application of the thrust delivered by the supported structure to the column will be different for the two cases. For a rocker, the thrust will be delivered through the pivot point and the point of contact with the top of the column, and will have an inclination equal to the rotation of the top of the column. For a roller, the thrust passes through the two points of contact between supported structure and roller and between roller and the top of the column, in general, it does not pass through the center of the roller, and has an inclination from the vertical, half as great as the rotation of the top of the column.

The difference in action of rocker and roller is demonstrated by Fig. 13. Fig. 13 (a) and (b) depicts the action of a rocker mounting. The relationships developed by the author are applicable to this mechanism. Fig. 13 (c) and (d) depicts the action of a roller mounting. The stability considerations are distinctly different from those of a rocker, and are developed subsequently by the writer.

Fixed Base Column, Loaded Through a Roller.—If the mechanism shown in Fig 13 (c) is subjected to a load of sufficient magnitude to induce buckling of the column, with both rotation and translation at the top of the column, the conditions shown in Fig. 13 (d) will be developed. Following procedures used by the author, the bending moment at any point on the column is given by the equation:

$$M_X = -E I \frac{d^2y}{dx^2} = P(y - \delta/2) - P \frac{\phi}{2} (L + 2R - x) \quad \ldots\ldots\ldots (45)$$

---

[a] July, 1960, by D. A. Sawyer.

[3] Cons. Struct. Engr., San Francisco, Calif.

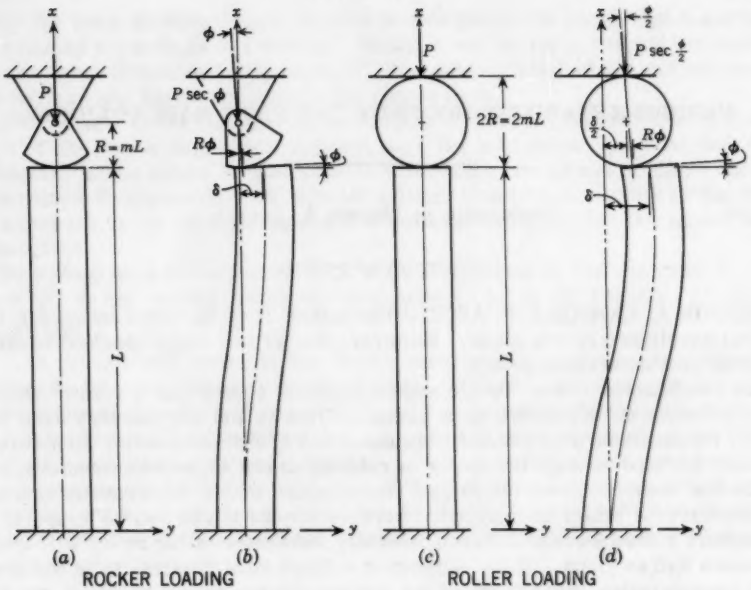

FIG. 13.—ACTION OF A ROCKER AND A ROLLING MOUNTING

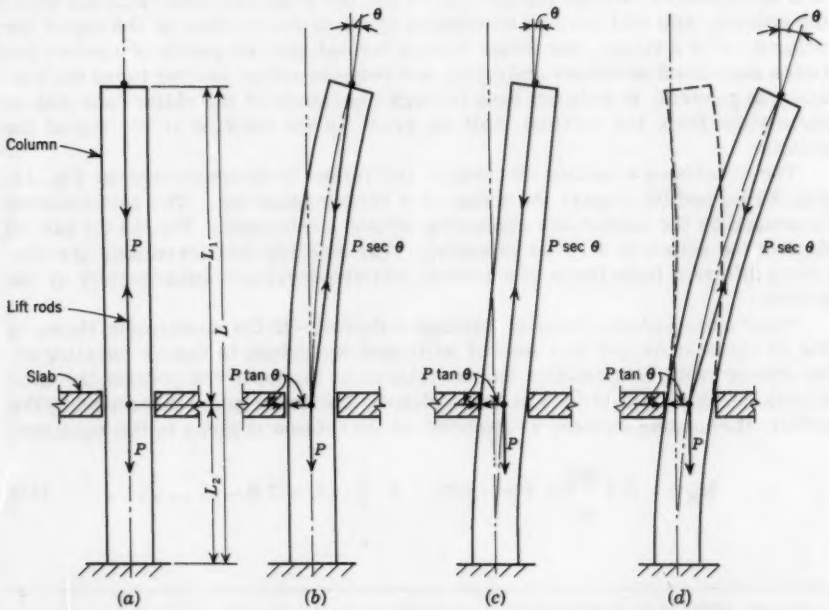

FIG. 14.—BUCKLING OF LIFT SLAB COLUMNS

The solution to this equation is:

$$y = A \cos kx + B \sin kx + \delta/2 + L \frac{\phi}{2} + R\phi - \phi \frac{x}{2} \quad \ldots\ldots (46)$$

where $k^2 = P/(E\ I)$

The boundary conditions are:

$$y = 0 \quad \text{at } x = 0 \ldots\ldots (47)$$

$$\frac{dy}{dx} = 0 \quad \text{at } x = 0 \ldots\ldots (48)$$

$$y = \delta \quad \text{at } x = L \ldots\ldots (49)$$

and

$$\frac{dy}{dx} = -\phi \quad \text{at } x = L \ldots\ldots (50)$$

Substitution of the boundary conditions into Eq. 46 gives the following:

$$A = -\delta/2 - L \frac{\phi}{2} - m\,L\,\phi \ldots\ldots (51)$$

$$B = \frac{\phi}{2k} \ldots\ldots (52)$$

$$3(1 + \cos kL) + k\,L\,(1 + 4\,m) \sin kL = 0 \ldots\ldots (53)$$

and

$$\phi = -\frac{k\,\delta \sin kL}{2 + \cos kL + k\,L\,(1 + 2\,m)\sin kL} \ldots\ldots (54)$$

Eq. 53 establishes the magnitude of load which is required for equilibrium with the column in its buckled state. It is satisfied by a value of $k\,L = \pi$. Since both terms of Eq. 53 are positive for all values of k L between zero and π, it is evident that this is the first mode of buckling. Using the relationship, $k^2 = \frac{P}{E\,I}$, the load corresponding to the first mode of buckling is determined to be

$$P_{cr} = \frac{\pi^2\,E\,I}{L^2} \ldots\ldots (55)$$

This is the classic Euler equation for buckling of a pin ended column.

From Eq. 54, by substituting a value of π for k L, the rotation of the top of the column is determined to be: $\phi = o$ when $k\,L = \pi$. The column then, in the first mode of buckling, has equal and opposite moments at top and bottom, and consequently a point of contraflexure at mid length. Note also that the critical load, for the first mode of buckling, is independent of the radius of the roller.

Lift Slab Columns.—The writer has previously had occasion to investigate the stability of lift slab columns, and has derived relationships which are identical in effect with those expressed by the author in Eq. 43 and 44. The writer finds, however, that Eq. 34 is not applicable to a conventional lift slab column.

Referring to the Fig. 12 (a), the column deflection, y, at the elevation of the slab must be equal to the slab translation, δ, as the column is encircled by a close fitting collar embedded in the slab. Also, the bending moment in the column at the elevation of the slab must be identically zero, regardless of the state of buckling, as the load applied by the lifting rods at the top of the column is directed along the rods and through the center of the collar, which remains centered on the column at slab level. Eq. 34 does not satisfy these conditions. Eq. 34 describes a structure in which there is no lateral movement of the slab during buckling of the column, and in which the clearance is so large that there is no contact between collar and column during buckling.

The buckling criteria can be expressed most simply and clearly in terms of the lengths of column segments from top of column to slab level and from slab level to column base. Fig. 14 (a) shows a column of height L, with the slab lifted to a level which divides the full height of the column into segments L_1 and L_2 above and below the slab respectively. Buckling may occur either above the slab, as in Fig. 14 (b), or below the slab, as in Fig. 14 (c), and in general will occur in one segment of the column only, the other segment remaining straight.

For buckling above the slab, the critical load is

$$P_{cr} = \frac{\cos\theta \ \pi^2 E I}{L_1^2} \quad \ldots\ldots\ldots\ldots\ldots\ldots \quad (56a)$$

At the initial state of buckling, θ is a small angle and can be set equal to unity, reducing the buckling criterion to

$$P_{cr} = \frac{\pi^2 E I}{L_1^2} \quad \ldots\ldots\ldots\ldots\ldots\ldots \quad (56b)$$

For buckling below the slab, the critical load is

$$P_{cr} = \frac{\pi^2 E I}{4 L_2^2} \quad \ldots\ldots\ldots\ldots\ldots\ldots \quad (57)$$

For buckling to occur throughout the length of the column, as in Fig. 14 (d), the critical load must be the same for both segments of the column. This requires that the slab be located at one third the height of column above the base, in which case L_1 is twice as large as L_2, and the two critical loads are equal. However, even though occuring simultaneously, the two types of buckling are independent of each other in direction and magnitude.

In actual lift slab operations, the lengths L_1 and L_2 are variable during the lift. The most critical stage for buckling as in Fig. 14 (b) is at the start of the operation when L_1 equals L. If the column is stiff enough to resist buckling at this stage, it cannot buckle as in Fig. 14 (c) until the slab has been raised to half height of the column.

The author's treatment, and the foregoing discussion, constitute only a brief introduction to the problem of lift slab column design. Some of the other elements which must be considered in a complete treatment of the subject are given subsequently, not necessarily in order of importance.

(1) The number of columns involved in a single lift is typically from eight to twelve, and may run to twenty or more. There often is considerable variation in the vertical loads carried by individual columns. The columns may or may not be of the same size and stiffness. A buckling failure as in Fig. 14 (c) involves the group action of all columns interconnected by the slab, some of which may be carrying loads above and others below that required to produce buckling of a single column acting independently. Also, failure may be initiated either by a lateral movement of the slab or, in some cases, by a rotational movement of the slab.

(2) The number of slabs is not limited to one, and may be a dozen or more. These are distributed throughout the height of the columns. At various stages of the lift they may be considered as simply supported by or rigidly connected to the columns, depending on the procedures followed.

(3) Conditions at the column bases may require some modification of the assumption of absolute rigidity.

(4) In addition to the vertical loads, it is necessary to provide for some horizontal forces acting on the structure, either due to accidental loadings, to wind forces, or to earthquake forces.

(5) In a practical structure, the effects of inaccuracies, uncertainties, and tolerances must be considered. The columns may have an initial curvature. They may not be set exactly plumb. The lifting jacks may not be exactly centered on the tops of the columns, and the rods may not engage the centers of the lifting collars in the slab. The collars cannot fit tightly around the columns, but require a clearance of 1/2 in. to 3/4 in. to prevent binding during the lift. Possible variation in rate of advance of the jacks may cause shift of loads between the various columns.

It should be apparent that the rational design of columns for a lift slab structure involves complexities not found in those for other, more traditional, types of construction. A thorough and authoritative treatment of the subject would be welcomed.

BASIC COLUMN STRENGTH[a]

Discussion by Donovan H. Lee

DONOVAN H. LEE,[18] F. ASCE.—It would seem likely to be of great interest to others as well as the writer if the authors would care to give their views on the following points.

Do they consider that the higher yield strength often found from coupons taken from the edges of beam flanges compared with the yield strength found at the meeting of the web with one of the flanges to be typical of I beam and H sections and that this is quite separate and independent of the effect of the residual stresses reported by them?

Also would they consider that, with a given steel chemical composition, thicker flanges and thicker webs more or less consistently show a reduced yield strength, which can be compensated for by a small increase of the carbon content of the steel?

It would be interesting to be sure that the authors consider that the rate of cooling is the only cause of the residual stresses reported by them, and also whether the difference in yield strength of coupons from different parts of the section is due to the somewhat lower temperature of the edges of the flanges when they pass through the finishing rolls or alternatively, partially because those parts become more worked during the rolling process.

---

[a] July, 1960, by Lynn S. Beedle and Lambert Tall.
[18] Cons. Engr., London, England.

ERRATA

Journal of the Structural Division

Proceedings of the American Society of Civil Engineers

July, 1960

p. 202, line 9 from bottom. Add the word "but" to the beginning of the line.

p. 204, lines 29 and 31. Change the words "discussion" to "discussions."

p. 205, line 32. Change "total time on one hour" to "total time of one hour."

p. 205, lines 48 and 49. Replace these lines by the following:

of the compass from the east through the north to the west, and the corresponding distances from the tower to the coastline varied between approximately 6 miles and 20 miles.

p. 206. Fig. 10 (b). Change "within a 5 minute intervals" to "within 5 minute intervals."

p. 207. Table 2. Change footnote a to "One minute mean speeds" and change footnote b to "Two second peaks."

p. 210. Table 3. From the caption, delete the material in parentheses. In the table change "Basic Wind - Velocity" to "Basic Wind - Velocity, in mph (See Figs. 5 and 6)." Also, insert the numbers 115 and 130 into the blank headings to the last two columns.

p. 212, item 5, line 3. Change "Table 1A or 1B" to "Table 3(a) or 3 (b)."

August, 1960

p. 75. In Eq. 47 add the term P_4 to the P-column. In Eq. 48 add the term P_4 after the terms P_1 P_2 P_3 and to the P-column. In the line above Eq. 48 change "P_1, P_2, and P_3" to "P_1, P_2, P_3, and P_4."

PROCEEDINGS PAPERS

The technical papers published in the past year are identified by number below. Technical-division sponsorship is indicated by an abbreviation at the end of each Paper Number, the symbols referring to: Air Transport (AT), City Planning (CP), Construction (CO), Engineering Mechanics (EM), Highway (HW), Hydraulics (HY), Irrigation and Drainage (IR), Pipeline (PL), Power (PO), Sanitary Engineering (SA), Soil Mechanics and Foundations (SM), Structural (ST), Surveying and Mapping (SU), and Waterways and Harbors (WW), divisions. Papers sponsored by the Department of Conditions of Practice are identified by the symbols (PP). For titles and order coupons, refer to the appropriate issue of "Civil Engineering." Beginning with Volume 82 (January 1956) papers were published in Journals of the various Technical Divisions. To locate papers in the Journals, the symbols after the paper number are followed by a numeral designating the issue of a particular Journal in which the paper appeared. For example, Paper 2270 is identified as 2270(ST9) which indicates that the paper is contained in the ninth issue of the Journal of the Structural Division during 1959.

VOLUME 85 (1959)

OCTOBER: 2189(AT4), 2190(AT4), 2191(AT4), 2192(AT4), 2193(AT4), 2194(EM4), 2195(EM4), 2196(EM4), 2197(EM4), 2198(EM4), 2199(EM4), 2200(HY10), 2201(HY10), 2202(HY10), 2203(PL3), 2204(PL3), 2205 (PL3), 2206(PO5), 2207(PO5), 2208(PO5), 2209(PO5), 2210(SM5), 2211(SM5), 2212(SM5), 2213(SM5), 2214 (SM5), 2215(SM5), 2216(SM5), 2217(SM5), 2218(ST8), 2219(ST8), 2220(EM4), 2221(ST8), 2222(ST8), 2223 (ST8), 2224(HY10), 2225(HY10), 2226(PO5), 2227(PO5), 2228(PO5), 2229(ST8), 2230(EM4), 2231(EM4), 2232(AT4)[c], 2233(PL3)[c], 2234(EM4)[c], 2235(HY10)[c], 2236(SM5)[c], 2237(ST8)[c], 2238(PO5)[c], 2239(ST8), 2240 (PL3).

NOVEMBER: 2241(HY11), 2242(HY11), 2243(HY11), 2244(HY11), 2245(HY11), 2246(SA6), 2247(SA6), 2248 (SA6), 2249(SA6), 2250(SA6), 2251(SA6), 2252(SA6), 2253(SA6), 2254(SA6), 2255(SA6), 2256(ST9), 2257(ST9), 2258(ST9), 2259(ST9), 2260(HY11), 2261(ST9)[c], 2262(ST9), 2263(HY11), 2264(ST9), 2265(HY11), 2266(SA6), 2267(SA6), 2268(SA6), 2269(HY11)[c], 2270(ST9).

DECEMBER: 2271(HY12)[c], 2272(CP2), 2273(HW4), 2274(HW4), 2275(HW4), 2276(HW4), 2277(HW4), 2278 (HW4), 2279(HW4), 2280(HW4), 2281(IR4), 2282(IR4), 2283(IR4), 2284(IR4), 2285(PO6), 2286(PO6), 2287 (PO6), 2288(PO6), 2289(PO6), 2290(PO6), 2291(PO6), 2292(SM6), 2293(SM6), 2294(SM6), 2295(SM6), 2296 (SM6), 2297(WW4), 2298(WW4), 2299(WW4), 2300(WW4), 2301(WW4), 2302(WW4), 2303(WW4), 2304(HW4), 2305(ST10), 2306(CP2), 2307(CP2), 2308(ST10), 2309(CP2), 2310(HY12), 2311(HY12), 2312(PO6), 2313(PO6), 2314(ST10), 2315(HY12), 2316(HY12), 2317(HY12), 2318(WW4), 2319(SM6), 2320(SM6), 2321(ST10), 2322 (ST10), 2323(HW4)[c], 2324(CP2)[c], 2325(SM6)[c], 2326(WW4)[c], 2327(IR4)[c], 2328(PO6)[c], 2329(ST10)[c], 2330 (CP2).

VOLUME 86 (1960)

JANUARY: 2331(EM1), 2332(EM1), 2333(EM1), 2334(EM1), 2335(HY1), 2336(HY1), 2337(EM1), 2338(EM1), 2339(HY1), 2340(HY1), 2341(SA1), 2342(EM1), 2343(SA1), 2344(ST1), 2345(ST1), 2346(ST1), 2347(ST1), 2348(EM1)[c], 2349(HY1)[c], 2350(ST1), 2351(ST1), 2352(SA1)[c], 2353(ST1)[c], 2354(ST1).

FEBRUARY: 2355(CO1), 2356(CO1), 2357(CO1), 2358(CO1), 2359(CO1), 2360(CO1), 2361(PO1), 2362(HY2), 2363(ST2), 2364(HY2), 2365(SU1), 2366(HY2), 2367(SU1), 2368(SM1), 2369(HY2), 2370(SU1), 2371(HY2), 2372(PO1), 2373(SM1), 2374(HY2), 2375(PO1), 2376(HY2), 2377(CO1)[c], 2378(SU1), 2379(SU1), 2380(SU1), 2381(HY2)[c], 2382(ST2), 2383(SU1), 2384(ST2), 2385(SU1)[c], 2386(SU1), 2387(SU1), 2388(SU1), 2389(SM1), 2390(ST2)[c], 2391(SM1)[c], 2392(PO1)[c].

MARCH: 2393(IR1), 2394(IR1), 2395(IR1), 2396(IR1), 2397(IR1), 2398(IR1), 2399(IR1), 2400(IR1), 2401(IR1), 2402(IR1), 2403(IR1), 2404(IR1), 2405(IR1), 2406(IR1), 2407(SA2), 2408(SA2), 2409(HY3), 2410(ST3), 2411 (SA2), 2412(HW1), 2413(WW1), 2414(WW1), 2415(HY3), 2416(HW1), 2417(HW3), 2418(HW1)[c], 2419(WW1)[c], 2420(WW1), 2421(WW1), 2422(WW1), 2423(WW1), 2424(SA2), 2425(SA2)[c], 2426(HY3)[c], 2427(ST3)[c].

APRIL: 2428(ST4), 2429(HY4), 2430(PO2), 2431(SM2), 2432(PO2), 2433(ST4), 2434(EM2), 2435(PO2), 2436 (ST4), 2437(ST4), 2438(HY4), 2439(EM2), 2440(EM2), 2441(ST4), 2442(SM2), 2443(HY4), 2444(ST4), 2445 (EM2), 2446(ST4), 2447(EM2), 2448(SM2), 2449(HY4), 2450(ST4), 2451(HY4), 2452(HY4), 2453(EM2), 2454 (EM2), 2455(EM2)[c], 2456(HY4)[c], 2457(PO2)[c], 2458(ST4)[c], 2459(SM2)[c].

MAY: 2460(AT1), 2461(ST5), 2462(AT1), 2463(AT1), 2464(CP1), 2465(CP1), 2466(AT1), 2467(AT1), 2468(SA3), 2469(HY5), 2470(ST5), 2471(SA3), 2472(SA3), 2473(ST5), 2474(SA3), 2475(ST5), 2476(SA3), 2477(ST5), 2478 (HY5), 2479(SA3), 2480(ST5), 2481(SA3), 2482(CO2), 2483(CO2), 2484(HY5), 2485(HY5), 2486(AT1)[c], 2487 (CP1)[c], 2488(CO2)[c], 2489(HY5)[c], 2490(SA3)[c], 2491(ST5)[c], 2492(CP1), 2493(CO2).

JUNE: 2494(IR2), 2495(IR2), 2496(ST6), 2497(EM3), 2498(EM3), 2499(EM3), 2500(EM3), 2501(SM3), 2502 (EM3), 2503(PO3), 2504(WW2), 2505(EM3), 2506(HY6), 2507(WW2), 2508(PO3), 2509(ST6), 2510(EM3), 2511 (EM3), 2512(ST6), 2513(HW2), 2514(HY6), 2515(PO3), 2516(EM3), 2517(WW2), 2518(WW2), 2519(EM3), 2520 (PO3), 2521(HY6), 2522(SM3), 2523(ST6), 2524(HY6), 2525(HY6), 2526(HY6), 2527(IR2), 2528(ST6), 2529 (HW2), 2530(IR2), 2531(HY6), 2532(EM3)[c], 2533(HW2)[c], 2534(WW2), 2535(HY6)[c], 2536(IR2)[c], 2537(PO3)[c], 2538(SM3)[c], 2539(ST6)[c], 2540(WW2)[c].

JULY: 2541(ST7), 2542(ST7), 2543(SA4), 2544(ST7), 2545(ST7), 2546(HY7), 2547(ST7), 2548(SU2), 2549(SA4), 2550(SU2), 2551(HY7), 2552(ST7), 2553(SU2), 2554(SA4), 2555(ST7), 2556(SA4), 2557(SA4), 2558(SA4), 2559(ST7), 2560(SU2)[c], 2561(SA4)[c], 2562(HY7)[c], 2563(ST7)[c].

AUGUST: 2564(SM4), 2565(EM4), 2566(ST8), 2567(EM4), 2568(PO4), 2569(PO4), 2570(HY8), 2571(EM4), 2572(EM4), 2573(EM4), 2574(SM4), 2575(EM4), 2576(EM4), 2577(HY8), 2578(EM4), 2579(PO4), 2580 (EM4), 2581(ST8), 2582(ST8), 2583(EM4)[c], 2584(PO4)[c], 2585(ST8)[c], 2586(SM4)[c], 2587(HY8)[c].

SEPTEMBER: 2588(IR3), 2589(IR3), 2590(WW3), 2591(IR3), 2592(HW3), 2593(IR3), 2594(IR3), 2595(IR3), 2596 (HW3), 2597(WW3), 2598(IR3), 2599(WW3), 2600(WW3), 2601(WW3), 2602(WW3), 2603(WW3), 2604(HW3), 2605(SA5), 2606(WW3), 2607(SA5), 2608(ST9), 2609(SA5)[c], 2610(IR3), 2611(WW3)[c], 2612(ST9)[c], 2613(IR3)[c], 2614(HW3)[c].

OCTOBER: 2615(EM5), 2616(EM5), 2617(ST10), 2618(SM5), 2619(EM5), 2620(EM5), 2621(ST10), 2622(EM5), 2623(SM5), 2624(EM5), 2625(SM5), 2626(SM5), 2627(EM5), 2628(EM5), 2629(ST10), 2630(ST10), 2631(PO5)[c], 2632(EM5)[c], 2633(ST10), 2634(ST10), 2635(ST10)[c], 2636(SM5)[c].

c. Discussion of several papers, grouped by divisions.

AMERICAN SOCIETY OF CIVIL ENGINEERS

OFFICERS FOR 1960

PRESIDENT

FRANK A. MARSTON

VICE-PRESIDENTS

Term expires October, 1960:
PAUL L. HOLLAND
LLOYD D. KNAPP

Term expires October, 1961:
CHARLES B. MOLINEAUX
LAWRENCE A. ELSENER

DIRECTORS

Term expires October, 1960:
PHILIP C. RUTLEDGE
WESTON S. EVANS
TILTON E. SHELBURNE
CRAIG P. HAZELET
DONALD H. MATTERN
JOHN E. RINNE

Term expires October, 1961:
THOMAS J. FRATAR
EARL F. O'BRIEN
DANIEL B. VENTRES
CHARLES W. BRITZIUS
WAYNE G. O'HARRA
FRED H. RHODES, JR.
N. T. VEATCH

Term expires October, 1962:
ELMER K. TIMBY
SAMUEL S. BAXTER
THOMAS M. NILES
TRENT R. DAMES
WOODROW W. BAKER
BERNHARD DORNBLATT

PAST PRESIDENTS

Members of the Board

LOUIS R. HOWSON
FRANCIS S. FRIEL

EXECUTIVE SECRETARY

WILLIAM H. WISELY

TREASURER

E. LAWRENCE CHANDLER

ASSISTANT SECRETARY

DON P. REYNOLDS

ASSISTANT TREASURER

ENOCH R. NEEDLES

PROCEEDINGS OF THE SOCIETY

HAROLD T. LARSEN
Manager of Technical Publications

PAUL A. PARISI
Editor of Technical Publications

MARVIN L. SCHECHTER
Associate Editor of Technical Publications

IRVIN J. SCHWARTZ
Assistant Editor of Technical Publications

COMMITTEE ON PUBLICATIONS

PHILIP C. RUTLEDGE, *Chairman*

THOMAS M. NILES, *Vice-Chairman*

TILTON E. SHELBURNE
WESTON S. EVANS
WAYNE G. O'HARRA
BERNHARD DORNBLATT